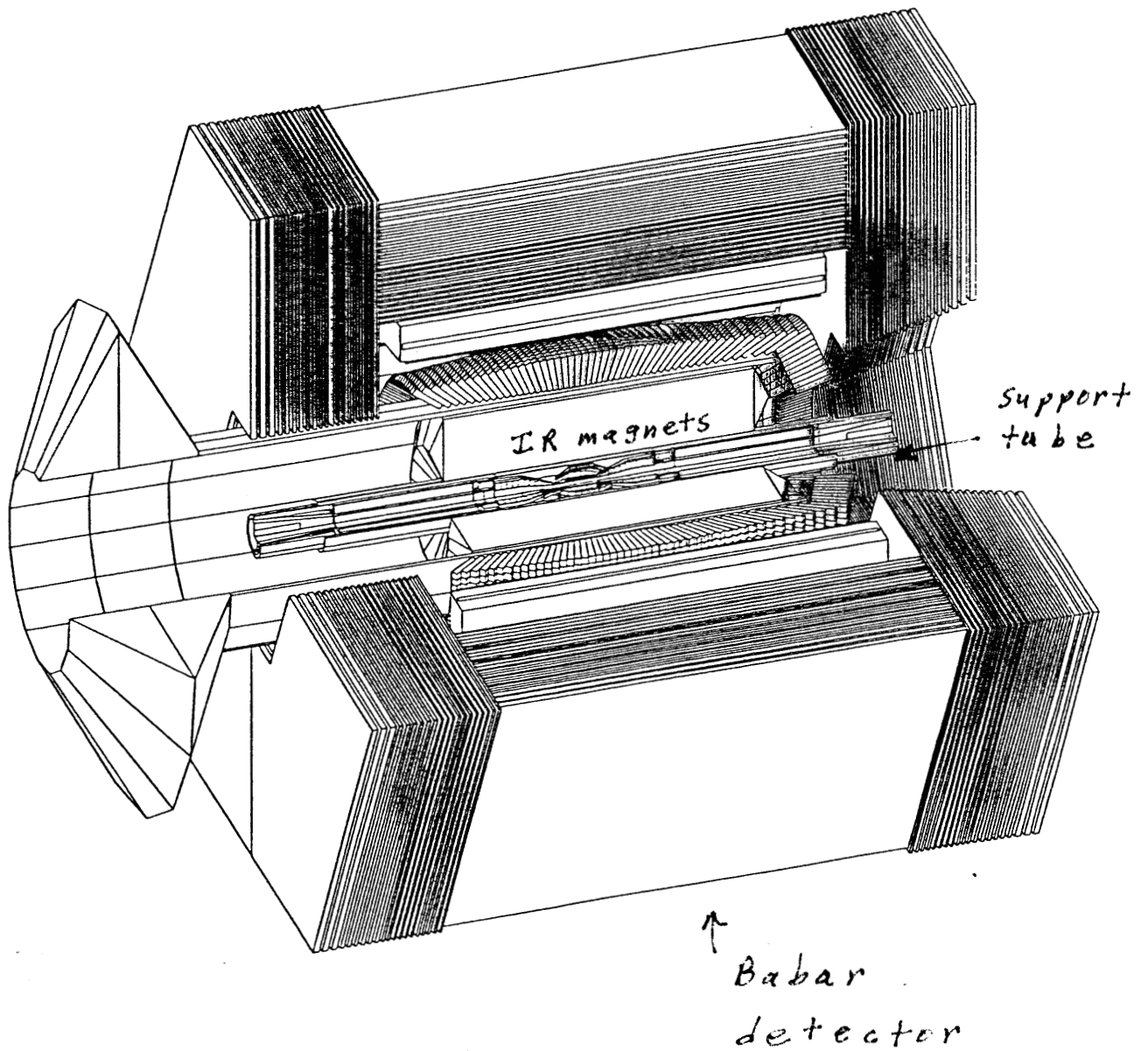


Magnet Alignment Tools
Developed At SLAC

Zack Wolf, SLAC
IMMW-XI

B Factory IR Support Tube Position Monitor



The support tube holds the IR magnets inside the Babar detector.

Support Tube Position Monitor

Goals And Constraints

Goals:

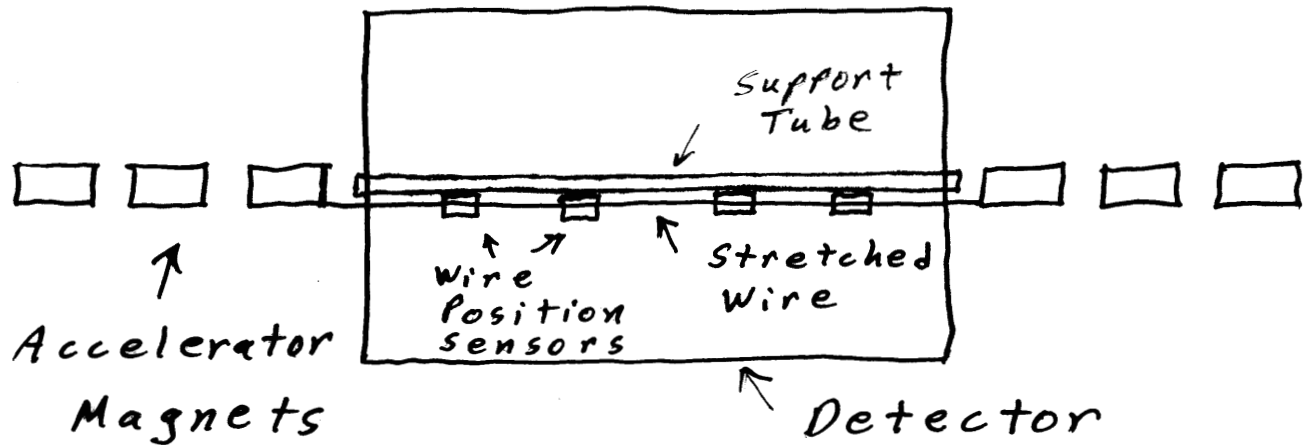
- 1) Monitor the position of the IR magnets relative to the accelerator.
- 2) Desired X and Y position accuracy: -10 microns

Constraints:

- 1) No budget for the project
- 2) Very limited space, 1 cm between the support tube and the detector
- 3) The sensors can not be above the support tube surface as the support tube is being inserted in the detector
- 4) No magnetic components can be used

Support Tube Position Sensor

General Approach

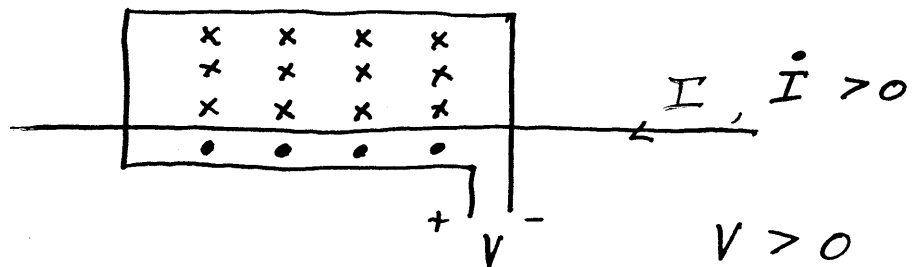
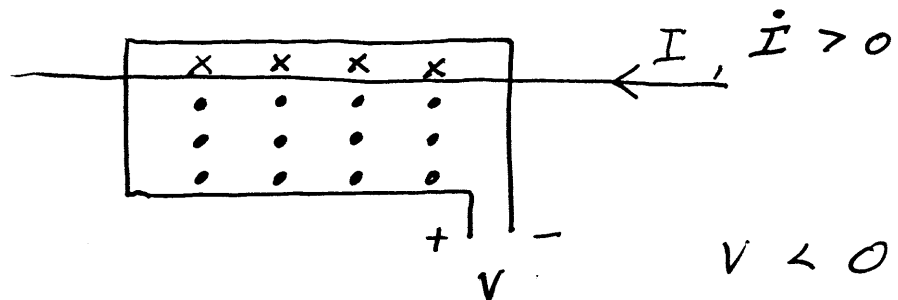
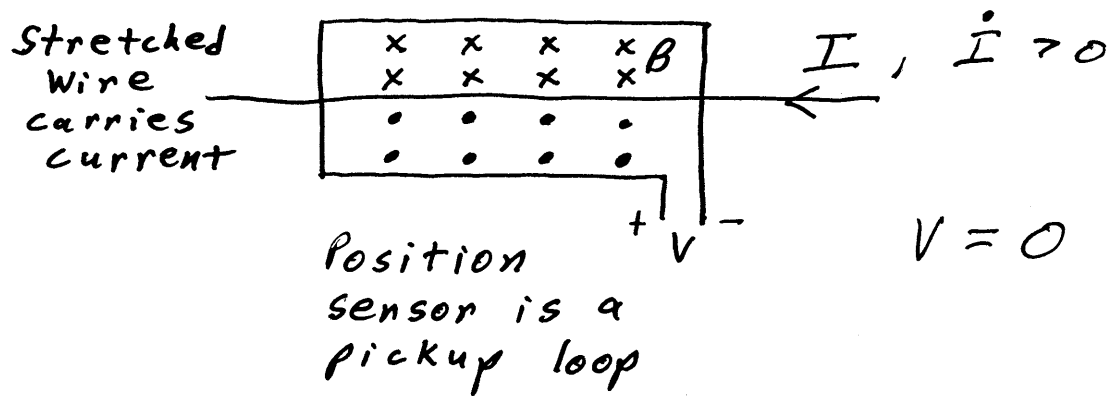


Stretch a wire between the accelerator magnets on each side of the detector.

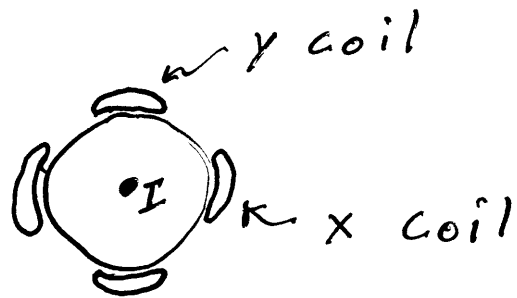
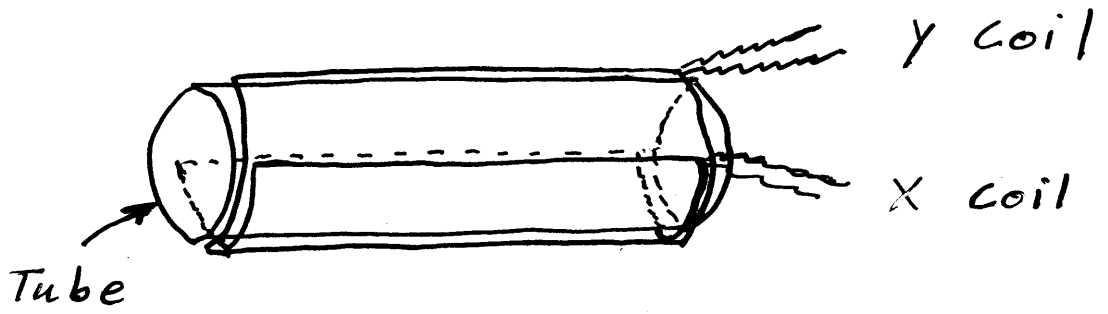
Measure the position of the support tube relative to the wire.

Support Tube Position Sensor

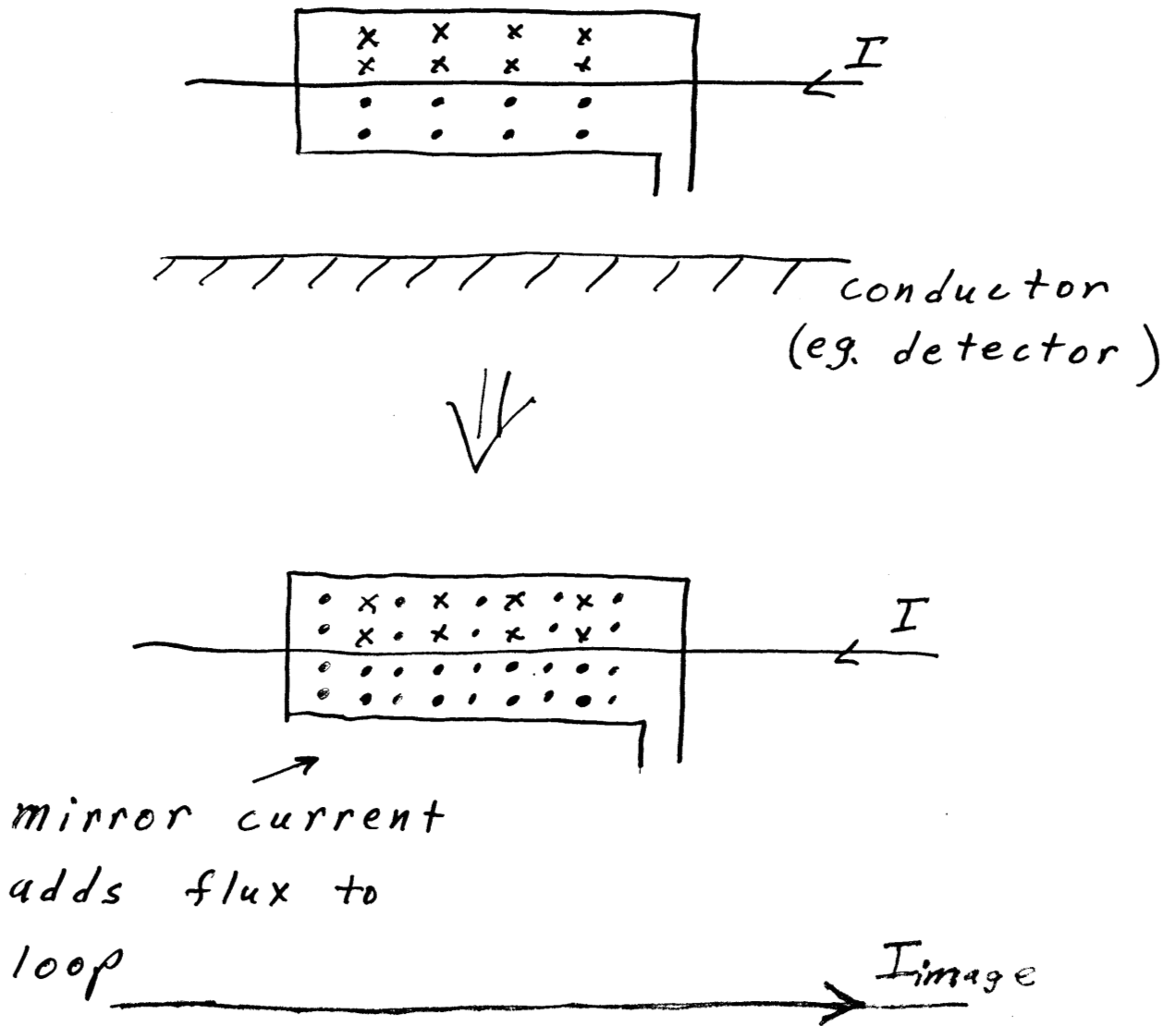
Principle of Operation



Sensor Design



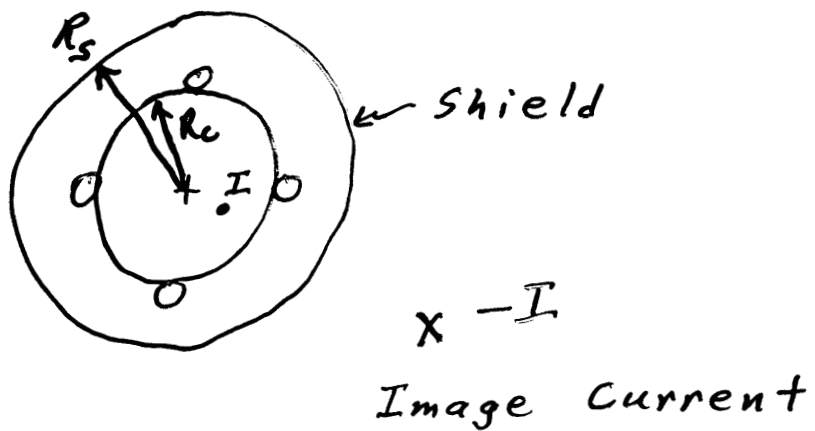
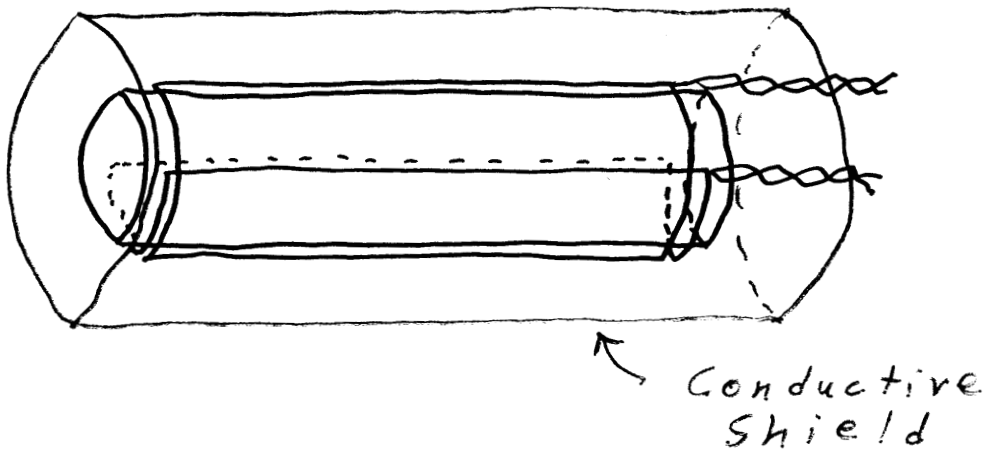
Eddy Currents Affect the Signal



Eddy currents in a nearby conductor have the same effect on the sensor signal as an image current.

Eddy Current Shield

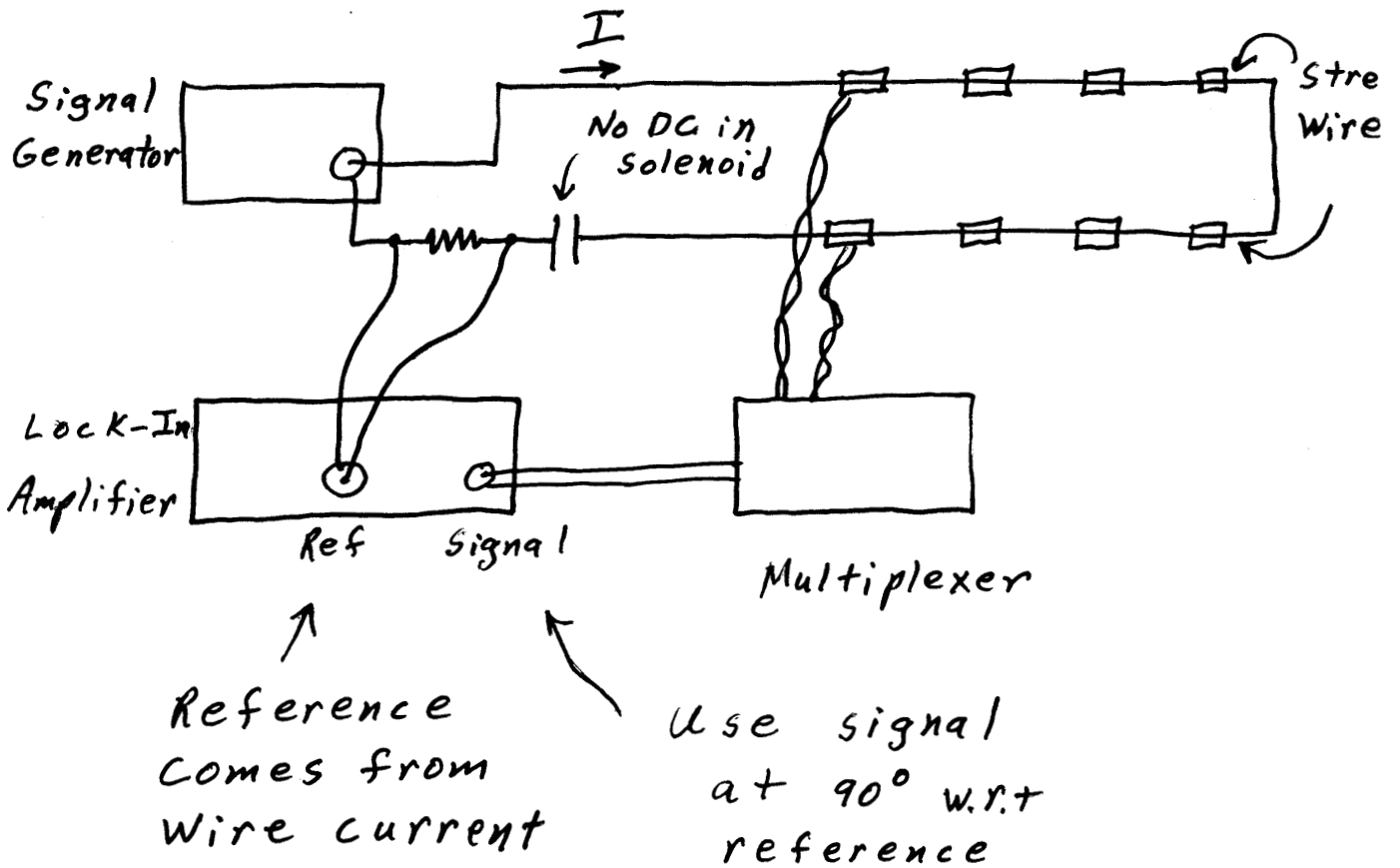
Add a shield so external conductors don't affect the sensor response.



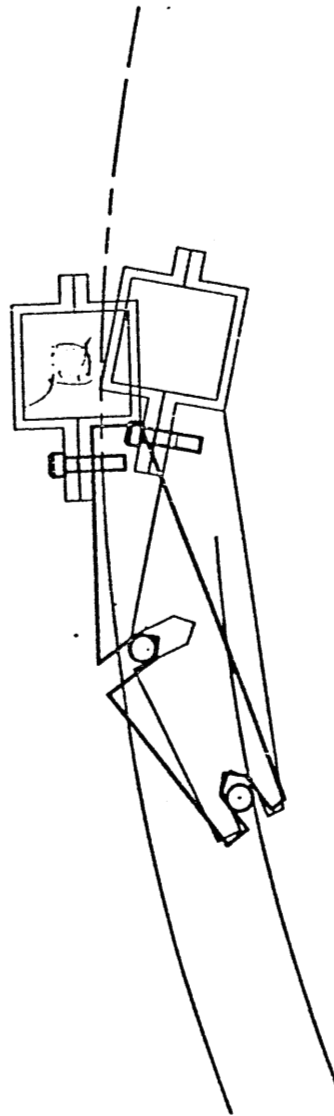
$$V = j \frac{\mu_0 W I N L}{\pi R_c} \left(1 - \frac{R_c^2}{R_s^2} \right) X$$

↗ effect of shield
↖ displacement of current from center

Support Tube Sensor Electronics



Sensor Pop-Up Mechanism



similar to
final design

SLAC Magnetic Measurements

Date: 01-02-1990

Time: 00:14:41

Project: Q1

Device Type: WPSENSOR

Device Name (Serial #): PROTO3

Operator: zw

Run Number: 3

Comment: test x response

Sensor Name = Proto 3, X

Sensor ID Number = 5

Wire Current = 4.084053E-02 Arms

Wire Current Frequency = 80074.5 Hz

Xwire (microns)	Ywire (microns)	Sensor Out (Vrms)	V/X (V/m)	V/Y (V/m)
-999.90	-0.05	-0.002244730	2.244954	-
-800.05	-0.05	-0.001774800	2.218361	-
-600.05	-0.10	-0.001315010	2.191501	-
-400.00	-0.05	-0.000875417	2.188543	-
-200.05	-0.05	-0.000445249	2.225688	-
0.00	-0.05	-0.000023713	-	-
200.00	-0.05	0.000397684	1.988420	-
400.05	-0.05	0.000819270	2.047919	-
600.00	-0.05	0.001253490	2.089150	-
800.00	-0.05	0.001700050	2.125062	-
1000.00	-0.05	0.002160800	2.160800	-

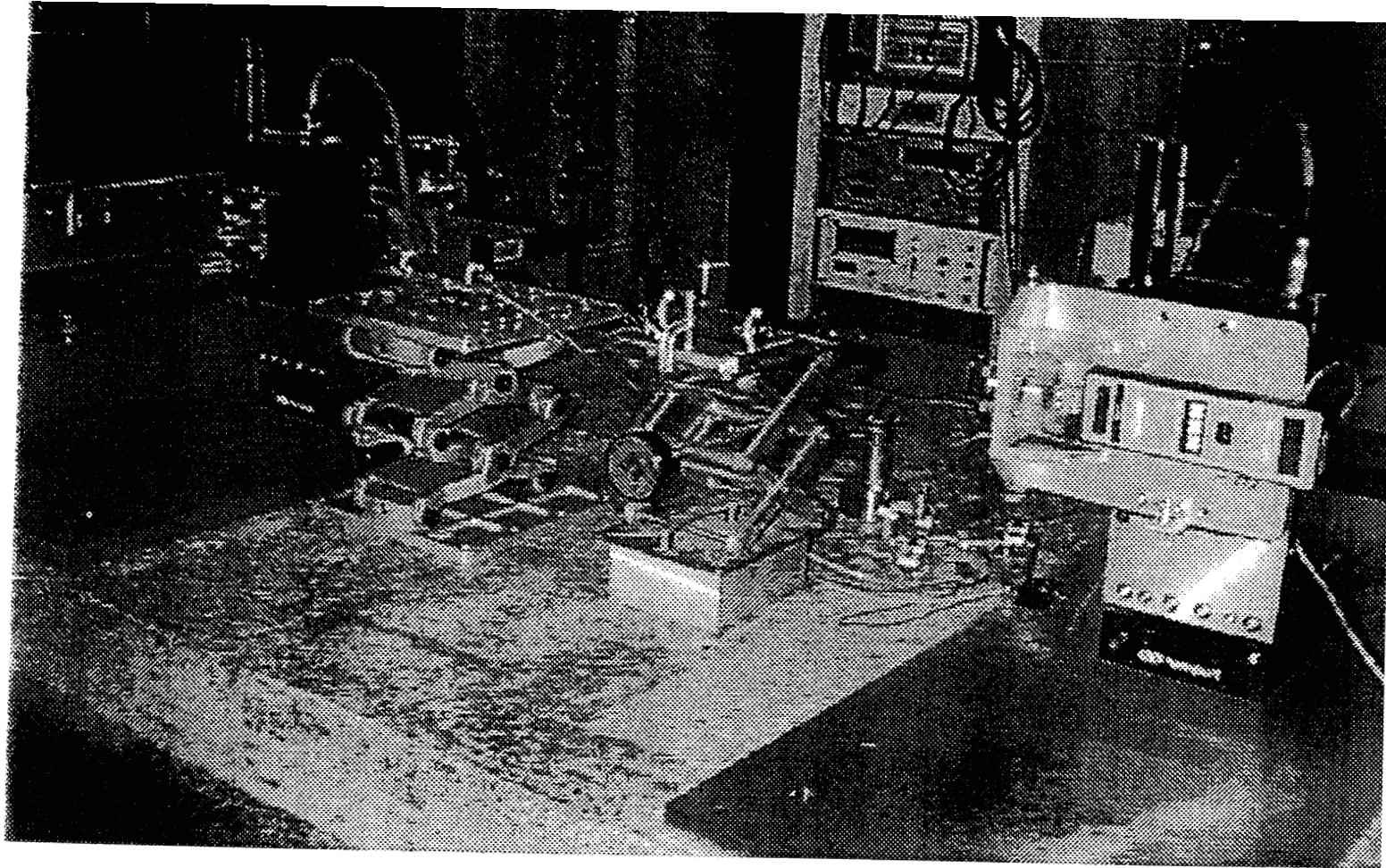
↑

↑

Sensor Parameters:

Lcoil = 0.055880 m
 Rcoil = 0.003556 m
 Ncoil = 30
 Rshield = 0.005080 m
 Skin Depth = 0.000265 m
 Rsh corr = 0.005345 m
 Iwire = 0.040841 Arms
 Fiwire = 80074.5 Hz
 Est dV/dx = 2.15987 V/m ←

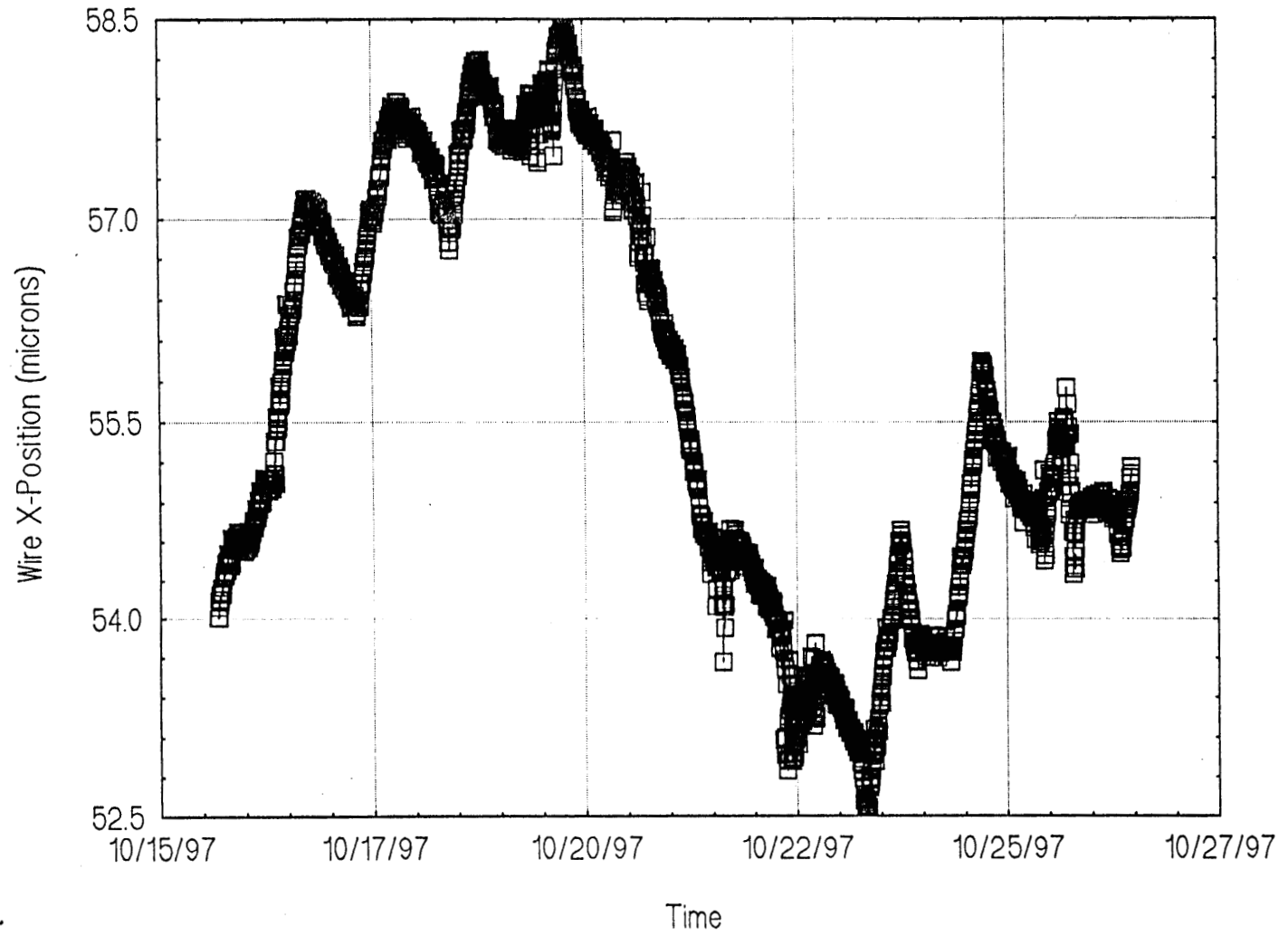
1) Sensitivity ~ $\frac{2 \mu V}{\mu m}$
 2) Sensor behaves as expected



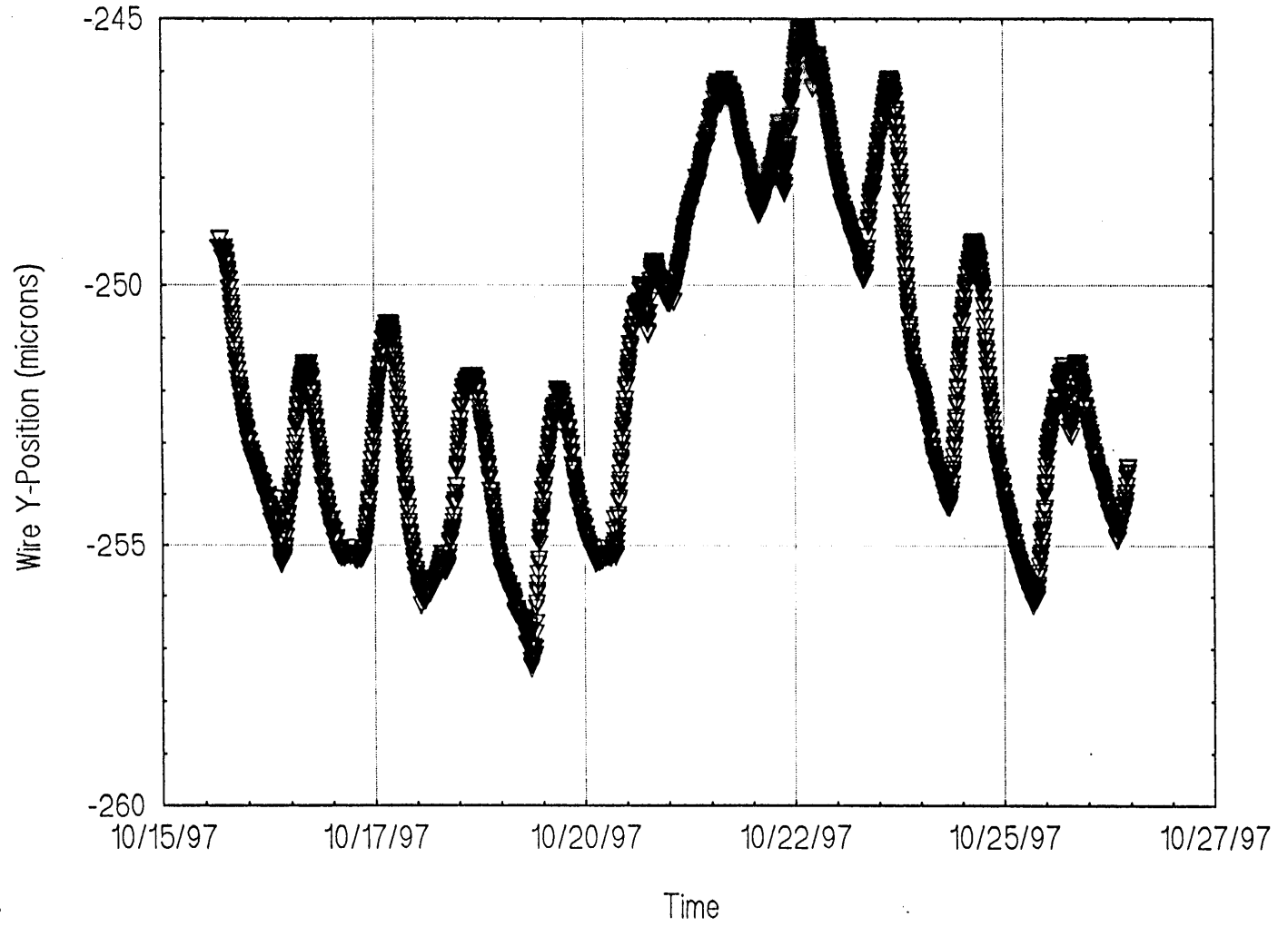
Two prototype sensors under test.

The x, y stages move the wire
to determine the sensor's response.

11 Day Stability Test



11 Day Stability Test



Alignment Tools For VISA

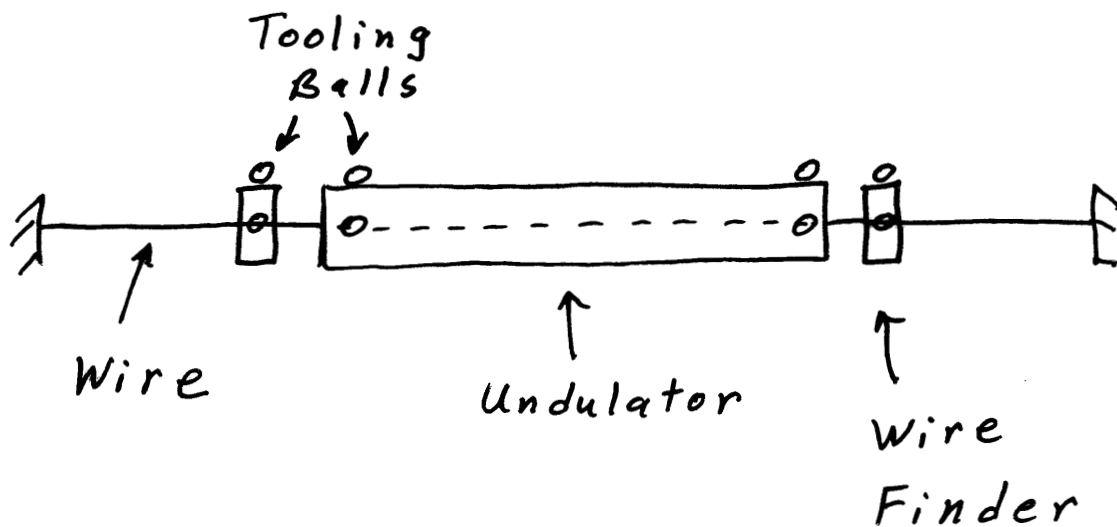
VISA [Visual to Infrared SASE (Self Amplified Stimulated Emission) Amplifier] is a FEL experiment being carried out at the BNL Accelerator Test Facility.

It is a step toward the LCLS being considered for SLAC.

VISA consists of four undulator segments each 99 cm long. The rms alignment errors for the four segments need to be less than 50 microns (2 mils).

The alignment is carried out in two steps. A pulsed wire system fiducializes the segments. Our wire finder relates the wire position to tooling balls. The segments are then placed on a reference laser beam. Our laser finder relates the laser beam position to tooling balls.

Wire Finder For VISA

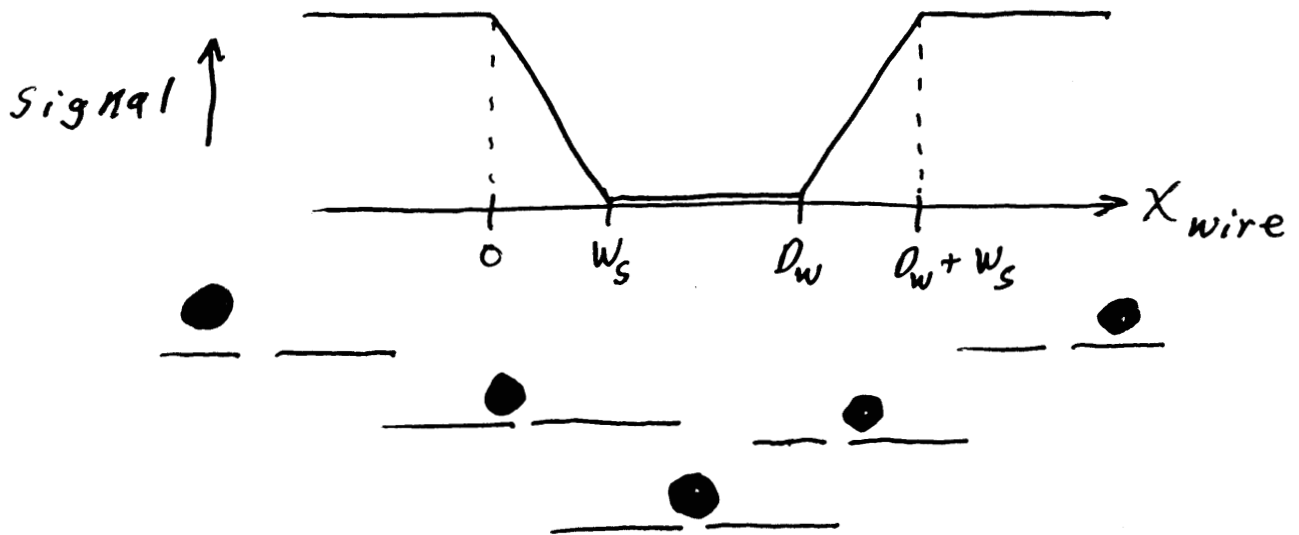
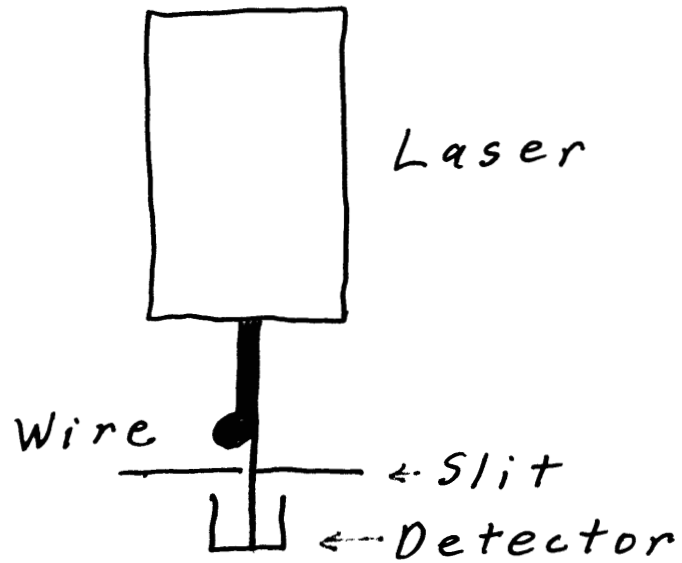


The wire is placed along the ideal trajectory using a pulsed wire technique.

The wire finder relates the wire position to tooling balls so the undulator can be fiducialized.

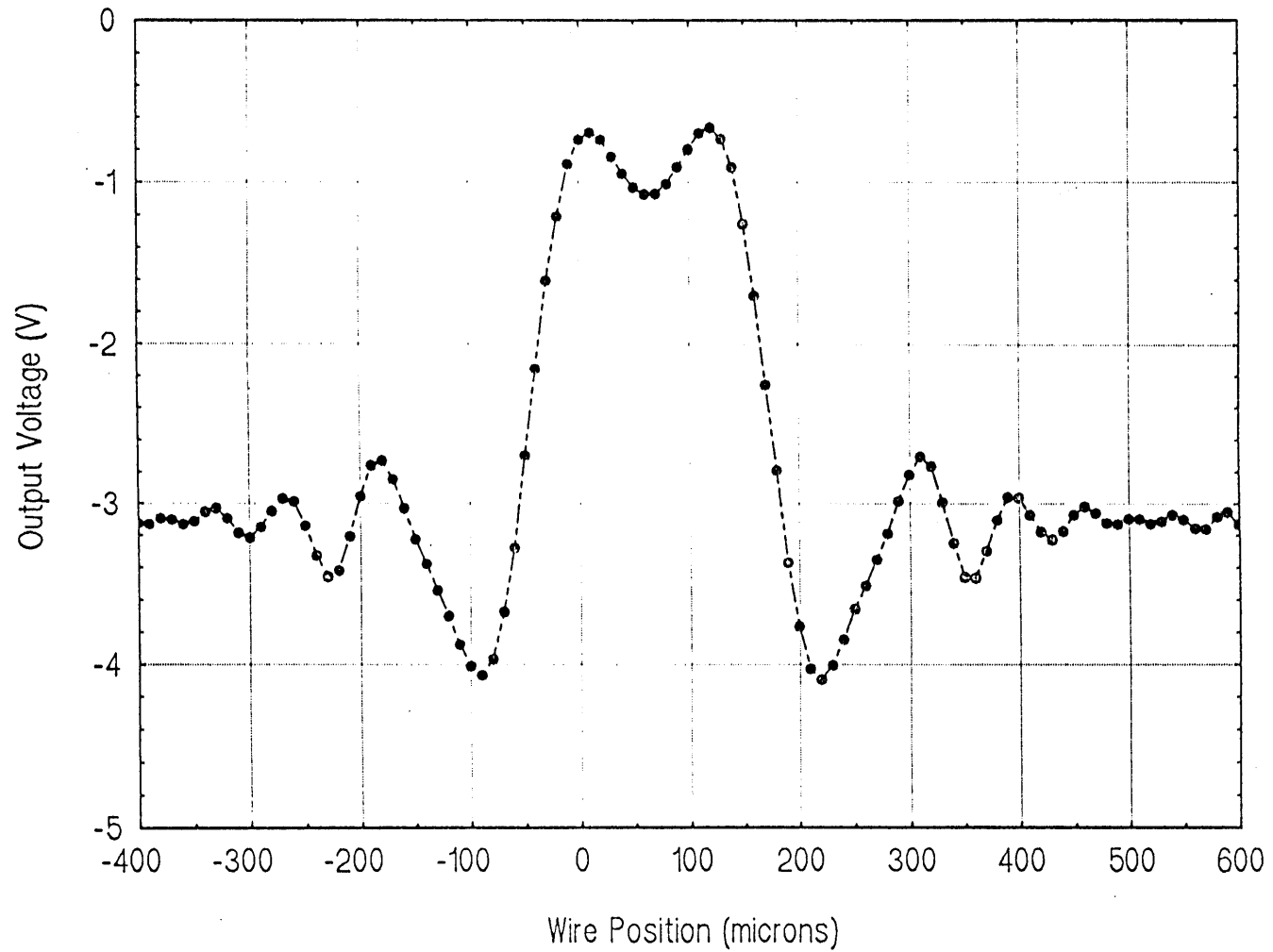
Zach Wolf

Principle of Operation



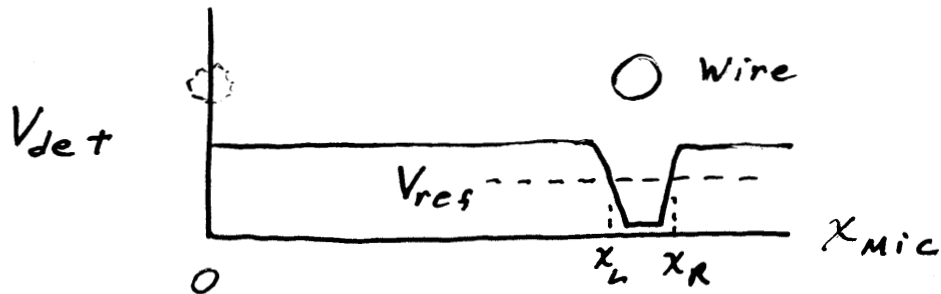
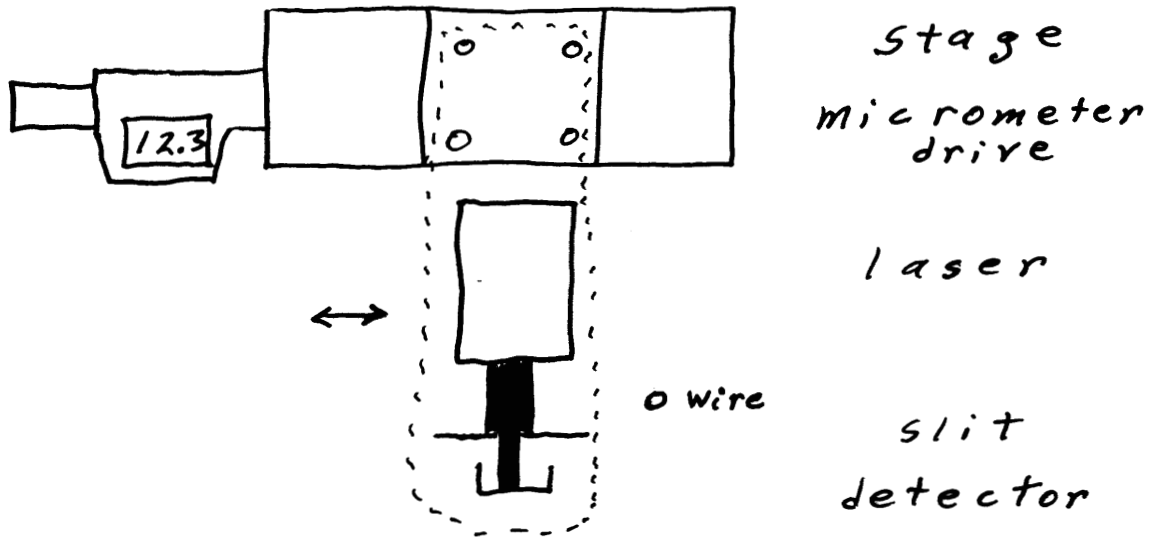
$$\text{Sensitivity} \sim \frac{3 \text{ V}}{50 \mu\text{m}} = \frac{60 \text{ mV}}{\mu\text{m}}$$

Laser Wire Position Sensor



Detector signal as a wire is moved across the slit.

Wire Finder Operation

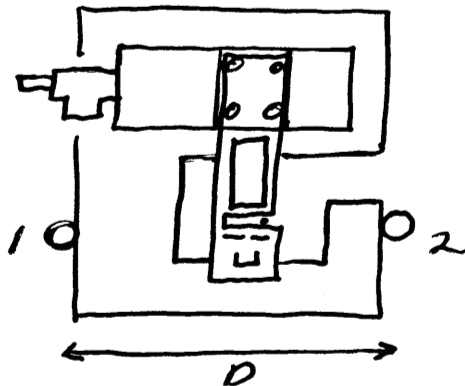


$$x_{mic}^{wire} = \frac{x_L + x_R}{2}$$

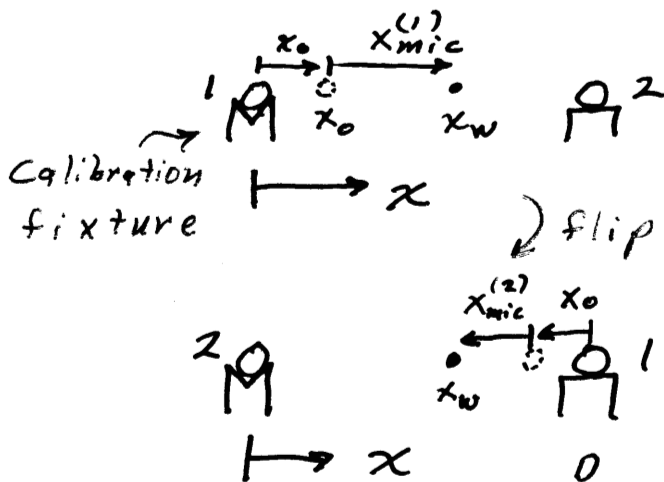
x_{mic}^{wire} is the position of the wire relative to a wire positioned where the micrometer reads zero.

A calibration is needed to get to absolute coordinates.

Wire Finder Calibration



Wire finder with tooling balls



$$x_w = x_0 + x_{mic}^{(1)}$$

(need x_0)

$$x_w = D - x_0 - x_{mic}^{(2)}$$

Subtract:

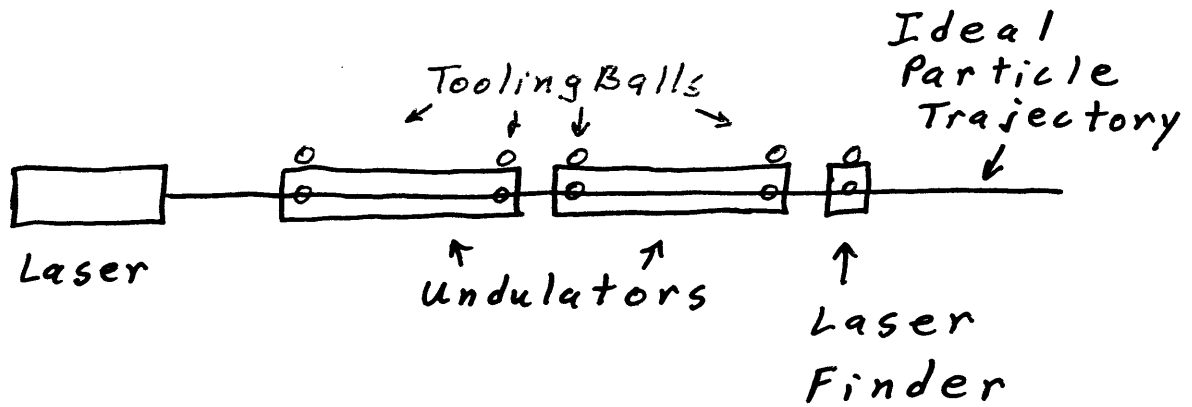
$$\begin{aligned} 0 &= x_0 + x_{mic}^{(1)} - D + x_0 + x_{mic}^{(2)} \\ &= 2x_0 - D + (x_{mic}^{(1)} + x_{mic}^{(2)}) \end{aligned}$$

$$x_0 = \frac{D}{2} - \frac{x_{mic}^{(1)} + x_{mic}^{(2)}}{2}$$

after calibration,

$$x_w = x_0 + x_{mic}$$

Laser Finder For VISA

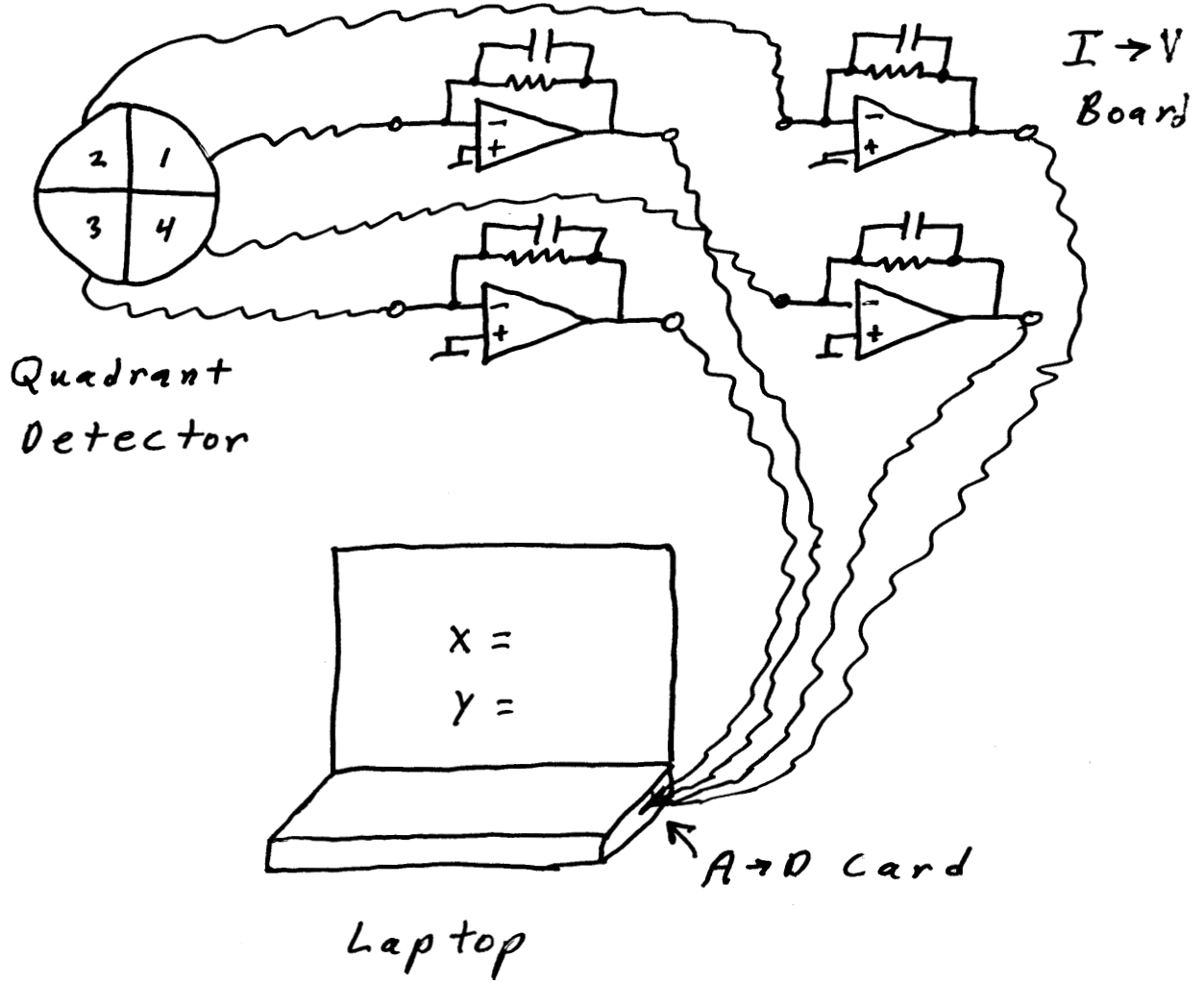


A laser beam is set up on the ideal particle trajectory.

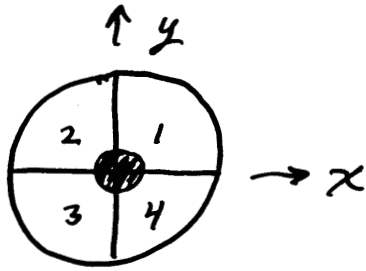
The undulator segments need to be positioned onto the beam.

The laser finder relates the laser beam to tooling balls so the undulator segments can be positioned.

Laser Beam Position Finder



Laser Beam Position Finder



Output :

$$V_1, V_2, V_3, V_4$$

Define :

$$V_T = V_1 + V_2 \quad V_B = V_3 + V_4$$

$$V_R = V_1 + V_4 \quad V_L = V_2 + V_3$$

Then,

$$x = K \frac{V_R - V_L}{V_R + V_L}$$

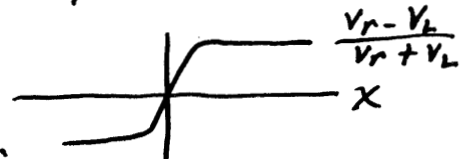
$$y = K \frac{V_T - V_B}{V_T + V_B}$$

K is determined experimentally

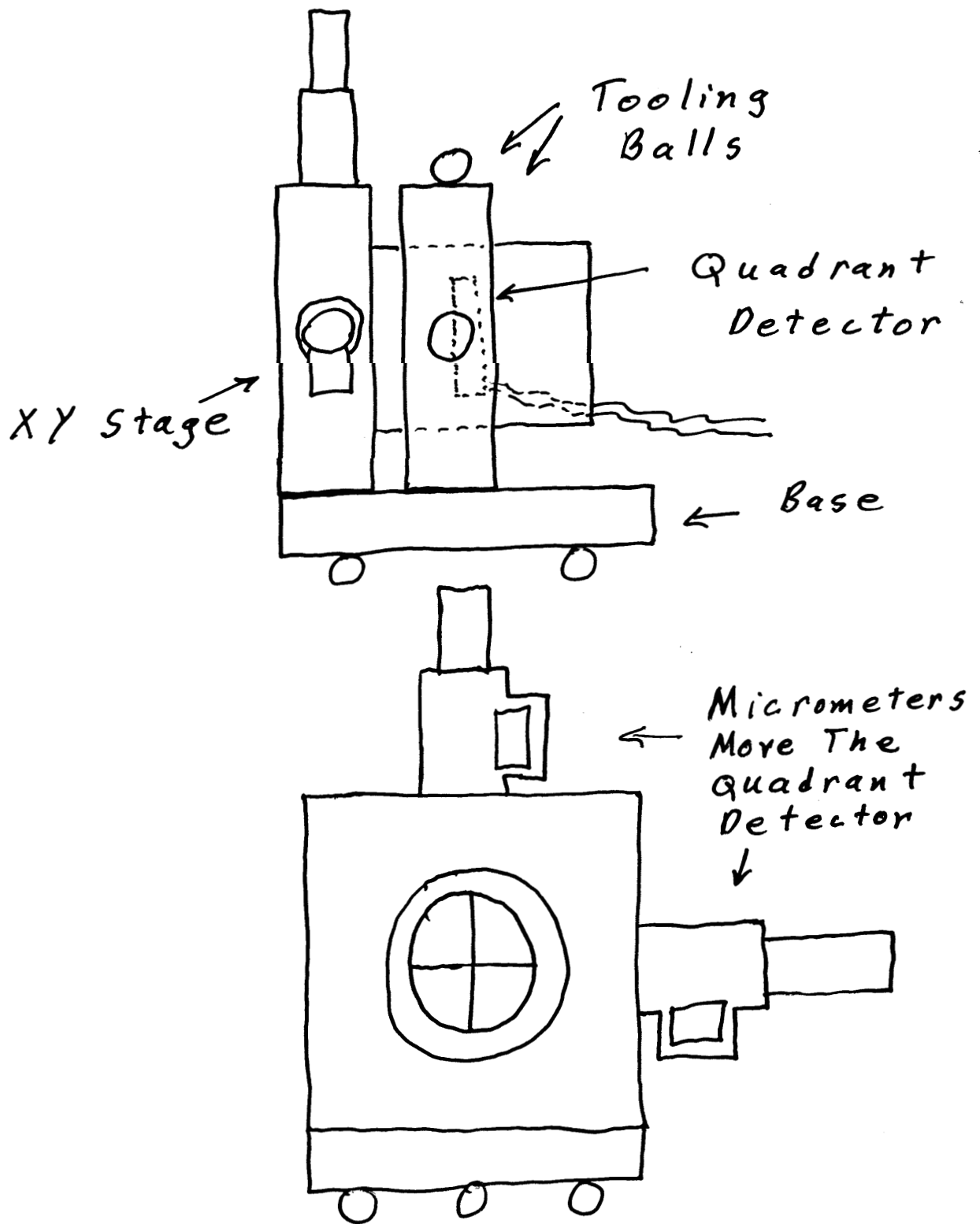
Very high sensitivity over a

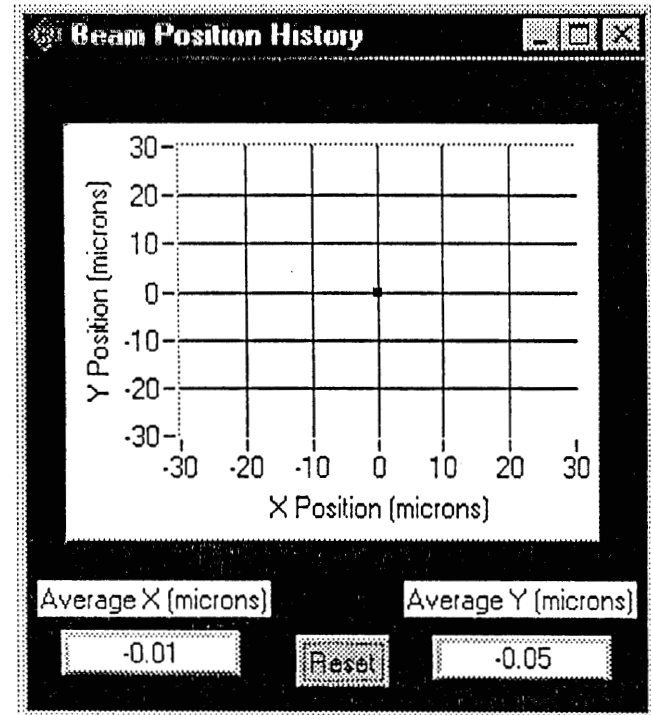
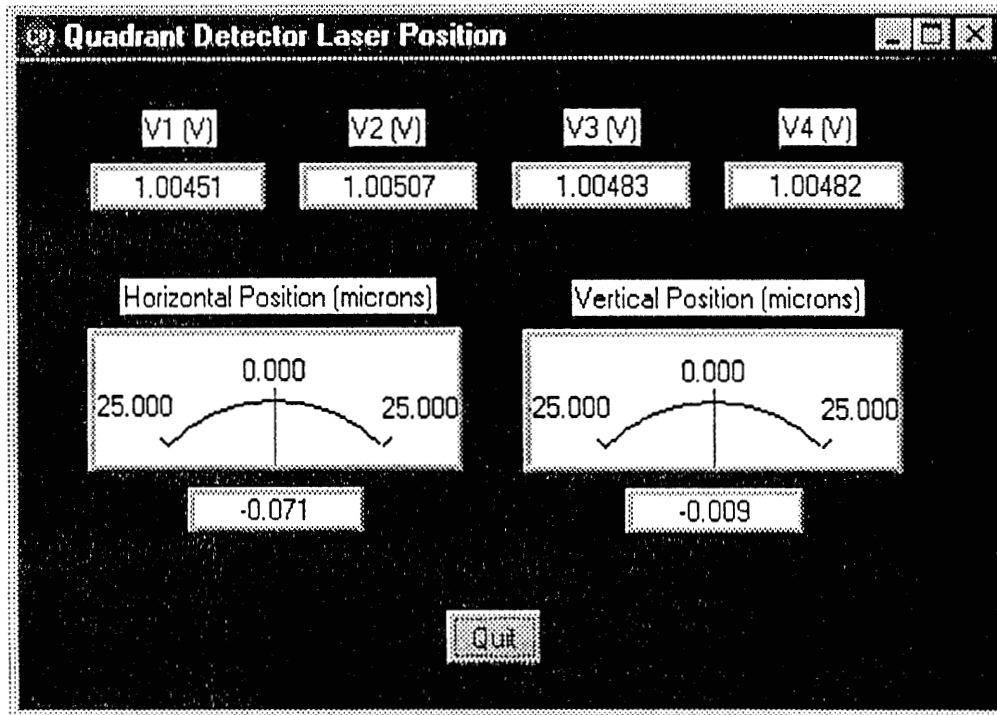
Small range

Use as null detector.



Laser Finder Construction





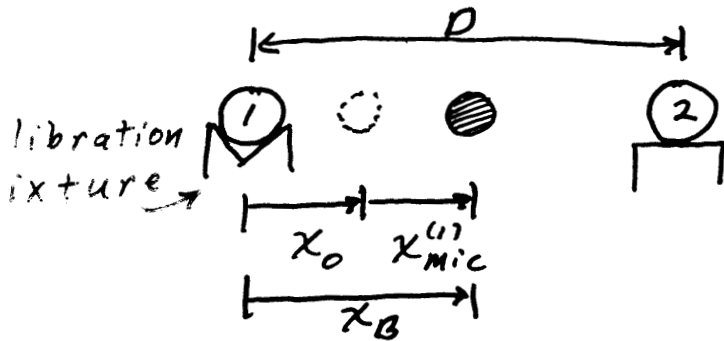
Lab Windows Interface gives the laser beam position relative to the quadrant detector.

Micrometers are used to move the detector onto the beam so the display reads $x=0$, $y=0$. The micrometer readings are used to relate the beam position to tooling balls.

Averaging in the history plot compensates for turbulent air refraction.

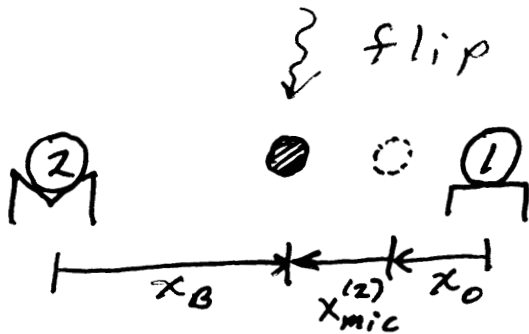
Laser Beam X Position

The quadrant detector is moved until it is centered on the beam.



$$x_B = x_0 + x_{mic}^{(1)}$$

(x_0 is the position of a beam centered on the detector when the micrometer reads zero)



$$x_B = D - x_0 - x_{mic}^{(2)}$$

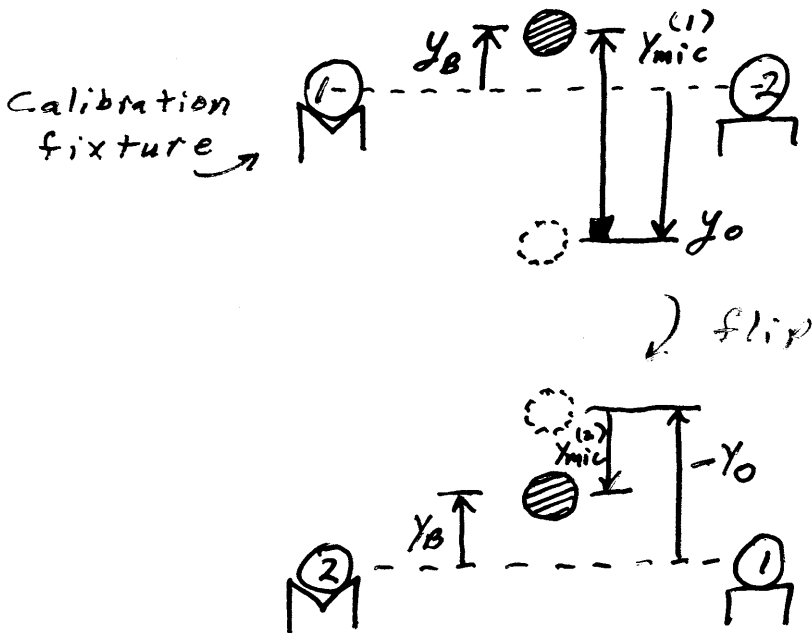
Calibration

$$x_0 = \frac{D}{2} - \frac{x_{mic}^{(1)} + x_{mic}^{(2)}}{2}$$

after calibration

$$x_B = x_0 + x_{mic}$$

Laser Beam Y Position



$$y_B = y_0 + y_{mic}^{(1)}$$

(y_0 is the position of a beam centered on the detector when the micrometer reads zero)

$$y_B = -y_0 - y_{mic}^{(2)}$$

Subtract:

$$0 = y_0 + y_{mic}^{(1)} - (-y_0 - y_{mic}^{(2)})$$

Calibration

$$y_0 = - \frac{y_{mic}^{(1)} + y_{mic}^{(2)}}{2}$$

after calibration

$$y_B = y_0 + y_{mic}$$

Magnet Mapping of the PHENIX Magnets Using Surface Method

Wlodek Guryn, BNL

ABSTRACT

We shall describe the mapping procedure, setup and give preliminary results of the magnet mapping of the PHENIX magnets. We used the surface mapping technique, where the flux of the magnetic field through the closed surface surrounding the volume of interest is measured. Given the absence of the current sources inside the surface, the magnetic potential satisfies Laplace equation, which is solved using Green's function method. Reconstructed field is compared to the measurements made on the inside of the volume of interest and to TOSCA simulations.

The contents of this talk were not available for inclusion in the proceedings.

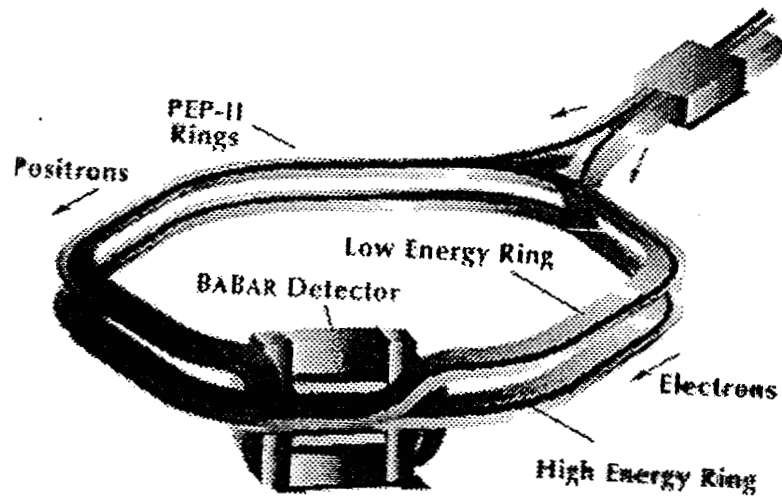
The Babar Detector Solenoid

Field Map

Zack Wolf
IMMW XI

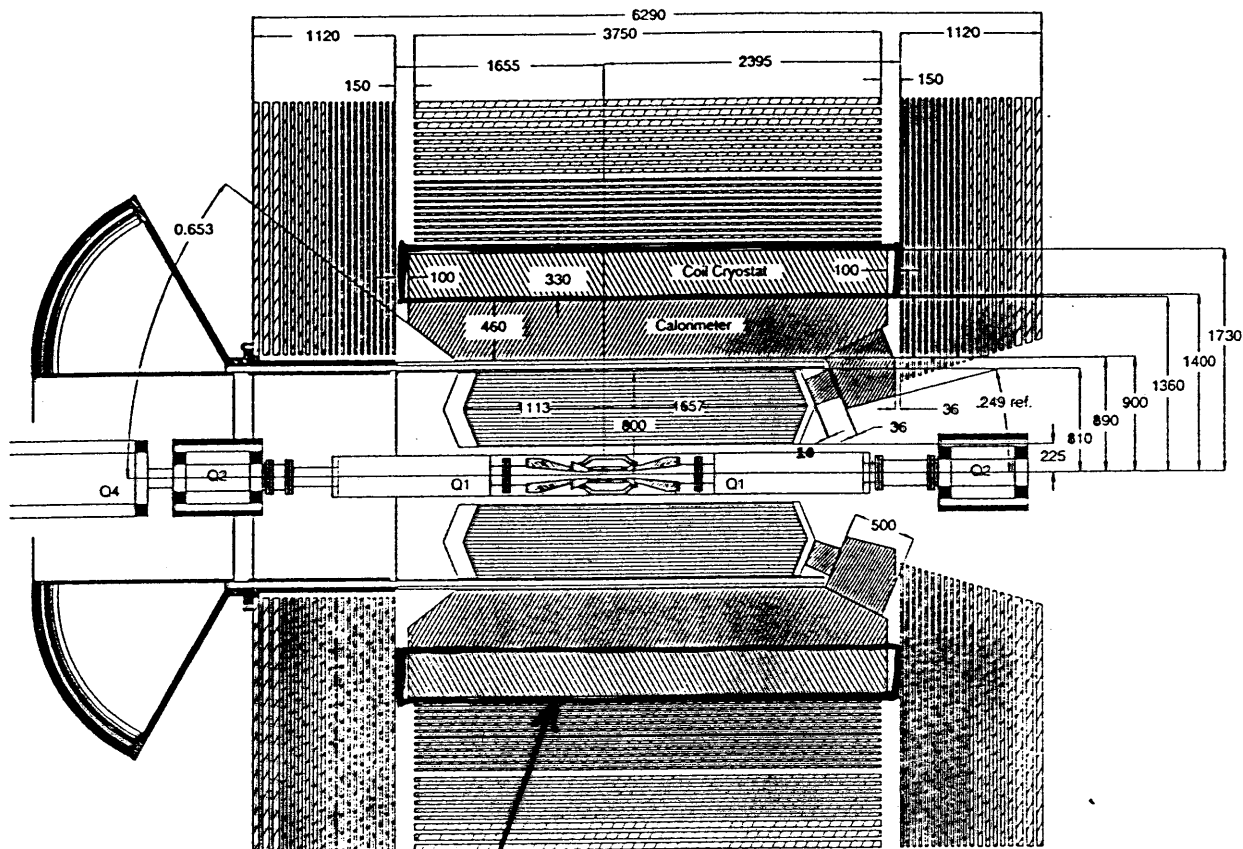
PEP II

SLAC B Factory



BABAR
Detector

Babar Detector



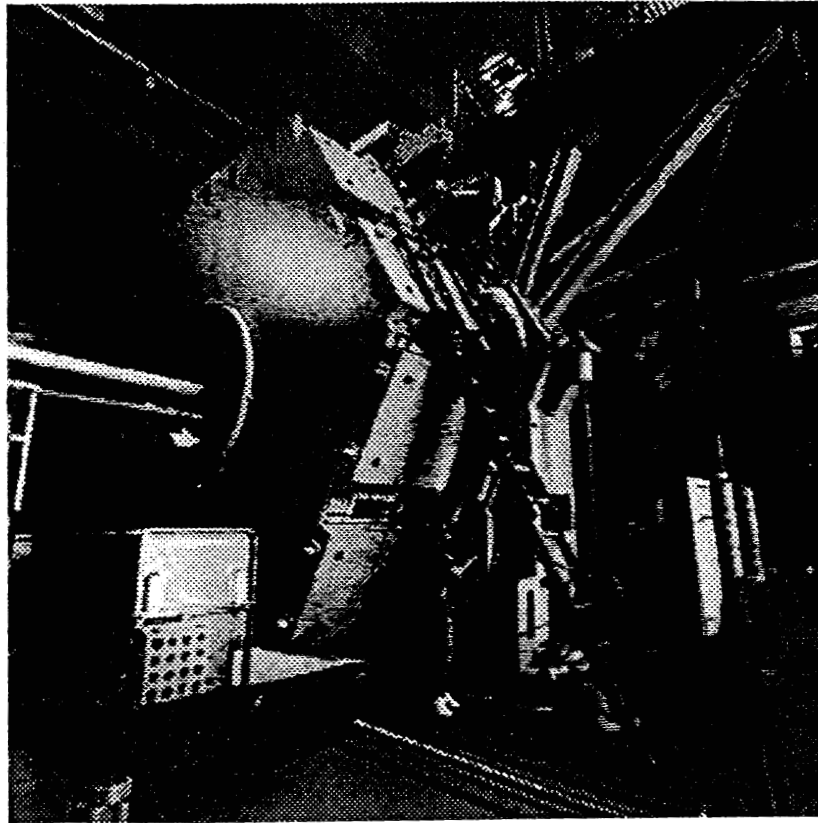
Superconducting
Solenoid

$$B = 1.5 \text{ T}$$

$$D = 2.8 \text{ m}$$

$$L = 3.46 \text{ m}$$

Babar Detector with Mapper



Babar Solenoid

There are 2 parts to the job of characterizing the solenoid.

- 1) Find B_z , B_r , B_ϕ on a grid inside the solenoid for particle tracking.
- 2) Find the effect of the solenoid on the accelerator.

Field In the Tracking Volume

Momentum resolution ($\approx 3\%$) sets the field map accuracy requirements,

Probe accuracy:

Standard values $.1\%$, $.01\%$

We bought $.01\%$ probes for B_z ,
 $.1\%$ probes for the smaller B_r, B_ϕ

Measurement grid:

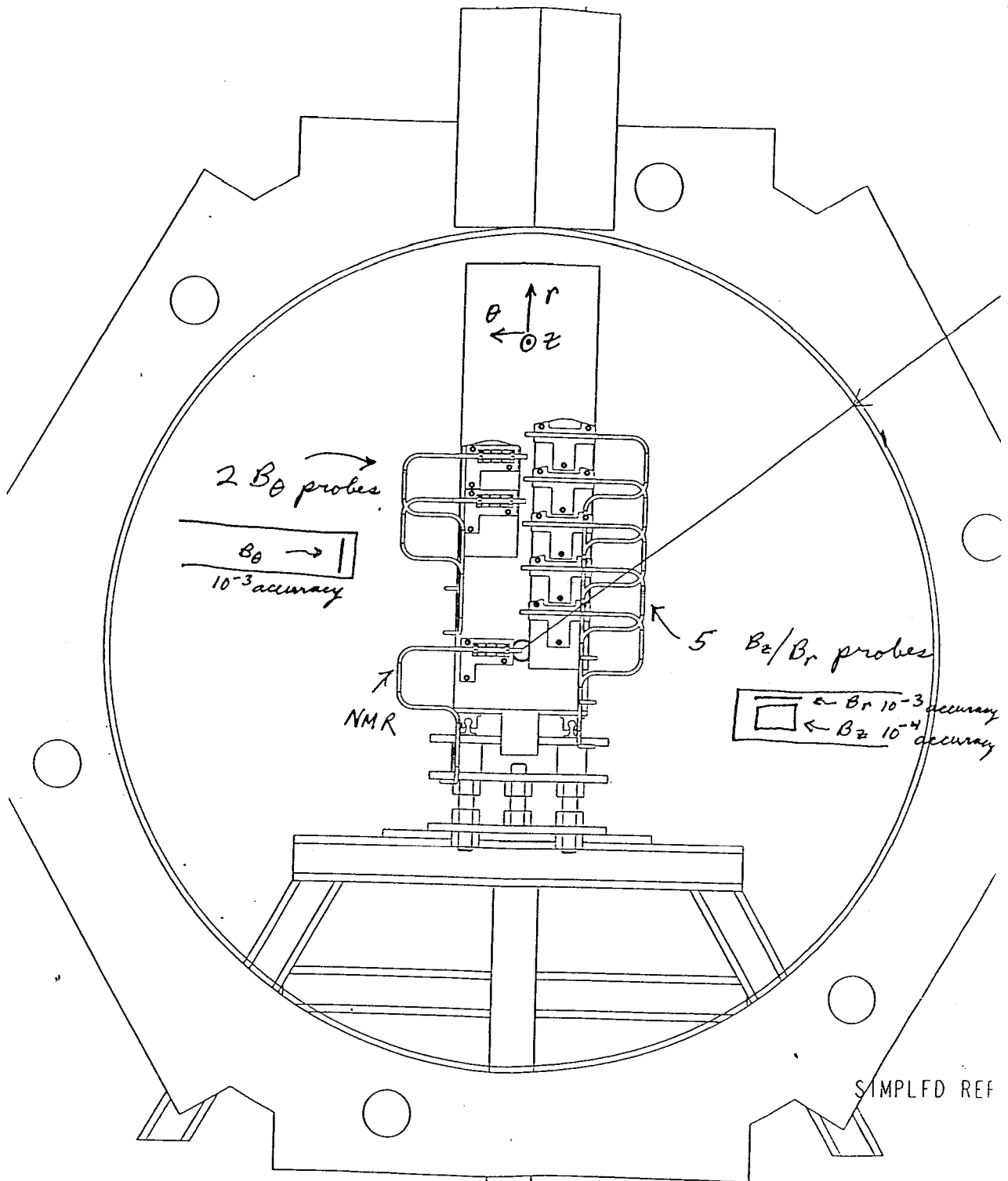
Set by interpolation errors between measurement points.

Computer modeling set the grid spacing at 7.5 cm
($\epsilon < .05\%$)

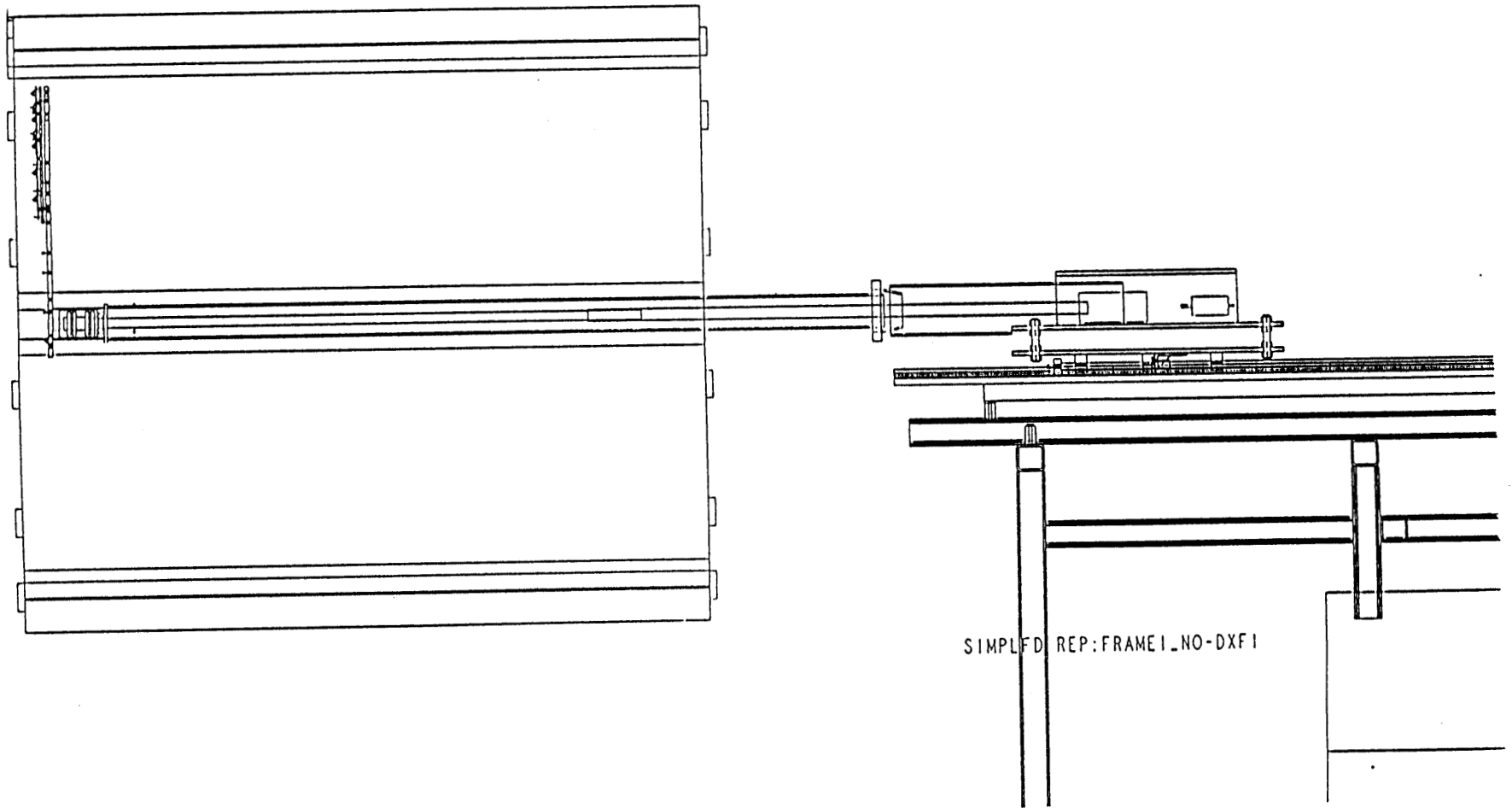
Our Approach

(Many compromises)

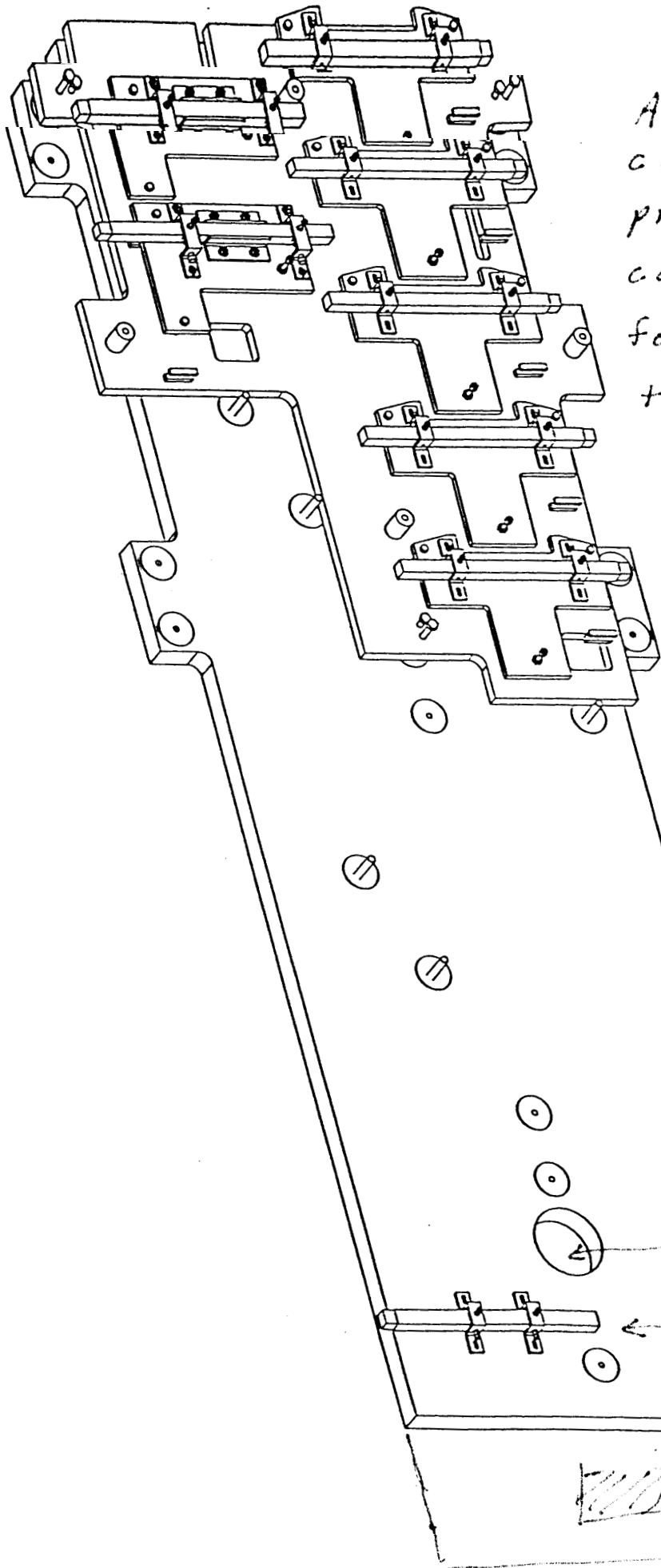
- 1) field gradients \Rightarrow Hall probes,
NMR only in solenoid center
- 2) minimal complexity inside
(+ better accuracy)
magnet \Rightarrow array of probes,
move in ϕ and z from outside
- 3) finite (small) budget \Rightarrow
probe plate which moves
to 4 ^{radial} positions, this is done
by hand, limits the number
of Hall probe we have to buy
- 4) space constraints \Rightarrow cantilevered
arm, everything on one end of
detector



Probes on an arm which rotates in ϕ and moves along the axis in z .



Schematic of the mapper



A Probe plate carries the Hall probes. The plate can be moved to four positions on the Hexcel arm,

(cardboard honeycomb with a G10 skin)

rotation axis

NMR

counter weight

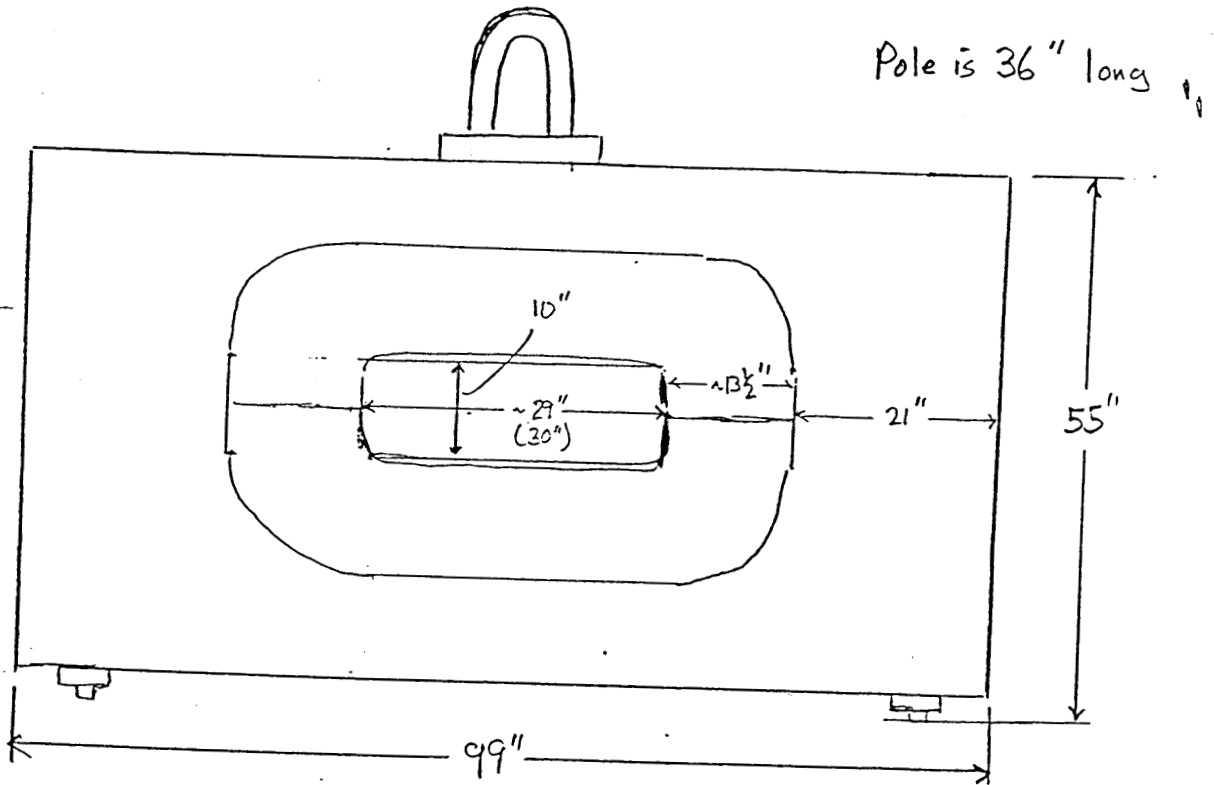
Keep B_z out of B_r and B_ϕ

- 1) Set up a calibration magnet with a large, homogeneous, vertical field
- 2) Put tooling balls on the probe plate and keep them in the horizontal plane.
- 3) Move each probe to the center of the magnet, level the tooling balls, adjust the B_r and B_ϕ probes to read zero.
- 4) Use the tooling balls to place the probe plate on the mapper.

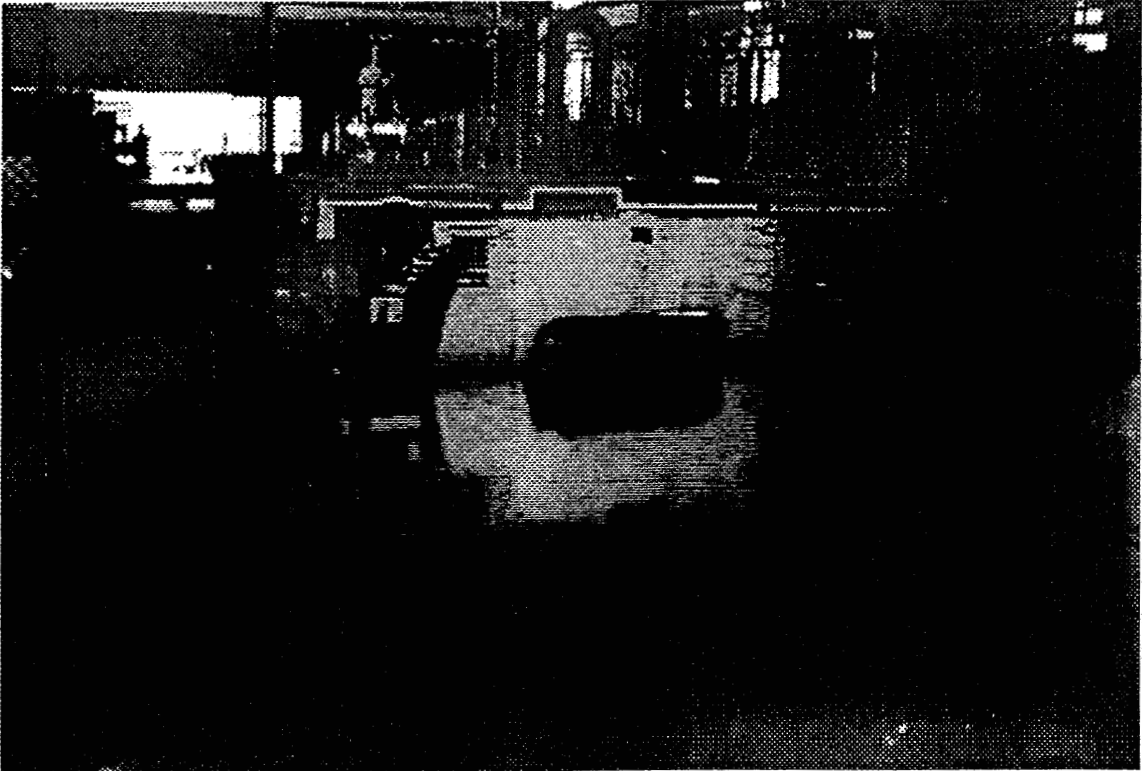
Probe Adjustment Magnet

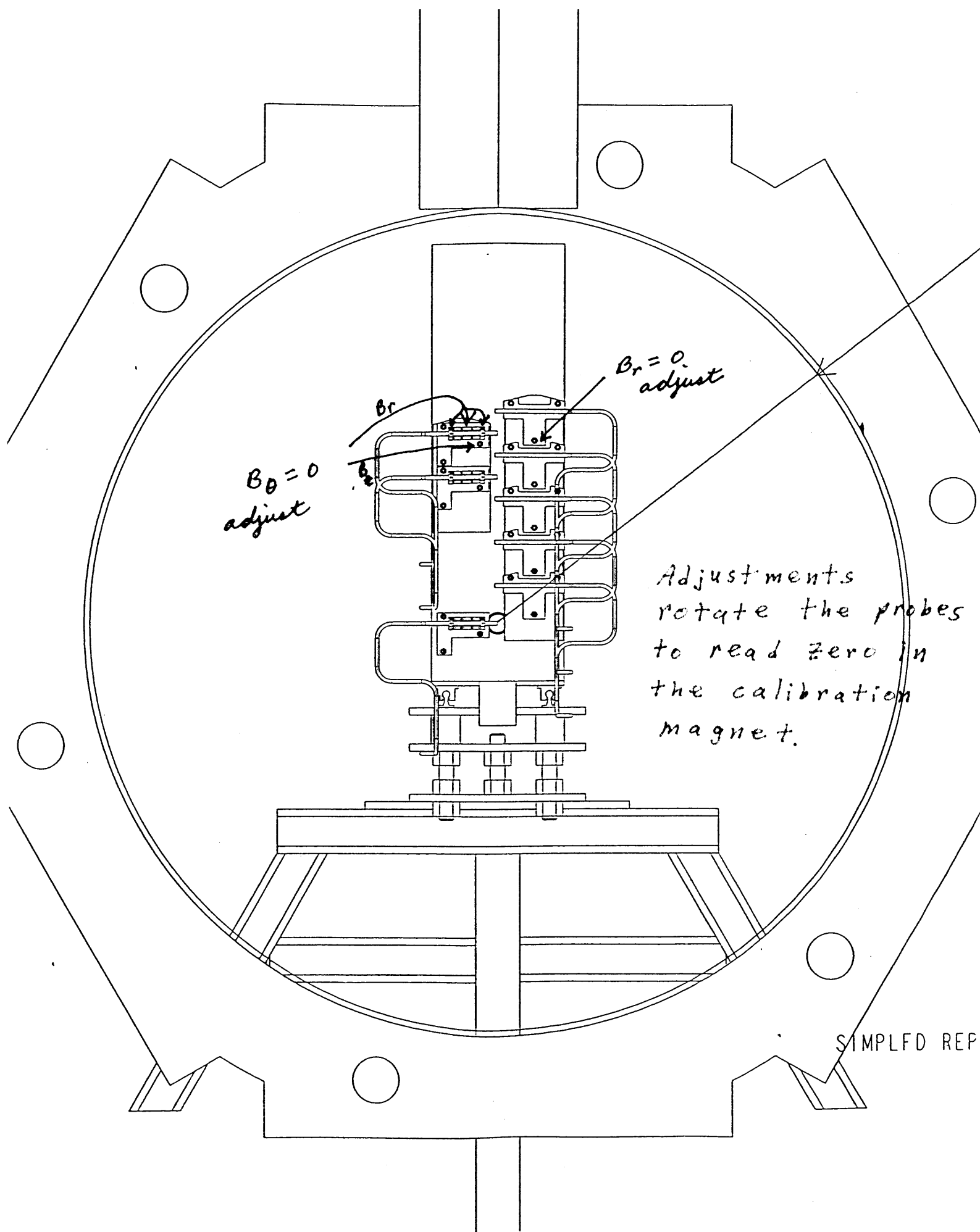
29 D 36 (10" Gap Height)
(or 30)

P.C. 19823 AEC # 178429 27 Tons



Probe Adjustment Magnet





$B_0 = 0$
adjust

$B_r = 0$
adjust

B_r

Adjustments
rotate the probes
to read zero in
the calibration
magnet.

SIMPLFD REP

Which Brand of Hall Probes to buy?

Problem: We were not able to align our Hall probes in a 1.5 T field.

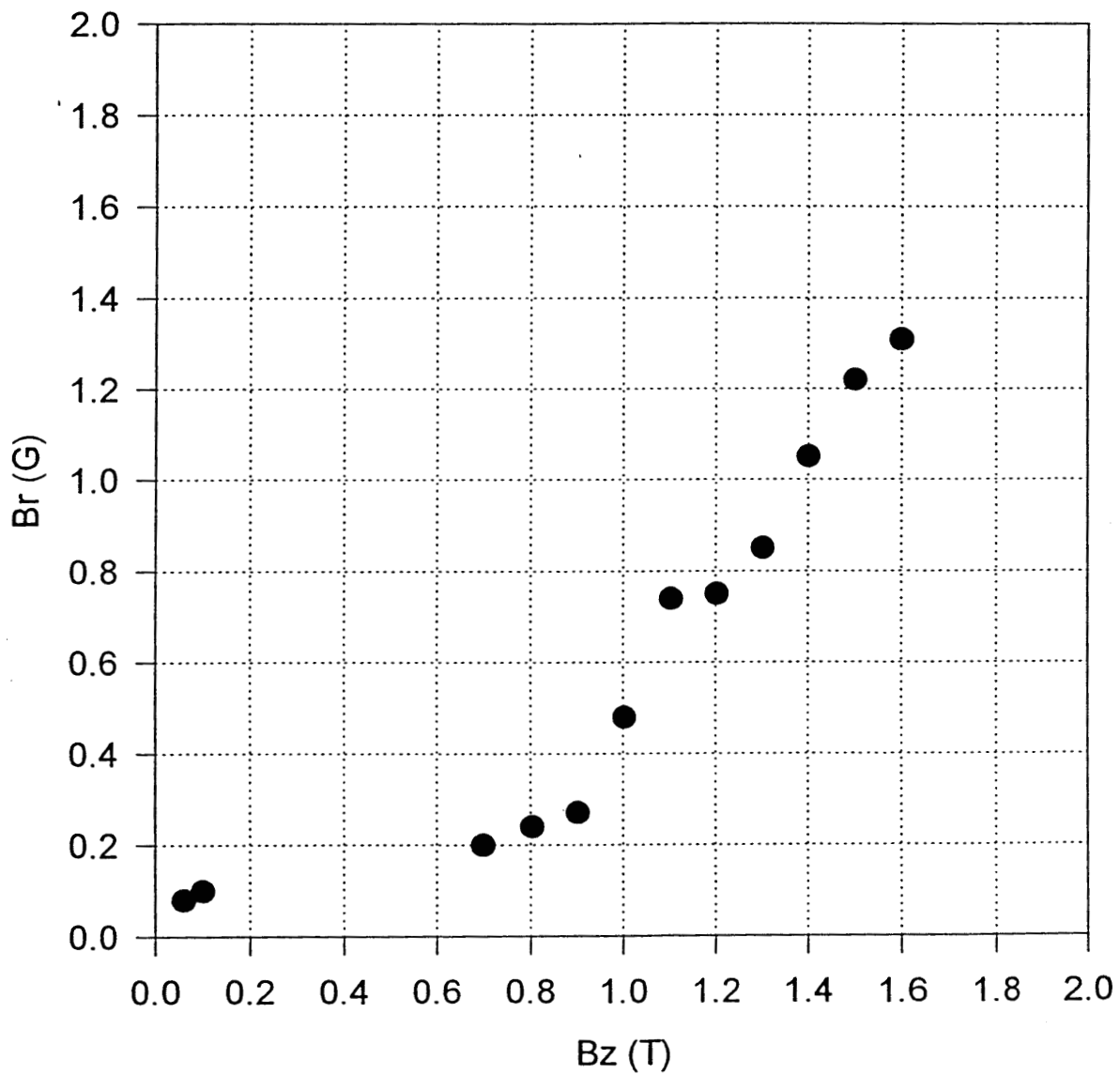
We needed probes we could align at low fields and would not be influenced by the planar 1.5 T field.



Sentron probes

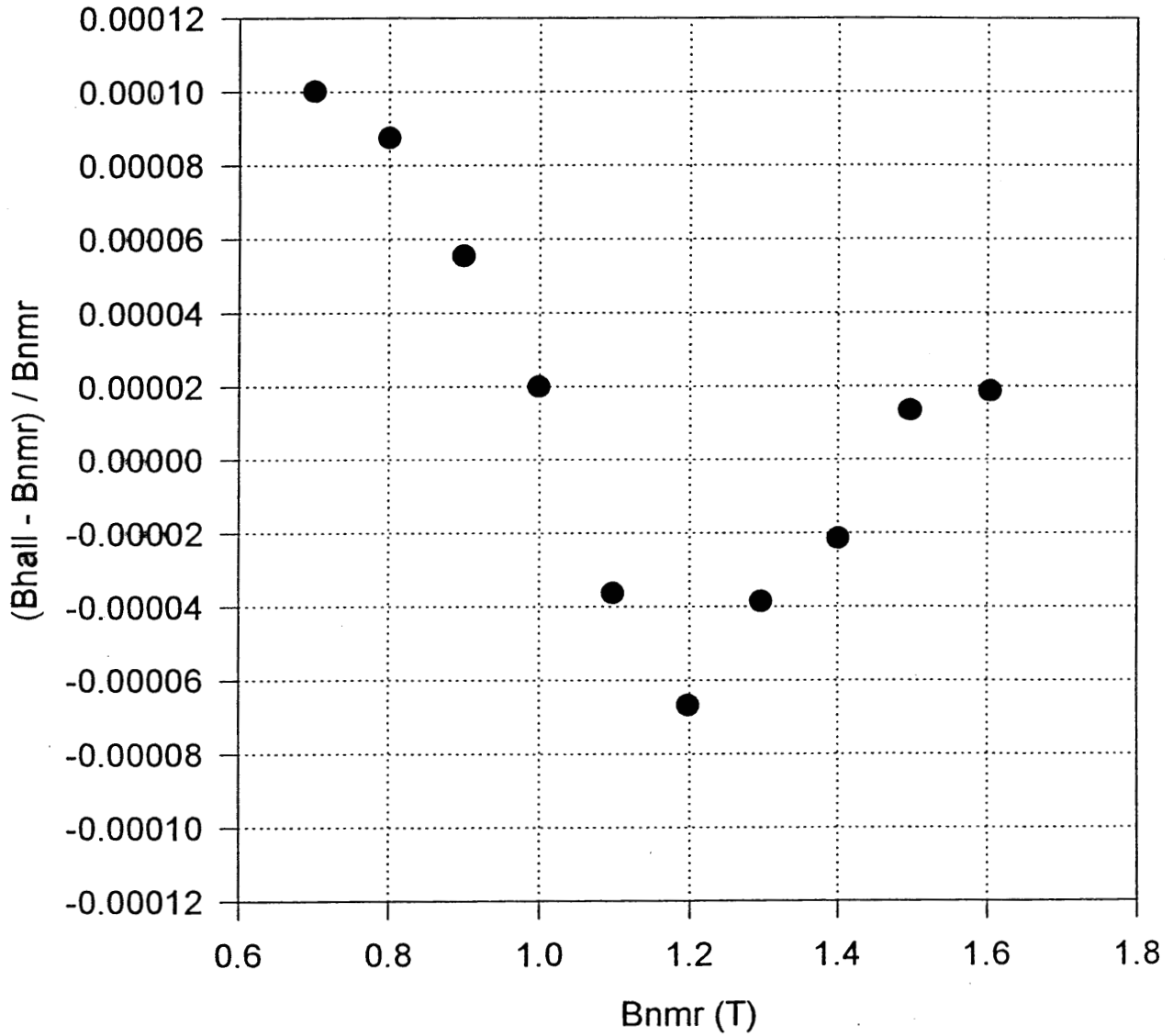
(Also, there is a cost savings in the analog voltage output.)

Sentron Hall Probe B_r vs B_z



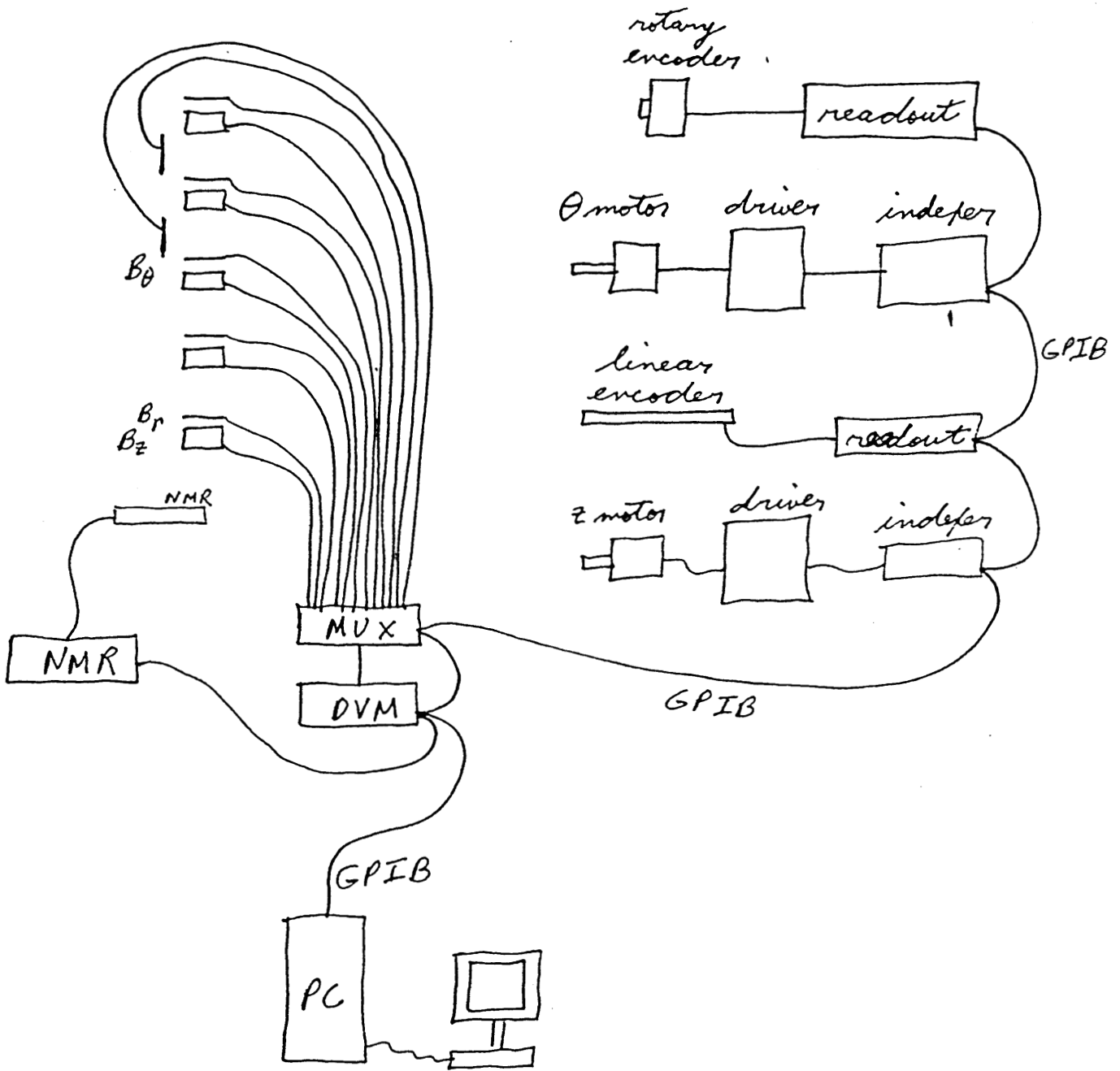
The B_r probes could be aligned at 1 kG and only give a 1.3 G error at 1.5 T. (Very small planar Hall effect.)

Sentron Hall Probe 10^{-4} Probe Accuracy



This Sentron probe was within its specified accuracy.

Data Acquisition System



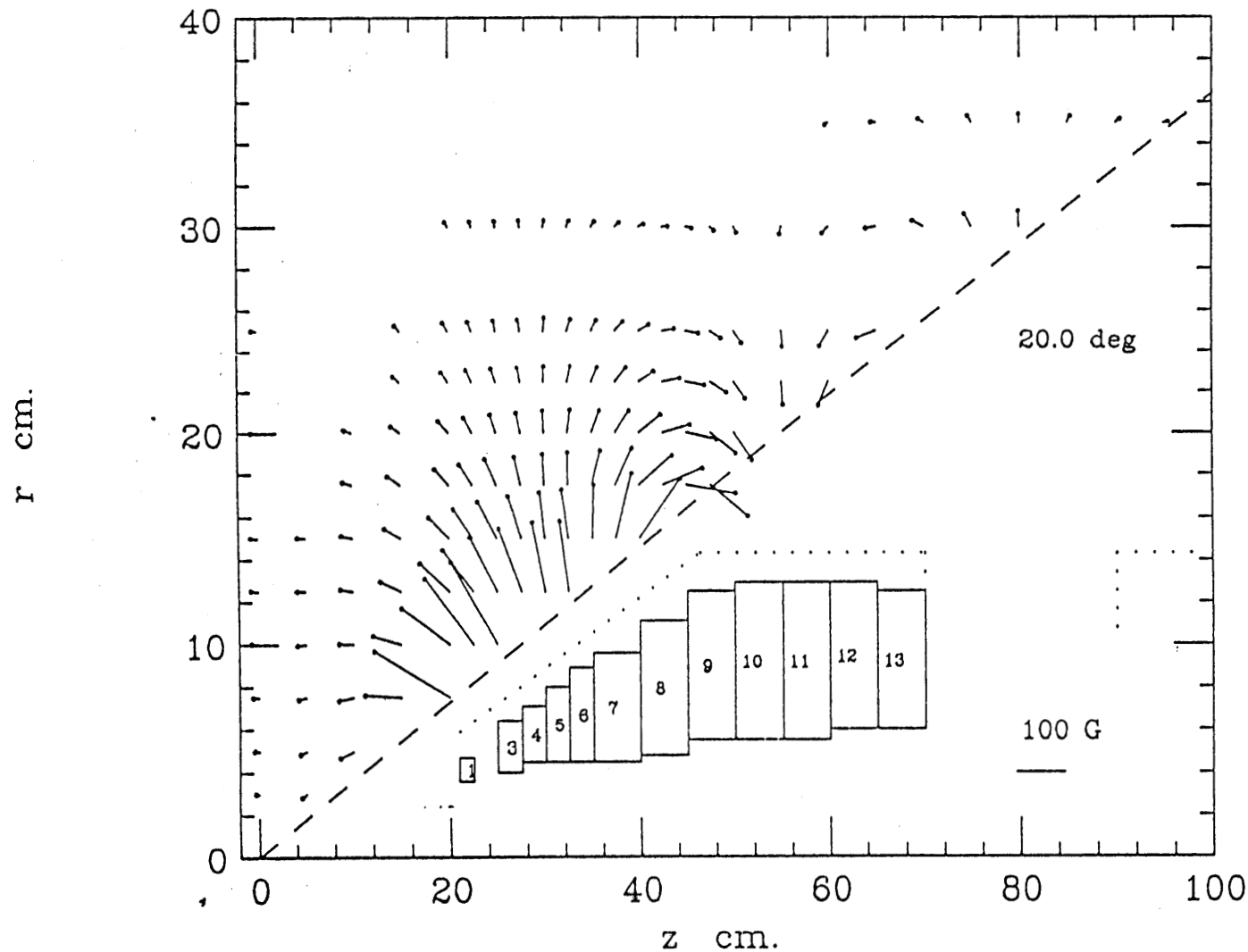
Additional signals (i.e. temperature, magnet current, ...) can go to the multiplexer.

Babar Solenoid Field Map Summary

In the end we got a successful field map, but...

- 1) The cantilevered arm approach required a lot of alignment time.
- 2) A couple Sentron probes broke before we started. Sentron provided support and gave us a loaner probe to use.
- 3) Several Sentron probes drifted during the map. It was important to move to the same location and take repeatable measurements at the beginning of each run.
- 4) A Group 3 backup probe drifted during the measurements.

Fwd. B1 (bz,br) for $\phi = -90$ deg.



The fields from the IR magnets need to be included in the total field in the tracking volume.

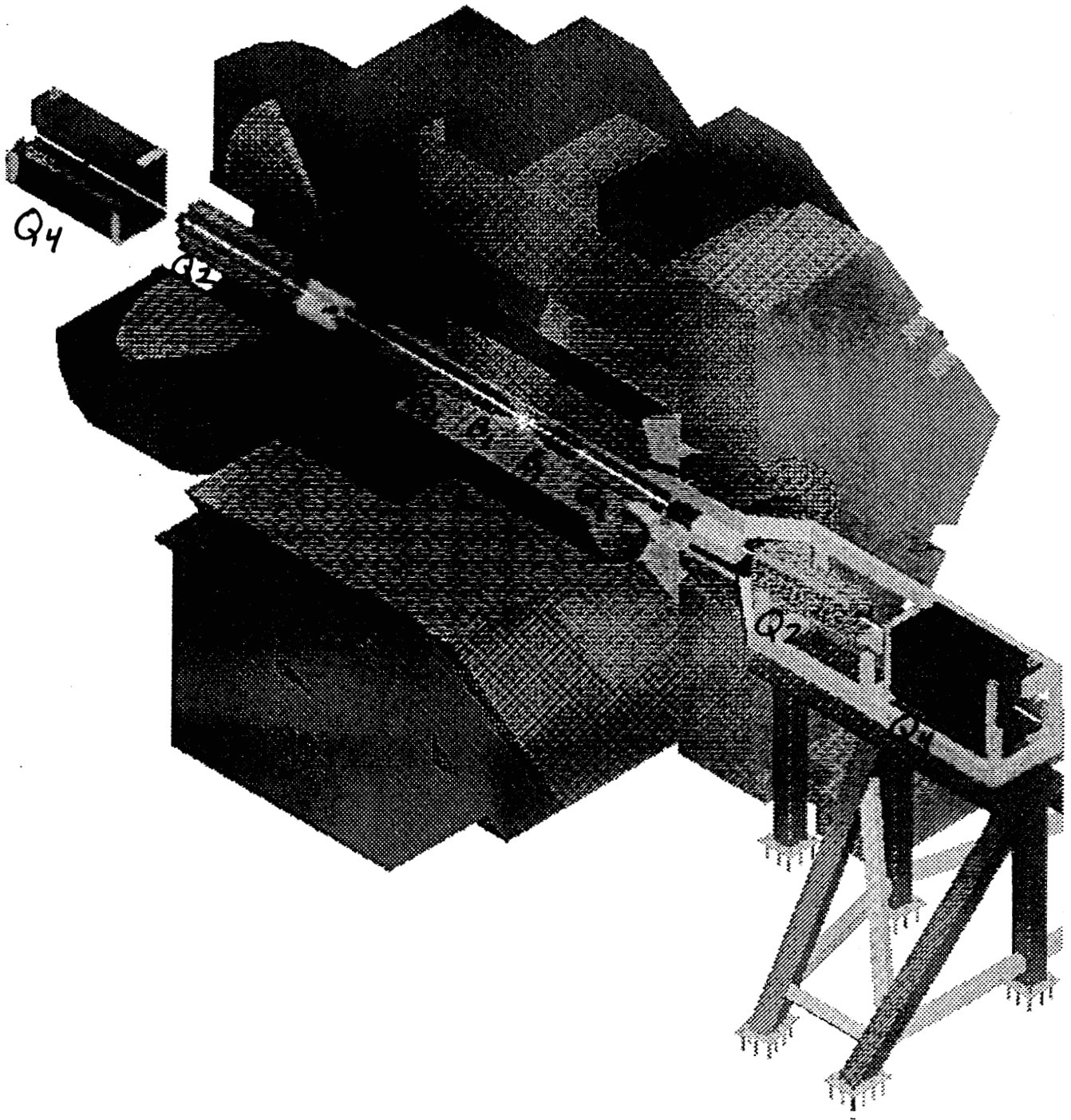
This required another field map.

Part II

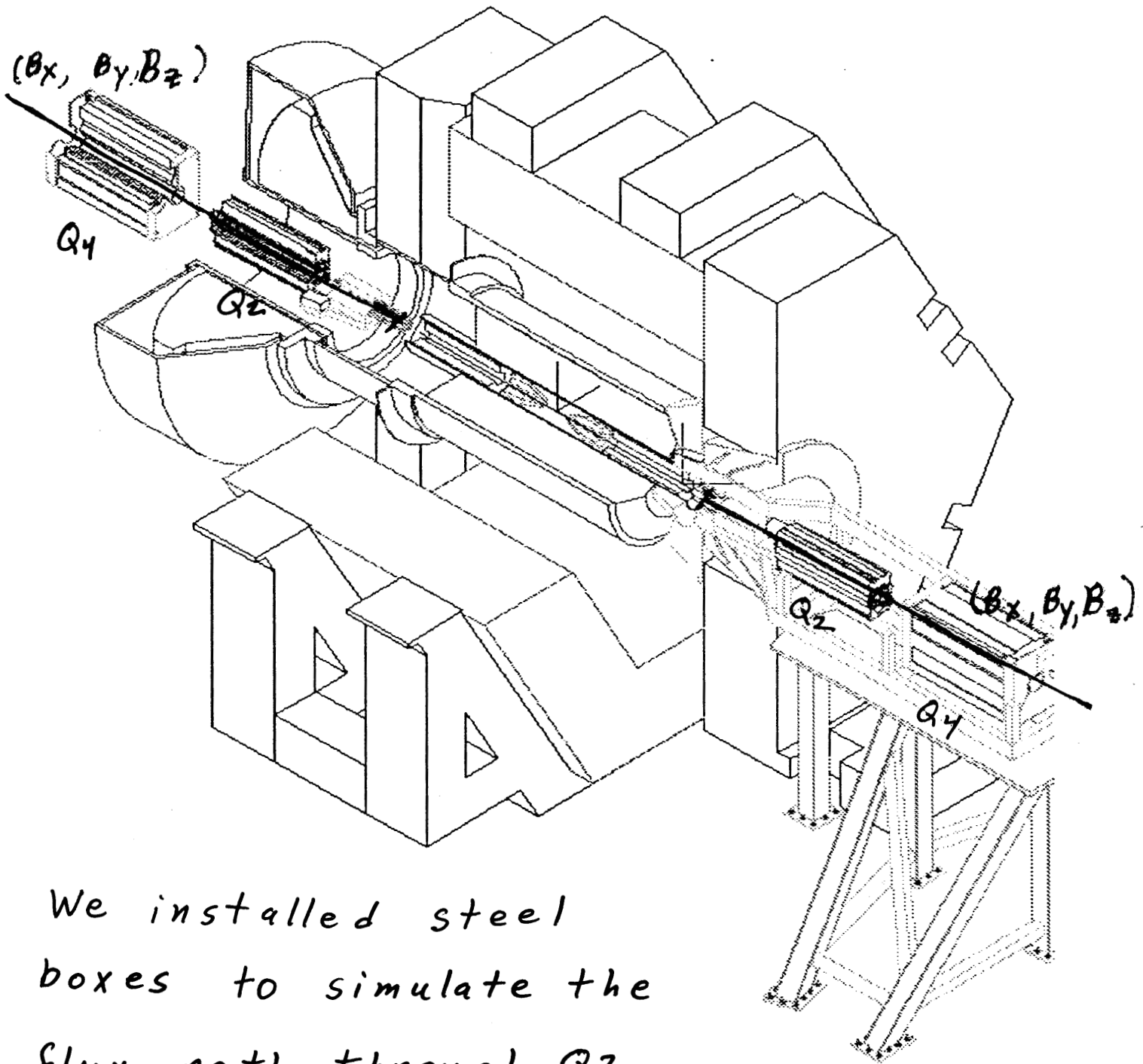
The effect of the solenoid on the accelerator needs to be determined.

- 1) Map \bar{B}_\perp along the beam in the end plug region. Dummy magnets were constructed and put in place to simulate the final configuration.
- 2) The solenoid field creates a skew octupole in an iron quadrupole. This needed to be characterized and corrected.
- 3) The solenoid field affects the permanent magnet IR magnets. This needs to be characterized. (Done in a different talk.)

PEP II IR Region and Babar

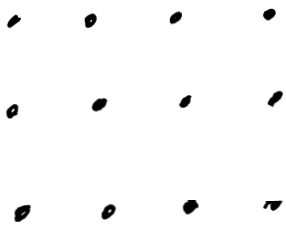
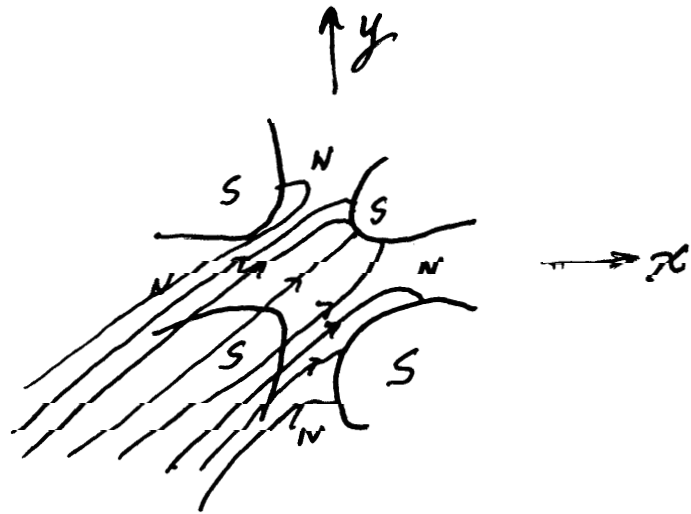


Measure B_{\perp} Along The Beams

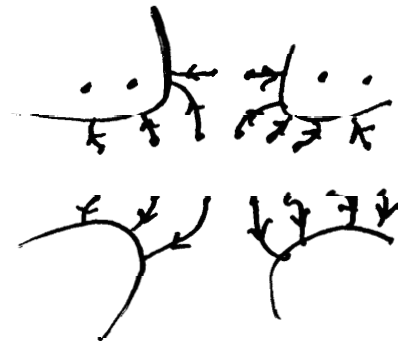


We installed steel boxes to simulate the flux path through Q2 and Q4. (The actual magnets were not ready for installation at this point.)

A Solenoid Field Going Into A Quadrupole Makes A Skew Octupole

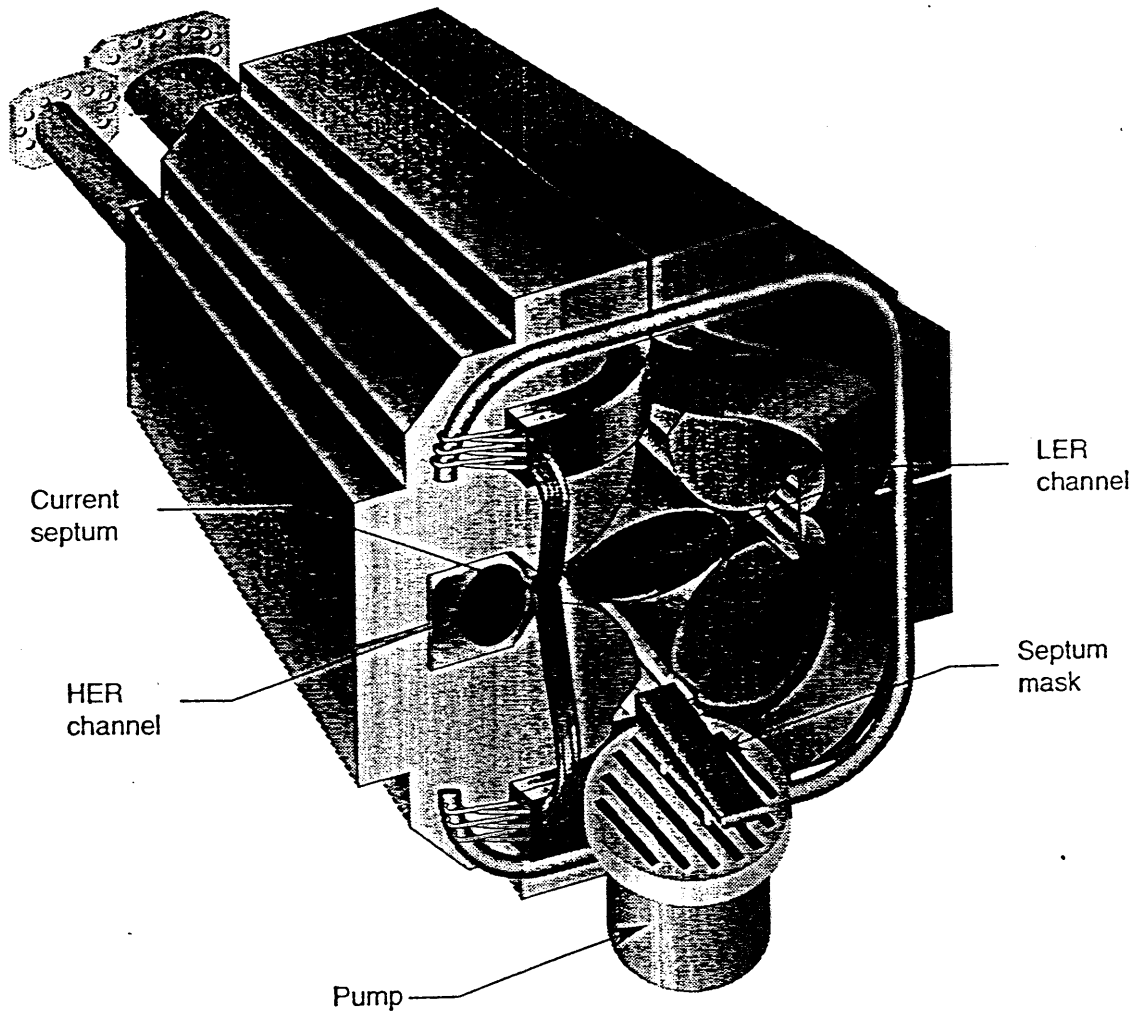


Solenoid Field
End View



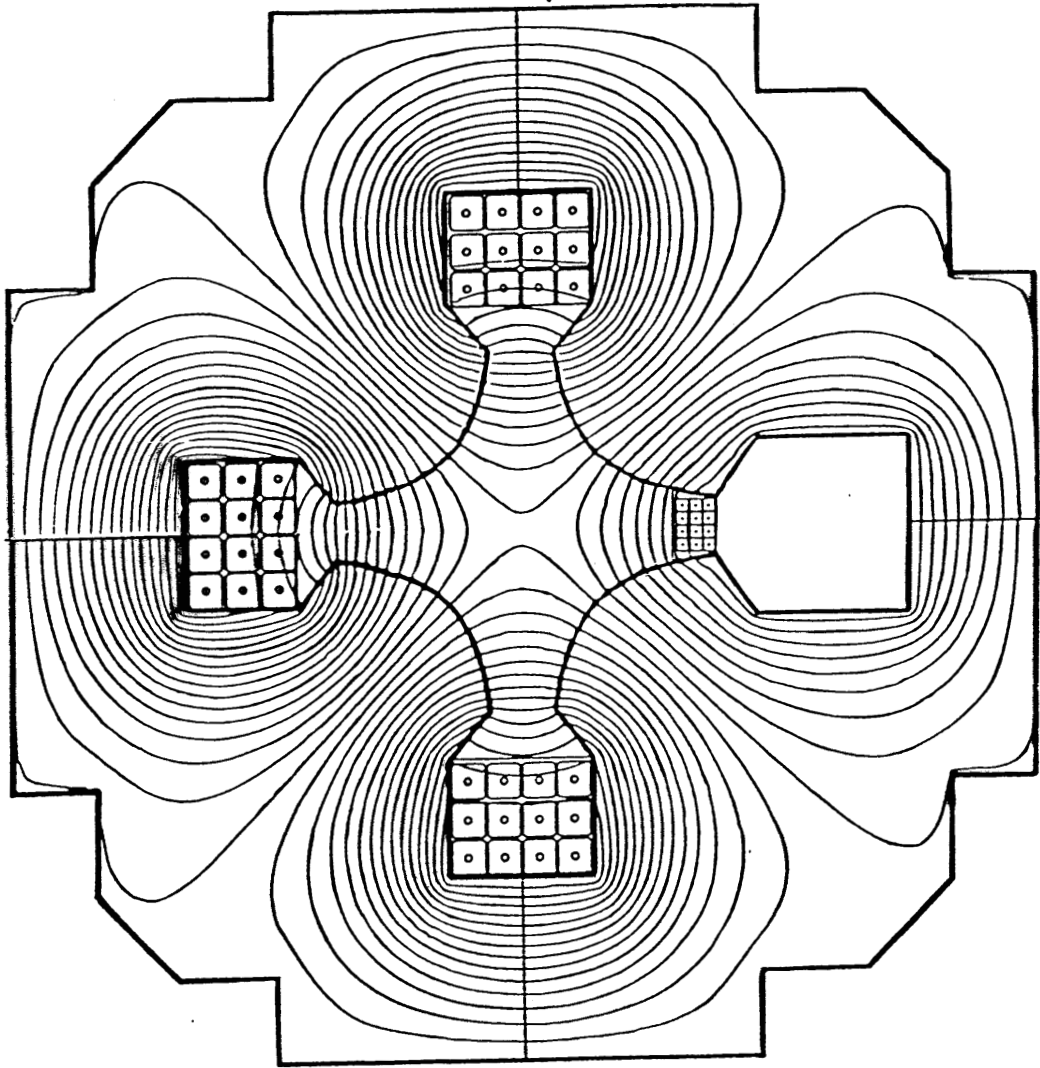
Solenoid Field
With Quadrupole
End View

Q2



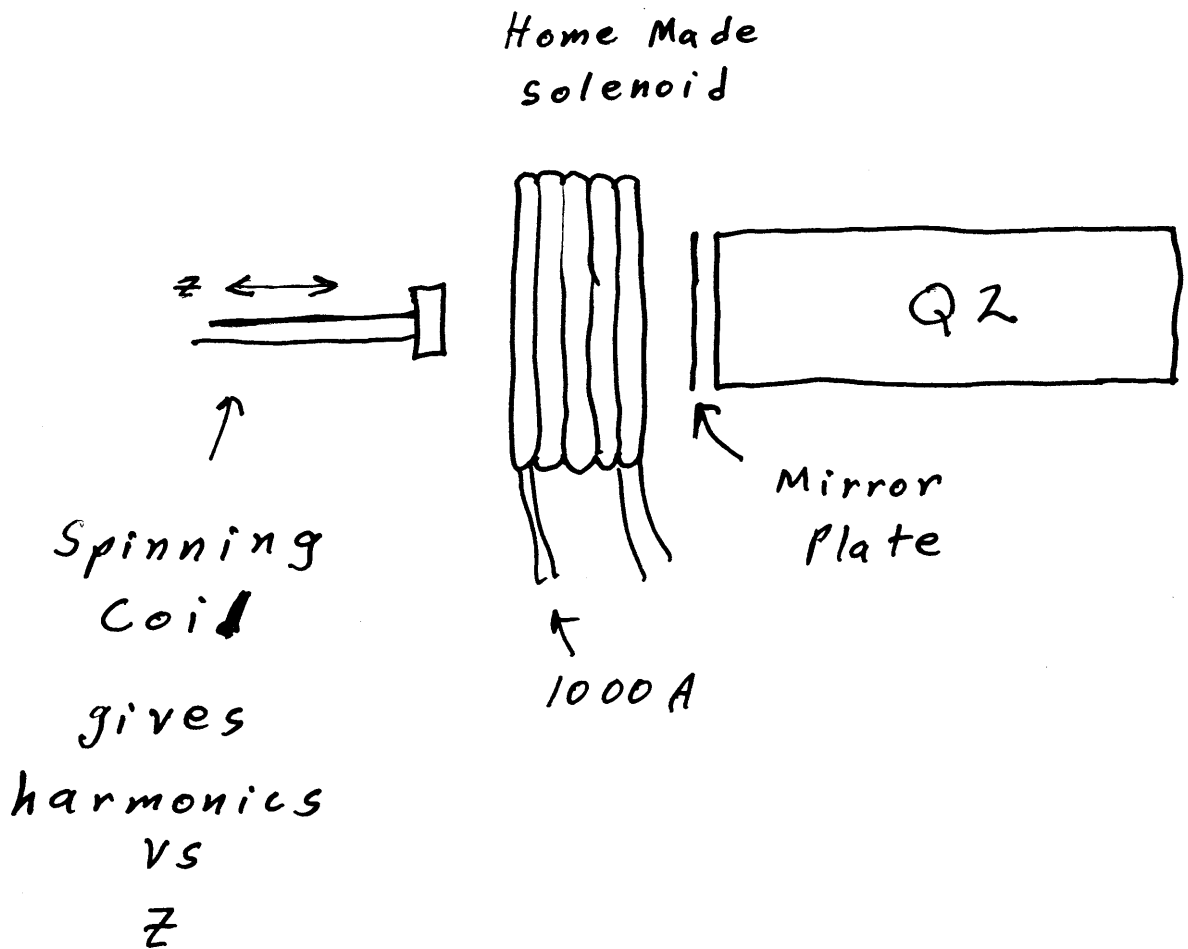
Q2 is a very complicated septum quadrupole. The induced skew octupole just makes things worse.

Q2

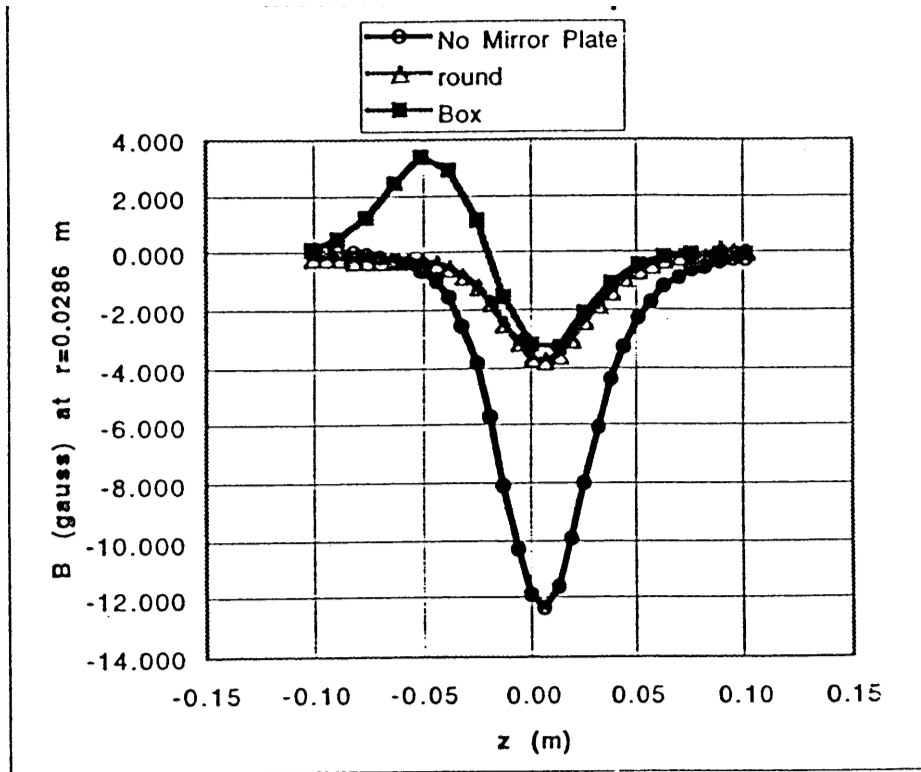


Q2 field pattern

Measure The Induced Skew Octupole In Q2

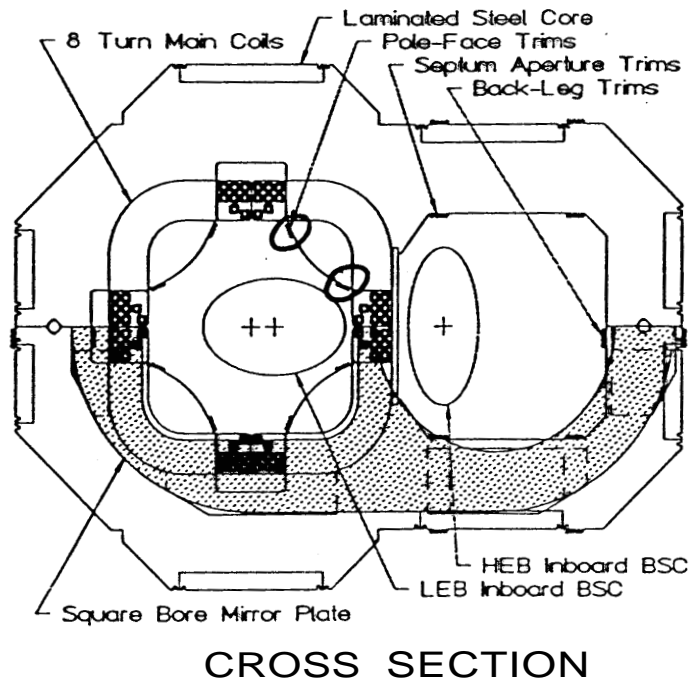


Induced Skew Octupole



The mirror plate was shaped (box) to minimize the integrated induced skew octupole.

Q2



Windings were also added to the poles of Q2 to cancel the induced skew octupole.

EUROPEAN ORGANIZATION FOR NUCLEAR RESEARCH

CERN – SL DIVISION

High Accuracy Field Mappings with a Laser Monitored Travelling Mole

B.Dehning, G.Mugnai, F.Roncarolo

Abstract

The LEP spectrometer is an alternative method adopted to predict the LEP beam Energy. A bending magnet is flanked on either side by three beam position monitors (BPM) used to determine the deflection angle of the beam. This angle, together with the integral of the magnetic field along the beam trajectory, allows the calculation of the beam energy. In order to reach the desired accuracy on the energy a relative precision of a few 10^{-5} on the magnetic field integral is necessary. The magnet is a full-iron core dipole, 5.75 m long, of the MBI type used in the LEP injection region. It has been specially designed in order to have high field uniformity.

Geneva, Switzerland

October 21, 1999

1 Introduction

The beam energy calibration at LEP 2 is based on an extrapolation method. The very accurate resonant depolarisation (RD) [4] procedure measures the LEP beam energies up to 60 GeV [3], with a relative accuracy of less than $1 \cdot 10^{-5}$. Sixteen NMR probes distributed in fixed locations along the bending magnets are calibrated at each beam energy point measured with the RD method.

When the particle beams are colliding at physics energies ($\approx 100 \text{ GeV}$ in 1999) the energy is predicted via a linear extrapolation from the NMR readings.

A similar calibration is done between the same NMRs and the LEP flux-loop measurements. A loop covering the cross section of the dipole field has been placed inside the LEP dipoles. The voltage induced in this loop while cycling the magnets provides a measurement of the field integral.

The beam energy model is rather complex and takes into account several correction factors such as the “train effect” [1], orbit changes due to earth tides [7], and field changes due to thermal effects. The error estimate on the LEP beam energies during the 1998 run is 25 MeV, corresponding to a relative error $\approx 2.5 \cdot 10^{-4}$.

Further information about the beam energy calibration at LEP is included in [5] and [6].

The LEP spectrometer has been conceived to be an alternative method for the beam energy determination, providing a *direct* energy measurement. The concept consists in detecting the change in the bending angle θ through the beam position monitors (BPM) and evaluating the total integral B-field seen by the particles while travelling inside the spectrometer magnet (see Fig. 1). The beam energy is then calculated, being

$$\Delta\theta \propto \frac{\int_L B dl}{E_{beam}} \quad (1)$$

2 Measurement Requirements

The LEP beam energy calibration goal is to keep the error smaller than $1 \cdot 10^{-4}$. Considering the beam position measurements and the total integral field evaluation to be linearly independent, the single errors add quadratically. This leads to the requirement of an error

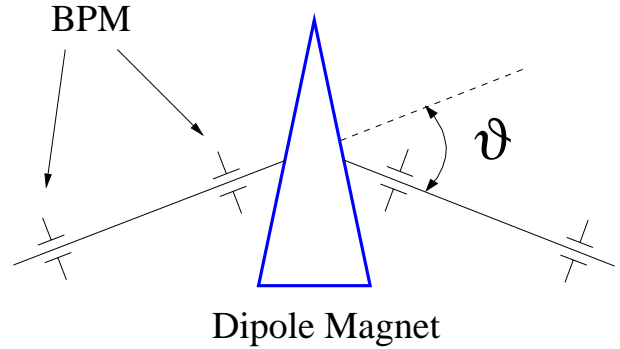


Fig. 1: LEP Spectrometer schematic layout

in the field mappings not larger than $3 \cdot 10^{-5}$.

The total integral field seen by the particles along the magnet is evaluated during the LEP operation by reading the field in four fixed locations. The aim of the mapping was the estimation of the total integral by sampling

$$\frac{\Delta \int B dl}{\int B dl} = f(B_{ref}) \quad (2)$$

and outline its possible changes with environmental conditions. For this reason a first series of maps have been carried out in the laboratory scanning different temperature levels and magnet conditioning.

The “mole” measurements were performed as a cross check and above all to investigate possible changes due to the magnet transportation in the LEP tunnel and the final spectrometer alignment and setup (insertion of the vacuum chamber, etc ...).

The mapping has the aim of estimating the total integral by sampling the local B-field and approximating the integral with a sum:

$$\int_{s_1}^{s_2} B(s) ds \approx \sum_{i=1}^N B_i \cdot \delta s_i \quad (3)$$

3 Measurement Setup Overview

The system has been developed to be accurate in the *length* and *field* measurement as well as transportable (laboratory-LEP tunnel) without compromising the reproducibility.

In Fig. 7 a general overview of the measurement set up is shown and the main elements are:

- the mapping mole sliding inside the beam pipe inserted in the dipole gap; two NMR probes and a search coil are installed on the mole as field monitors.
- the laser interferometer pointing to the retroreflector mounted on the mole;
- the digital integrator which processes the signal induced on the coil. (Rack)
- the acquisition system (also in the rack), including the NMR teslameters, a DAC introduced to compensate the integrator drift and the OS-9 CPU used as interface between the instruments and the Unix based data storage.

4 Reference Probes

The positioning of the four reference NMR probes has been carefully studied by scanning locally the B-field, in the region between the dipole lower pole and the beam pipe. A device able to move an NMR probe in the three dimensions in a small region has been used and an example of the field behavior is shown in Fig. 2.

The reference NMRs have been placed following such analysis, choosing four locations where the field has the smallest gradients in all directions ($\text{dB/B} ; 10^{-5} \text{ mm}^{-1}$). In such a way the error due to possible small misplacements of the probes after their removal and/or substitution (during all the spectrometer operation) is negligible. After choosing the optimal locations, some special supports have been designed and mounted in order to guarantee a high precision of every probe's repositioning, since for the aim of the spectrometer project as a whole it is important to monitor the local field always at the same locations.

Among the other components, a small variable ferromagnetic capacitor is inserted in the probes body, to allow the auto-tuning of the instrument around the resonance signal. Interference between two NMR probes has been observed when the head of one probe is less than 10 cm away from the body of the other probe.

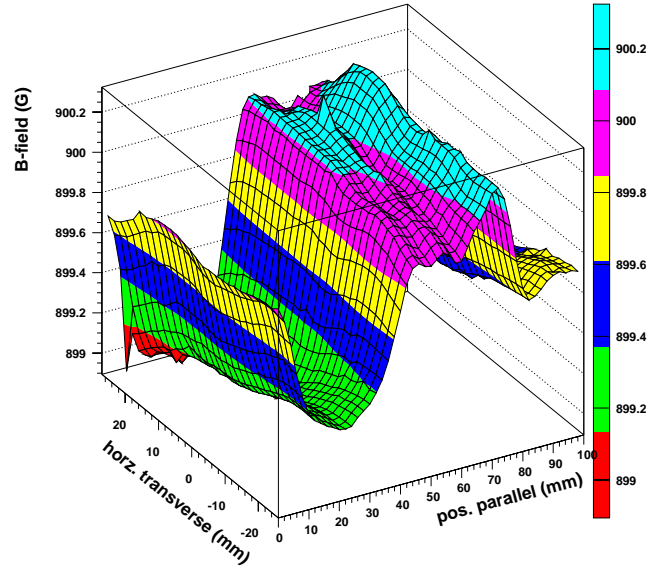


Fig. 2: Example of the local field monitoring around the reference NMR probes: the B-field is scanned at different horizontal positions for 100 mm in the longitudinal direction.

Such was the case during the LEP spectrometer magnet mapping, every time that the movable probes were passing by the fixed ones (see Fig. 3).

During the data analysis average values of the reference probes were calculated, not taking into account the peaks due to the aforementioned disturbances.

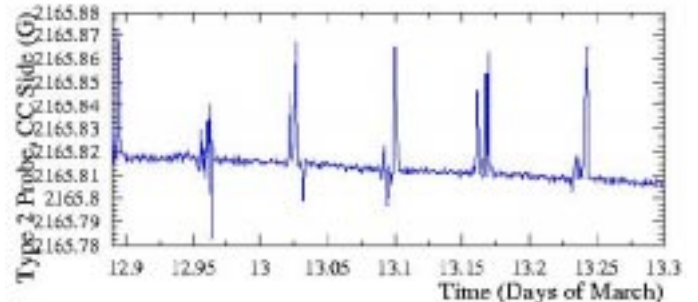


Fig. 3: In the readings of the reference probes it is possible to distinguish the peaks (one for each map) due to the interference between the movable and fixed probe.

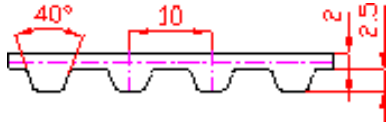


Fig. 4: Profile of the toothed belt used to pull the mole.

5 Mapping Mole

The mapping has been carried out with a mole travelling inside the vacuum chamber. A schematic diagram is shown in Fig. 6. The device has been designed in order to fulfill the requirements on the measurement accuracy. Fully non-magnetic materials have been chosen and basic static-dynamic calculations were executed to guarantee the necessary mechanical stability against stretching and torsion.

Four bronze-beryllium springs are inserted in each of the upper wheels' supports, in order to keep them stably pushed against the vacuum pipe walls. The vacuum chamber in the spectrometer magnet is lifted up by 2 mm from the center of the dipole yoke, in order to guarantee enough space between the lower pole tip and the beam pipe for the four fixed NMR probes. The alignment was carefully studied and the geometry was designed to put the NMR probes and the search coil in the center¹ of the dipole gap, making them slide along the ideal beam trajectory.

Two different views are included in Fig. 5.

The chariot is pulled by a toothed belt driven by a stepping motor. The belt has been chosen to have good elastic properties and stable behavior in time and temperature changes. A special internal structure in kevlar (non magnetic) was preferred to the standard steel one. The profile of the belt is illustrated in Fig. 4. The two ends of the belt are clamped at the extremities of the mole and two pulleys (one fixed on the stepping motor axis) are mounted externally to the vacuum chamber to make the belt turn and close the loop.

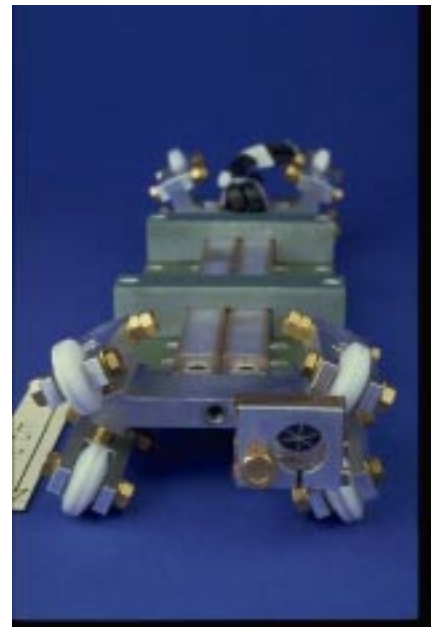
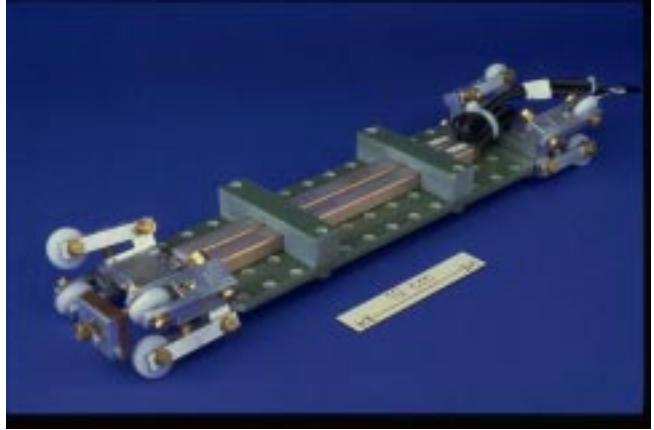


Fig. 5: Two pictures of the mapping mole.

¹More precisely: the two NMR probes are in the vertical center and symmetrically positioned with respect to the horizontal center.

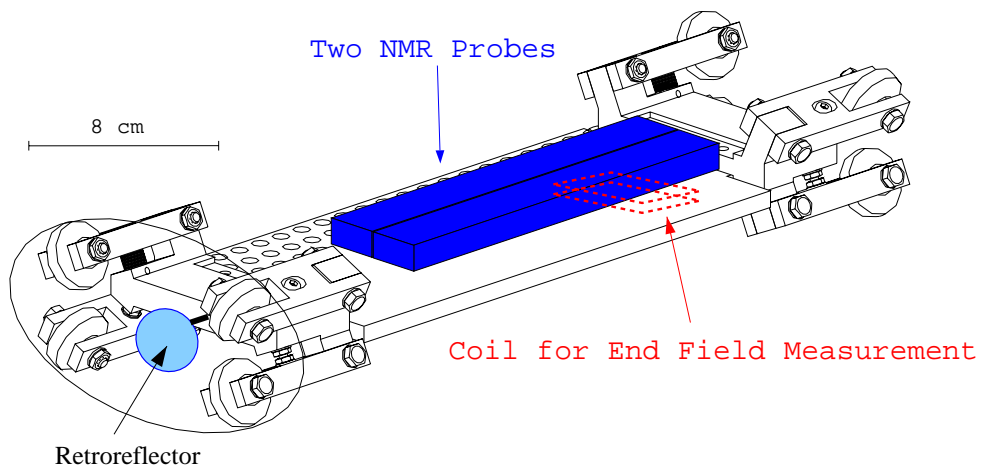


Fig. 6: Schematic diagram of the mole.

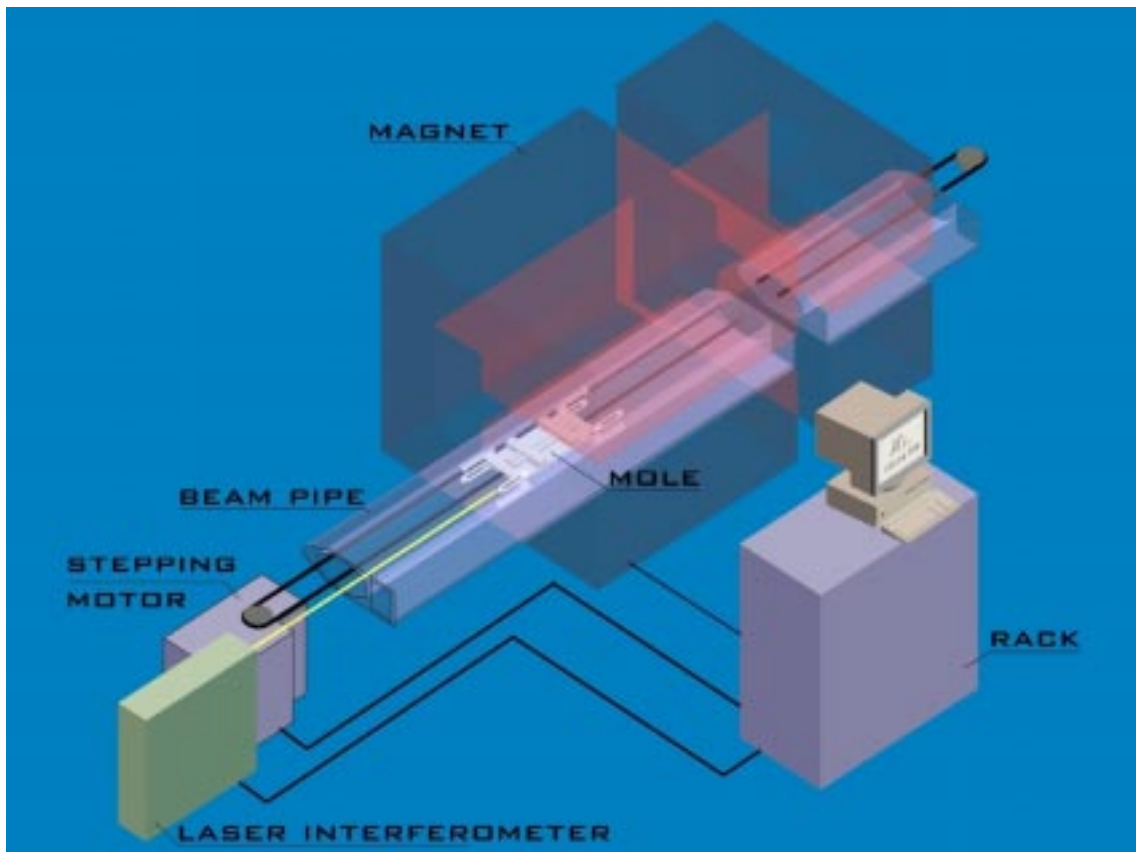


Fig. 7: Set up overview

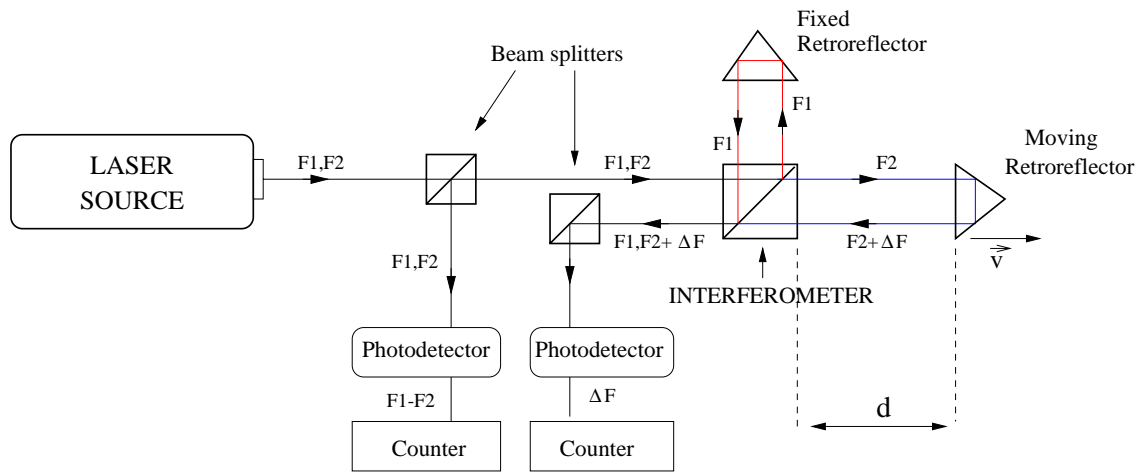


Fig. 8: Laser interferometer diagram.

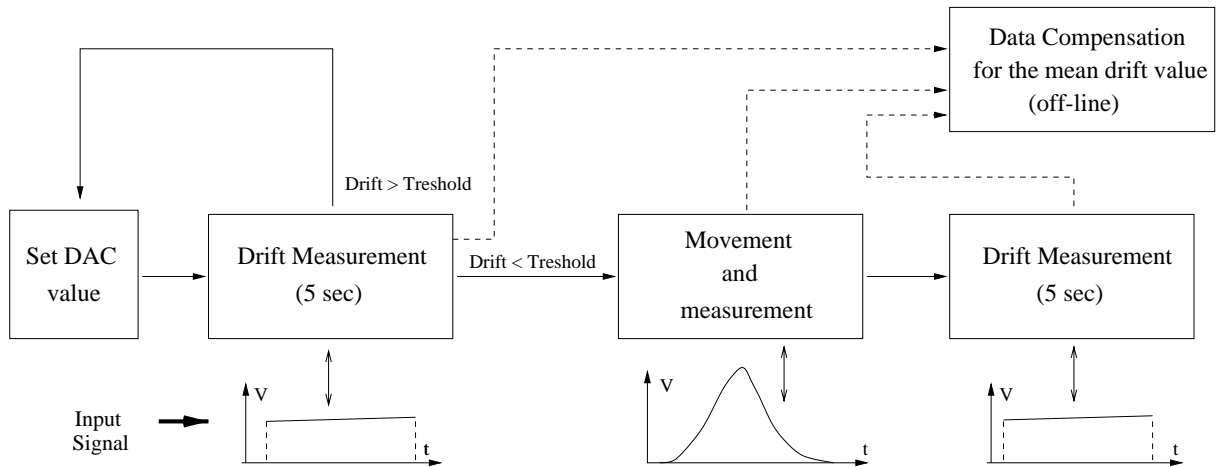


Fig. 9: Diagram of the drift-compensation cycle.

6 Displacement Measuring Interferometer

An accurate position monitoring is needed to evaluate the total integral field according to Eq. 3. For this purpose a laser source was adopted in order to perform a linear interferometer distance measurement. The diagram of the system is shown in Fig. 8.

The laser tube uses a helium-neon source which emits light with a well known and stable wavelength ($\lambda = 632.8$ nm). The beam passes through a magnetic field created inside the laser head to split the light into two frequencies (F_1 with right circular polarisation and F_2 with left circular polarisation) via the *Zeeman effect*. The difference between the two frequencies is about 2 MHz and the tube cavity is tuned in order to have equal intensity for the two components. The light beam passes through two plates which convert the polarisation of the two components from right and left circular to linear horizontal and vertical. At this point the beam has a diameter of 1 mm and travels through a telescope collimator which expands it. An aperture at the output of the tube restricts the beam diameter to ≈ 7.6 mm.

A first beam splitter deflects about 20% of the light to a reference detector. Within this detector another splitter divides the beam into two parts each of them containing both the frequencies. The *reference frequency* $F_1 - F_2$ is produced when F_1 and F_2 interfere. The outputs of the photo-detectors have a frequency $F_1 - F_2 \approx 2$ MHz; the DC component is used to send the *lock signal*², while the AC component is used to develop the *reference signal*.

The main light beam is transmitted to the interferometer, where a polarising beam splitter allows one frequency component (F_2) to pass whilst the other one (F_1) is deflected by 90 degrees. One of the two reflectors after the interferometer (see Fig. 8) is fixed and the beam is reflected with same frequency (F_1) which is used as reference. The other one is moving with a velocity v away from (or towards) the interferometer and the returning beam has thus a Doppler shifted frequency

$$F_2^I = F_2 \left(1 + \frac{v}{c}\right) = F_2 + F_2 \frac{v}{c}. \quad (4)$$

The two light beams recombine again in the interferometer and go back to the main unit, where it is elab-

orated by a Doppler detector. Within the detector the signal is optically demodulated and sent to a photo-detector whose output (*Doppler shifted signal*) has the frequency

$$\Delta F = F_1 - F_2^I = F_1 - F_2 - F_2 \frac{v}{c} \quad (5)$$

The reference and Doppler shifted signals are converted into logical pulses and sent to two different counters. Each counter stores in a register the number of wavelengths, of frequency $F_1 - F_2$ and ΔF respectively. Analytically the signal processing is the following:

- the reference detector determines the number of wavelengths of the signal with frequency $F_1 - F_2$ over a time period Δt :

$$\int_{\Delta t} (F_1 - F_2) dt = N_{F_1 - F_2}^{\Delta t} \quad (6)$$

- the second detector processes the return beam of frequency $\Delta F = F_1 - F_2^I$, counting the number of wavelengths over the same period Δt :

$$\begin{aligned} \int_{\Delta t} \left(F_1 - F_2 - F_2 \frac{v}{c}\right) dt &= \\ &= N_{F_1 - F_2}^{\Delta t} - \frac{F_2}{c} \int_{\Delta t} v dt \end{aligned} \quad (7)$$

- the difference between the right-hand parts of Eq. 6 and Eq. 7 is computed as:

$$\begin{aligned} \Delta N &= N_{F_1 - F_2}^{\Delta t} - \left(N_{F_1 - F_2}^{\Delta t} - \frac{F_2}{c} \int_{\Delta t} v dt\right) = \\ &= \frac{F_2}{c} \int_{\Delta t} v dt \end{aligned} \quad (8)$$

- the velocity can be expressed as $v = dL/dt$ and Eq. 8 becomes:

$$\Delta N = \frac{F_2}{c} \int_{\Delta t} \frac{dL}{dt} dt = \frac{F_2}{c} \cdot L_{\Delta t} \quad (9)$$

The relative displacement of the retroreflector during the period Δt is thus:

$$L_{\Delta t} = \frac{c}{F_2} \Delta N = \lambda_2^{vac} \Delta N \quad (10)$$

where ΔN is the the difference of the values stored in the two internal registers and λ_2^{vac} is beam light wavelength in vacuum (for non vacuum environments see section 6.1).

²This means that the instrument is ready to be read.

6.1 Error analysis

Unless the measurement is performed in vacuum the beam light wavelength has to be corrected for the index of refraction of air ($\lambda \rightarrow \lambda/n_{air}$). The index depends on the temperature, humidity and pressure of the environment where the measurement is performed. For example an increase in the air density (high pressure or low temperature) results in a lower light velocity and thus in a smaller laser beam light wavelength. Eq. 10 becomes:

$$L_{\Delta t} = \frac{\lambda_2^{vac}}{n_{air}} \Delta N \quad (11)$$

On the instrument adopted for this set of measurements the value of the index of refraction of air (which can be expressed also like $n_{air} = c/w = \lambda_{vac}/\lambda_{air}$, being w the velocity of light in air [10]) can be changed through a set of thumb-wheels located on the display unit.

The resolution of the instrument is 10 nm and the firm providing the laser source (HP) gives the following values for the accuracy [10]:

- 1 ppm/ $^{\circ}C$
- 1 ppm/2.8 mm Hg
- 1 ppm/90 %change in rel. humidity

Further information about the error analysis is included in [11].

7 Magnetic Field Monitors

The aim of a mapping is to evaluate the total integral magnetic field characteristic of a magnet, including the fringe regions where the field decreases to zero. In order to guarantee the zero-field conditions outside the magnet, the portions of vacuum chamber located around half a meter away from the magnet faces have been wrapped with a μ -metal material used to screen the external electromagnetic fields.

The field in the dipole core is around two times the field in the iron-concrete LEP bending dipoles:

$$\begin{aligned} E_b = 22 \text{ GeV} & \Rightarrow B \approx 0.047 \text{ T} \\ E_b = 100 \text{ GeV} & \Rightarrow B \approx 0.222 \text{ T} \end{aligned}$$

7.1 Central Region and Reference Probes

The NMR probes adopted (Metrolab Probe Head 1072, Range Type 1 and Range Type 2) cover magnetic fields between 0.043 and 0.026 T. The resolution is $1 \cdot 10^{-7}$ T (or 1 Hz). The guaranteed accuracy is better than ± 5 ppm and the relative accuracy better than ± 0.1 ppm in uniform fields [9]. Three teslameters (Metrolab PT2025) and three multiplexers have been used, dividing the NMR probes on the three instruments:

- fixed NMRs type 1;
- fixed NMRs type 2;
- movable NMRs (type 1).

The reference probes of the same range have been read via a multiplexer in order to avoid possible interference when two Teslameters operates almost at the same frequency.

7.2 End Field Region

In order to cover the field range not covered by the NMR probes a search coil has been installed on the mole. The coil was realized at CERN and is made of about one thousand turns around a rectangular frame (2.5×1 cm).

The motion of the mole in the end field region, where the field gradient is high enough, induces a voltage between the coil terminals, being (for each step):

$$\Phi = \frac{\Delta B}{A} \quad (12)$$

where Φ is the flux, ΔB the field change between two locations and A the coil area. An example of the signal detected during one step is shown in Fig. 10.

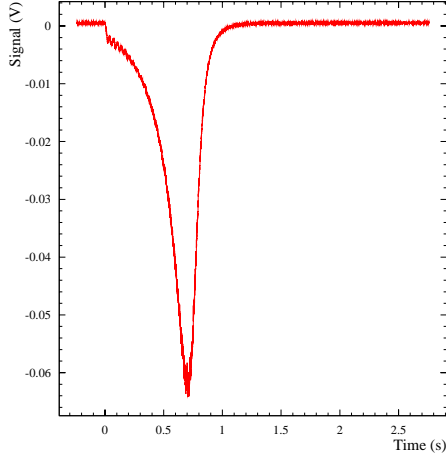


Fig. 10: Voltage induced on the search coil

8 Magnet Conditioning

Before every ramp a *degaussing cycle* was performed and once the nominal energy for the map was reached, a cycle of *bending modulation* was done. Both procedures, plus the ramp to the nominal energy followed the standard LEP operation:

- Degaussing Cycle
 $25\text{ A} \rightarrow 500\text{ A} \rightarrow 25\text{ A}$ for five times at a ramp speed of 50 A/s .
- Ramp
 $25\text{ A} \rightarrow I_{nominal}$ at a ramp speed of 2.3 A/s
- Bending Modulation
 $I_{nominal} \rightarrow I_{nominal}(1+0.03\%) \rightarrow I_{nominal}$
for 7 times at a ramp speed of 2.3 A/s

The bending modulation consists of a conditioning cycle, applied to improve the stability of the actual working point [2]. After such repeated excitation, in case of a variation in the power supply or any change in the excitation current, the magnetic field has a significant smaller jump (Fig. 11). In fact it happens that after the first small increase of the current during the bending modulation, the magnetic field increases by a relative amount of the order of $5 \cdot 10^{-5}$, much less for the following cycles and reaches a saturation after the seventh cycle. The phenomenon is displayed in Fig. 11.

9 Mapping Procedure

The mapping procedure was based on the following steps:

- Forward direction:

double end field map of the non-connection side with two shifted starting positions;

core map with the two NMR probes;

double end field map of the connection side with two shifted ending positions.

- Symmetric procedure for the backward direction.

Tests in the laboratory showed that it was enough to sample the core end-field every 2 cm to ensure negligible errors in the field integral, compared with a denser sampling.

For the end-region it was found a compromise between sampling-frequency and signal amplitude and, as mentioned above, the procedure foresaw two scans for each map (step size of 1 cm), with the starting point shifted by .5 cm.

The measurement of the coil area (see Eq. 12) has been carried out off-line ramping the magnet with the coil still in dipole core. To reduce the uncertainty, the coil area has been also calibrated on-line after each map, as explained at the end of the next paragraph.

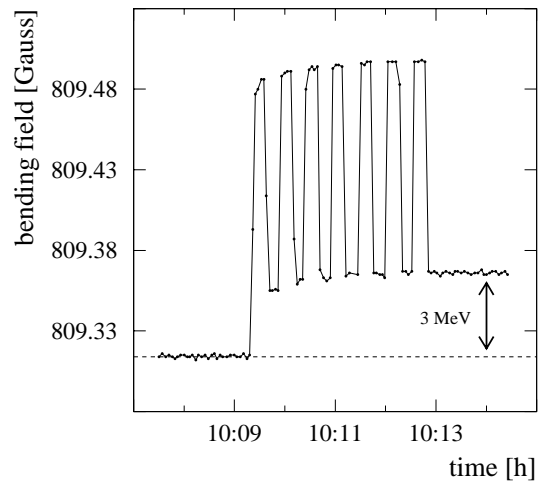


Fig. 11: Effects of the bending modulation treatment, measured on a LEP bending dipole.

Motor Resolver	Integrated Signal [V · s]	Drift after the DAC cycle [V]	Drift after the movement [V]	Initial Position [mm · 10 ⁵]	Final Position [mm · 10 ⁵]
...
5633	0.0008426	0.0000002	0.0000002	114908616.0	115897216.0
5655	0.0010228	0.0000002	0.0000002	115897232.0	116887528.0
5676	0.0012060	0.0000001	-0.0000006	116887568.0	117876392.0
5698	0.0014027	0.0000001	-0.0000013	117876448.0	118870160.0
5720	0.0015800	0.0000002	0.0000008	118870264.0	119855448.0
5741	0.0017901	0.0000001	0.0000001	119855488.0	120849856.0
5764	0.0019837	0.0000000	0.0000009	120849888.0	121839536.0
5786	0.0022223	0.0000001	-0.0000011	121839536.0	122836328.0
5809	0.0024536	-0.0000001	-0.0000001	122836320.0	123825696.0
5832	0.0027356	0.0000000	0.0000004	123825696.0	124816392.0
5856	0.0030329	-0.0000001	-0.0000004	124816352.0	125804672.0
...

Table 1: Example of raw data from the end field map

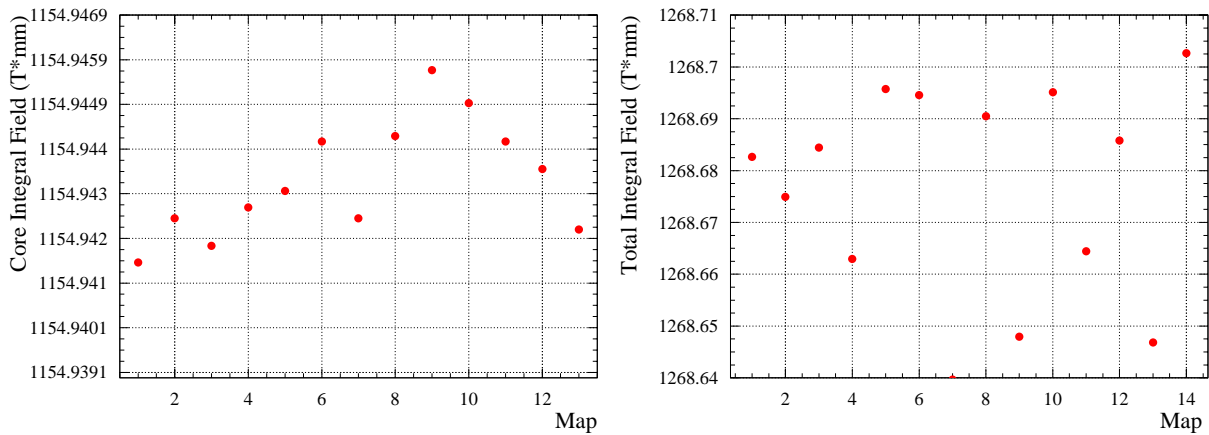


Fig. 12: Core region integrals and total integrals measured in the laboratory

To be independent from the absolute accuracy of the integrator³, a calibration of the system has been performed after every endfield measurement. The field inside the dipole gap (i.e. limit between “central field” and “fringe field”) was in fact precisely known, by the NMR probes installed on the mole. The difference between this value and the “zero field” value was set equal to the integral of the induced coil voltage, divided for the coil area:

$$B_{NMR} - B_0 = \Delta B = \frac{\int u dt}{A} \quad (13)$$

this procedure overcomes all system drifts developing in a time longer than the measurement period (including, for example, possible variation of the coil area).

11 Mapping Results

The travelling mole has been used both in the laboratory and in the LEP tunnel after the transportation of the magnet.

In Fig. 13 an example of the field profile is presented; the central region is measured with two NMR probes.

In Fig. 12 the reproducibility of the system for some maps is given:

- better than $1 \cdot 10^{-5}$ in the central region (NMRs)
- Few 10^{-5} on the total $\int B dl$

The maps displayed are performed at $I=480$ A ($E_{beam}=100$ GeV). They are not all consecutive and no temperature corrections are applied. The only off-line operation is the normalization for the reference probes, necessary to compare maps sometimes realized at slightly different working points.

The last two figures represent a final result for the LEP spectrometer total integral calibration. They include all the maps performed during the calibration, the “arm” measurements in the laboratory, the mole measurements in the laboratory and the mole measurements in the LEP tunnel.

Performing a linear fit of all the maps as function of the reference probes readings and calculating the residuals to the fit itself (Fig. 14), provides an estimate of the error in predicting the total B-field

³ $\frac{\Delta \int u dt}{\int u_{max} dt} = 1 \cdot 10^{-4}$, see [8].

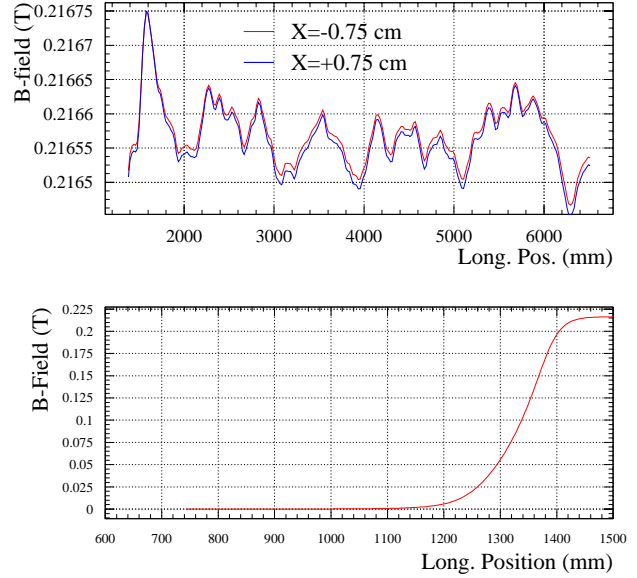


Fig. 13: Core region (top) and end-field (bottom) field profile

integral during the spectrometer operation (reading the reference probes).

More in detail, the main interest will be on the ratio between the integrals at different energies and the quantity

$$\frac{\int B^{E_2} dl}{\int B^{E_1} dl} = \frac{f(B_{ref}^2)}{f(B_{ref}^1)} \quad (14)$$

leads to the estimate of the error without possible systematic energy dependences. Fig. 15 shows this quantity.

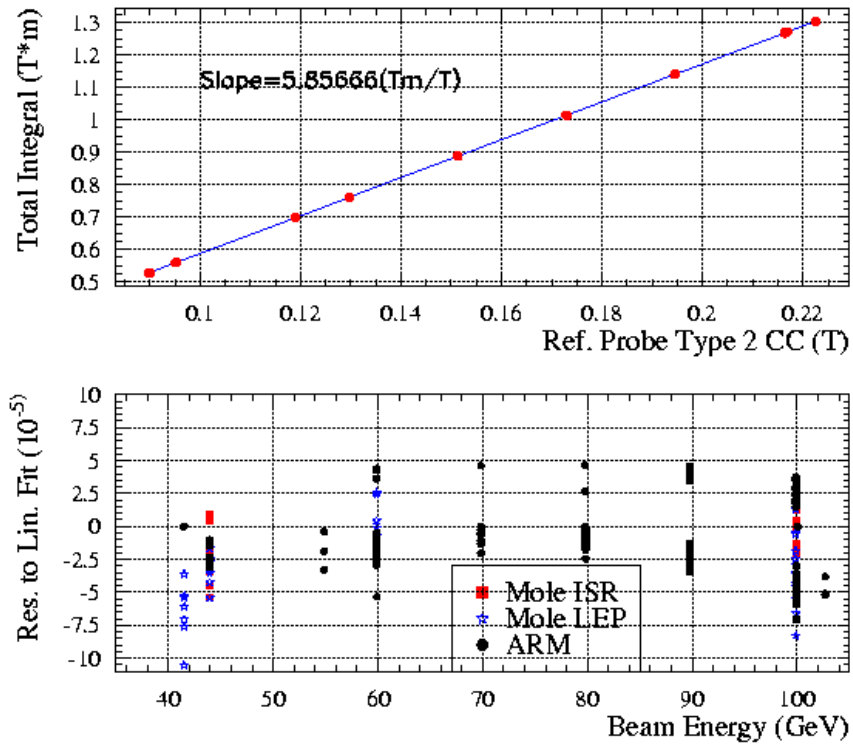


Fig. 14: Linear fit integral vs reference probes and residuals.

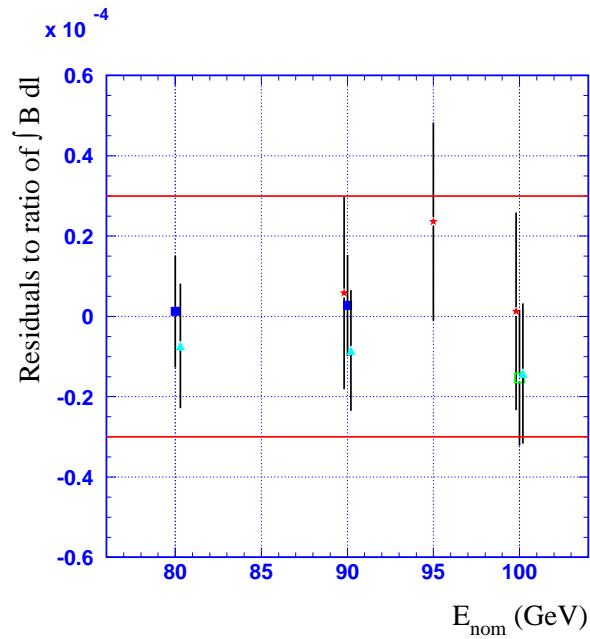


Fig. 15: Error estimate on the integral ratios.

12 Conclusions

The LEP spectrometer dipole magnet has been first mapped in the laboratory with a movable arm carrying an NMR probe and two hall probes for the fringe fields. Such a setup provided a large number of measurements, scanning the different accessible parameters, like the cooling water temperature and slightly different magnet conditioning.

The *Mole* system reached the aim of cross-checking the first method in the laboratory and investigate possible effects of the magnet transportation in the LEP tunnel and any variation in the magnetic field due to the different environmental conditions and the final setup of the LEP spectrometer.

The measurements showed a high reproducibility of the system and the agreement between the two mapping methods gives an estimate of the total integral field with the aimed accuracy of $3 \cdot 10^{-5}$.

13 Acknowledgements

We would like to thank all the people involved in the measurements.

Enrico Bravin has constantly followed up the progress of the work, always being available for discussions and problem-solving.

Several ideas by John Matheson and Jan Prochnow were helpful indeed. Thanks to all the people in the LEP Energy Calibration and Spectrometer Groups, and thanks to G.P.Ferri, who helped us in developing and installing the whole system for the mapping mole.

J.Bilan was very kind in giving us a search coil produced with high accuracy by his group.

References

- [1] Bravin E. et al., CERN, "The Influence of Train Leakage Currents on the LEP Dipole Field", 1997, SL-Note 97-047 BI.
- [2] Galbraith, P. et al., CERN, "Jumps in the Magnetic Field induced by Current Spikes", 1993, CERN SL note/93.
- [3] Assmann R. et al., CERN, "Observation of Radiative Spin-Polarization at 60.6 GeV", Article presented at PAC'99, New York.
- [4] L.Arnaudon et al., CERN, "Accurate determination of the LEP beam energy by resonant depolarisation", 1994, CERN SL/94-71.
- [5] The LEP Energy Working Group, CERN, "Calibration of center-of-mass energies at LEP1 for precise measurements of Z properties", 1998, CERN SL/98-12, CERN-EP/98-40.
- [6] The LEP Energy Working Group, CERN, "Evaluation of the LEP center-of-mass energy above the W-pair production threshold", 1998, CERN SL/98-73, CERN-EP/98-191.
- [7] L.Arnaudon et al., CERN, "Effects of terrestrial tides on the LEP beam energy", 1994, CERN SL/94-07 BI.
- [8] P.Galbraith, CERN, "Portable Digital Integrator", 1993, Note Technique 93-50, AT-MA/PG/fm.
- [9] Metrolab Instruments S.A., "High precision NMR Teslameters", Technical Specifications, Geneva, Also available @ <http://www.metrolab.com>.
- [10] Hewlett Packard, "Laser Measurement System Operator", Operation Manual.
- [11] Federico Roncarolo, Personal home page @ <http://home.cern.ch/froncaro/www/tesi.html>.

Recycler Measurement System

P. Schlabach, Fermilab

- 1) Recycler
- 2) Measurement System
- 3) Problems / Results
- 4) Comments

→ RECYCLER

- 8 GEV STORAGE RING
FOR \bar{P} RECOVERED FROM
TEVATRON
- IN MAIN INJECTOR TUNNEL
ABOVE M.I. MAGNETS
- ALMOST ENTIRELY BUILT
OF PERMANENT MAGNETS

Permanent Magnets at Fermilab

R&D phase (1995-96):

- 1) understand material properties (ferrite & compensator)
 - a. temperature compensation
 - b. uniformity of materials (magnetization, H_c, permeability, ..)
 - c. stability to thermal, temporal, radiation, mechanical effects
- 2) develop manufacturing techniques; built prototype magnets

Magnets for 8 GeV Transfer Line (1996-97):

- * beamline to transport protons from Booster to new Main Injector
- * gain experience with permanent magnet technology
- * magnet factory set up at Bldg MP9
- * built 65 gradients, 45 dipoles, 10 quads to moderate field-quality specs
- * beamline commissioned in 1997

Magnets for Recycler Ring (1997-98):

- * 8 GeV storage ring for recovered p-bars from Collider
- * MP9 factory improvements (include measurement facility)
- * built 500 magnets to storage-ring quality specifications
(372 gradients, 111 quads, 17 specialty magnets)
- * magnet installation in progress
- * project cost \$12.6M

Recycler Ring Permanent Magnet List

<i>magnet</i>	<i># in ring</i>	<i># in beamlines</i>	<i># spares</i>	<i>total</i>	<i>status (as of 24 Aug 98)</i>
<i>gradients</i>					
RGF	108	2	3	113	complete
RGD	106	3	2	111	complete
SGF	64	7	4	75	complete
SGD	64	8	1	73	complete
<i>quadrupoles</i>					
50.8 cm (initial phase)	90	9	0	99	complete
101.6cm	10	0	2	12	in assembly
50.8 cm (upgrade)	32	0	0	32	to do later
<i>other:</i>					
mirror magnets	2	6	4	12	in assembly
Lambertsons	0	5	0	5	complete

Recycler Ring also includes some electromagnets:

trim quads (normal)	9
trim quads (skew)	4
sextupoles	28
trim dipoles (horizontal)	26
trim dipoles (vertical)	26
vertical bends (FMI-RR transfer)	10

Recycler Ring Gradient Magnet Specifications

<i>magnet</i>	<i>pole length (m)</i>	<i>BL (T-m)</i>	<i>gradient, 62 (units @ 2.54 cm)</i>	<i>sextupole, b3(units)</i>
arc focussing (RGF)	4.4958	0.61824	619.74	8.78
arc defocussing (RGD)	4.4958	0.61824	-598.08	-15.1
dispersion suppression, focussing (SGF)	3.0988	0.41216	1275.96	0.0
dispersion suppression, defocussing (SGD)	3.0988	0.41216	-1303.08	0.0

- Recycler MEASUREMENT SYSTEM NOT
A NEW SYSTEM

- NEW HARMONICS TEST STAND^{MEASUREMENT}
A

- ALMOST IDENTICAL TO MAIN
INJECTOR TEST STAND IN
THE FNAL MAGNET TEST
FACILITY

- LOCATED ~ 1 MILE FROM
MTF

- SOME NEW APPARATUS

- FLIPCOIL

- "Z-SCAN"

- ALL SYSTEM WERE INTEGRATED INTO
EXISTING M.I. MEASUREMENT
SCHEME

- BUT REALLY JUST ANOTHER
MAIN INJECTOR TEST STAND



F-0161-0P

Recycler Measurement Apparatus

- FLIP COIL
- Z SCAN SYSTEM
- HARMONICS MEASUREMENT STAND
- SSW

Recycler Gradient Magnet Assembly Strategy

Pre-assembly:

- * magnetize bricks in electromagnet (saturate)
- * prepare compensator packs (mix from different lots)

Assembly:

- * build pole subassembly
- * stack alternately bricks/compensator on flux return plates
- * assemble poles and flux return top, bottom, sides, end plates

Trimming:

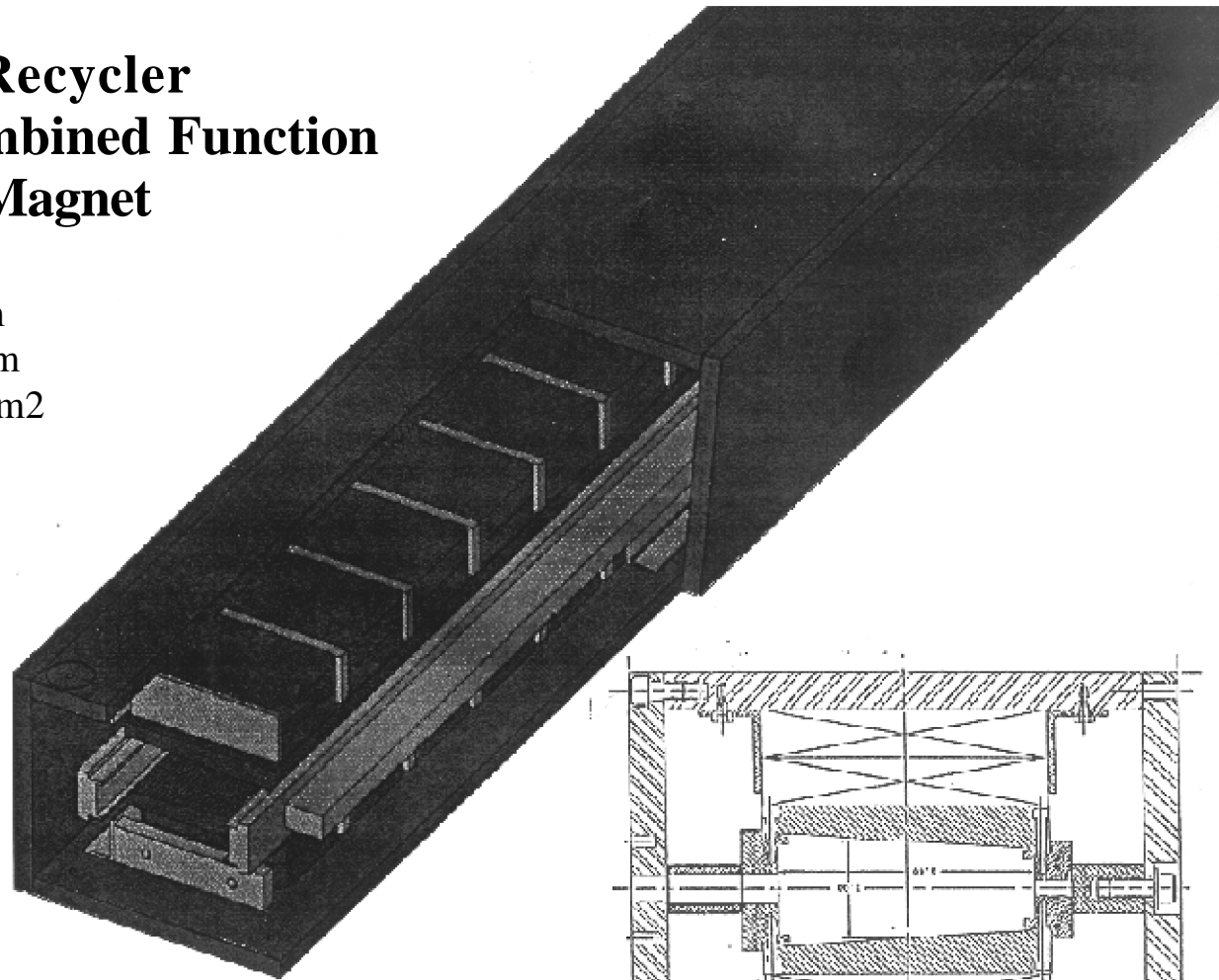
- * measure strength (flipcoil); adjust by adding/subtracting bricks
- * freeze magnet (0 C); measure strength of cold magnet (flipcoil)
- * warm up to room temperature & measure strength again to get compensation; adjust amount of compensator
- * measure longitudinal profile (Hall probe); determine bend center & adjust by brick / compensator redistribution
- * measure harmonics (rotating coil); calculate custom end shim profile.
- * install shims and remeasure harmonics

Production history:

- * began 11/97, complete 7/98: **373** magnets
- * average production rate: **40** magnets/month (2/day)
- * peak rate (Apr 98): **3.6** magnets/day

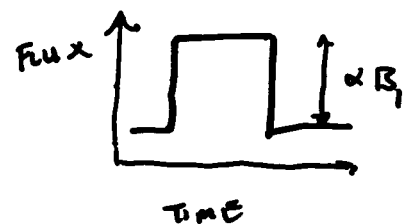
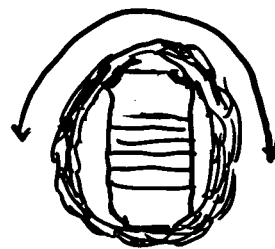
Fermilab Recycler Typical Combined Function Permanent Magnet

L 4.50 m
BL 0.618 T-m
B'L 1.51 T-m/m
B''L 1.67 T-m/m²



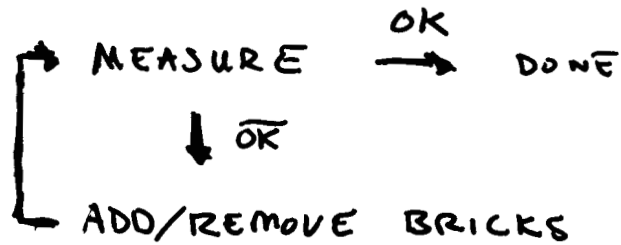
FLIP COIL

- MEASURE INTEGRAL STRENGTH OF DIPOLE OR GRADIENT MAGNET
- 1ST BUILT FOR USE IN PRODUCTION OF PERMANENT MAGNETS FOR 8 GEV TRANSFER LINE
- 10 TURN WINDING ON AL. FORM
- HOUSED IN STAINLESS STEEL TUBE
- SUPPORTS AT EACH END + 1 IN BODY
- MOTORIZED (WHEDECO DRIVE SYSTEM)
- SIGNAL INTEGRATED BY ANALOG INTEGRATOR
- INTEGRATOR READ BY HP ~~3458~~ 3457 DVM (SEE PROCEEDINGS OF LAST IMMW FOR MORE)

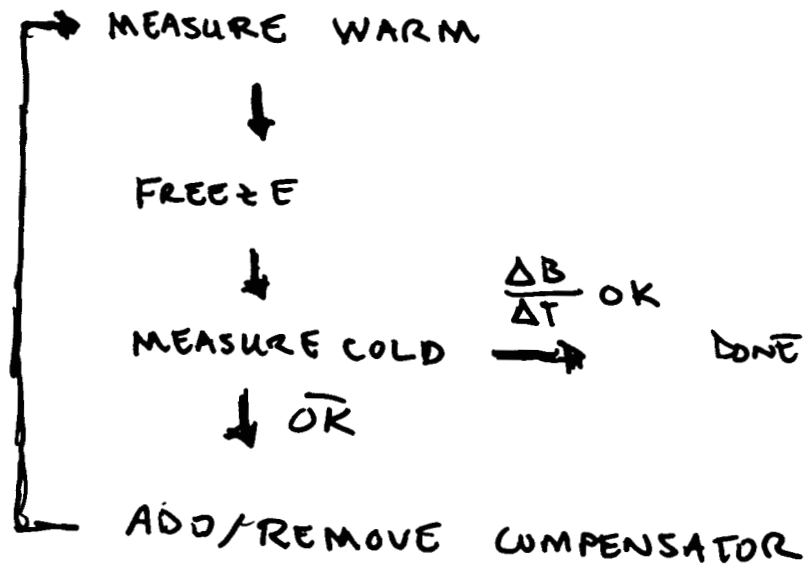


FLIP COIL (2)

- USED TO TUNE MAGNET STRENGTH



- USED TO TUNE TEMPERATURE COMPENSATION



Z SCAN

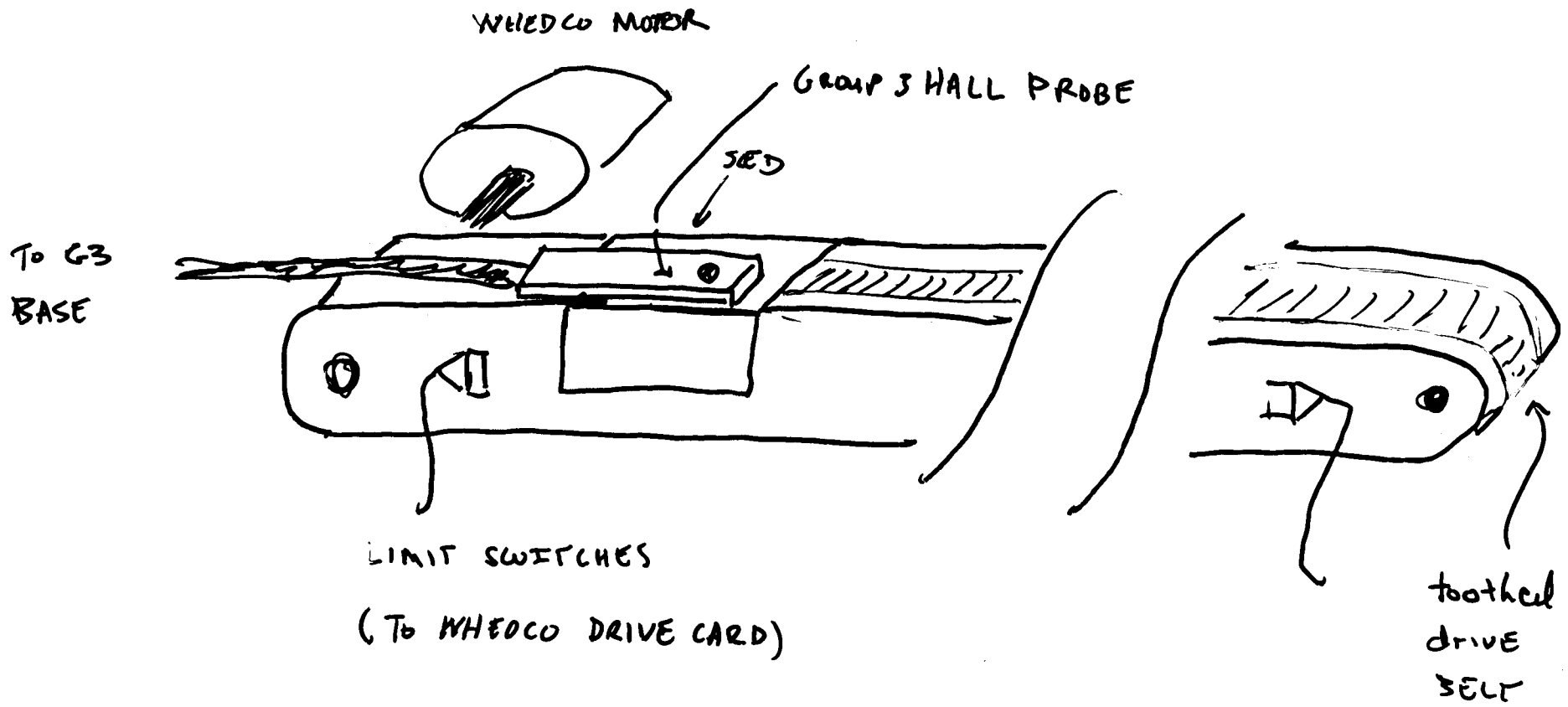
- MEASURE DIPOLE AS A FUNCTION OF LONGITUDINAL POSITION
- HALL PROBE MOUNTED ON A SLED PULLED ALONG A RAIL IN MAGNET APERTURE

(Slow sketch)
- USED WHEPCO DRIVE CARD, TRANSLATOR MOTOR
- GROUP 3 HALL PROBE READ BY GPIB VIA GPIB BUS EXTENDER
- POSITION MEASUREMENT
 - SEQUENCE STARTED BY SENDING THE SLED FORWARD
 - PULL BACK AGAINST LIMIT SWITCH
 - SET $z = 0$
 - POSITION THEN MEASURED FROM NO. OF MOTOR ROTATIONS
 - WHEN FAR LIMIT WAS SET; CHECK # ROTATIONS AGAINST KNOWN ~~DIFFER~~

Z SCAN (2)

DISTANCE BETWEEN LIMITS

- VERY SIMPLE SYSTEM, EASY TO USE,
WORKED WITHOUT ANY PROBLEMS
- EACH MAGNET WAS SCANNED
 - CHECK FOR LONGITUDINAL FIELD
ANOMALIES
 - COMPUTE LONGITUDINAL CENTER OF
FIELD
 - USED TO PLACE MAGNET IN TUNNEL



ROTATING COIL HARMONICS MEASUREMENT

- (ALMOST) IDENTICAL TO MTF STANDS
- 2 PROBES USED FOR GRADIENTS

WASHING
MACHINE
MOTION

- MORGAN COIL 1.6" OD, 16' L
WINDINGS: $n = 1, 2, \dots, 6, 10$

MERIDIAN
SLIP
RINGS

- TANGENTIAL COIL 1.1" OD, 16' L
WINDINGS: TAN, $n = 1, 2 \otimes 2$
BUILT FOR RECYCLER

- BOTH SUPPORTED BY 5 FIXTURES IN
MAGNET BODY & REFERENCED TO
POLE TIPS

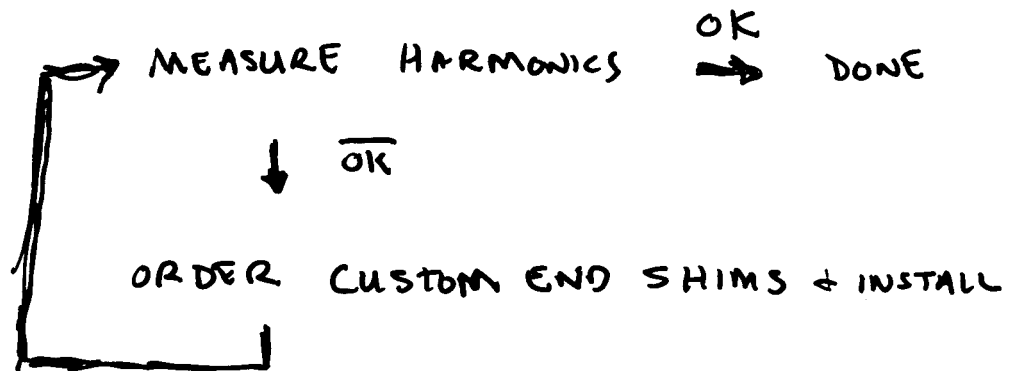
- M.C. 1 POSITION
 - T.C. 3 POSITIONS
- } IN BORE

- MOST MEASUREMENTS MADE WITH
MORGAN COIL
- TAN COIL USED FOR CROSS-CHECK, SCANS
ACROSS BORE

HARMONICS (2)

- MEASUREMENT CYCLE

- STRENGTH, TEMP. COMPENSATION
ALREADY TUNED



SSW

- FIELD SCANS IN BORE
- CALIBRATION OF ROTATING COIL WINDINGS
- SPECIALTY MAGNETS

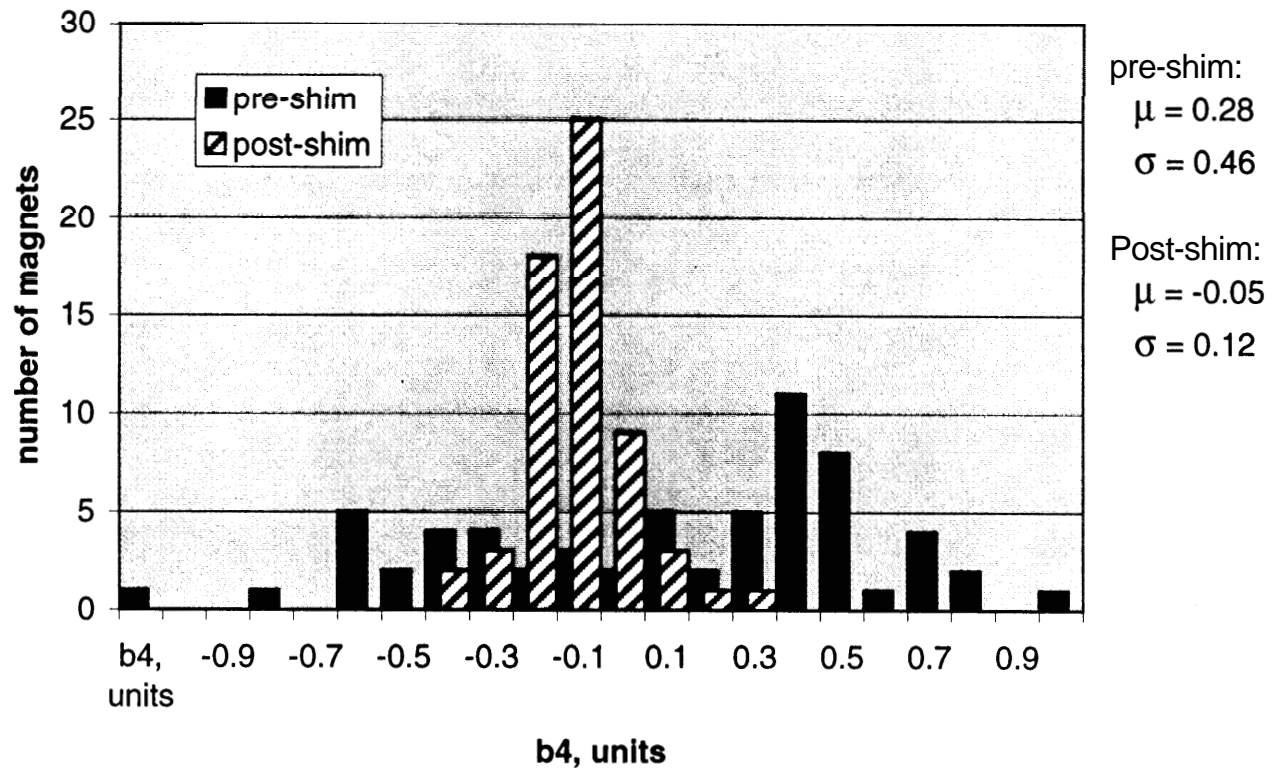
QUADS

- STRENGTH, TEMP. COMP., HARMONICS TUNED
- ALL DONE WITH ROTATING COIL

PROBLEMS

- TANGENTIAL PROBE WAS FINISHED LATE
 - COMMISSIONED DURING STARTUP OF GRADIENT PRODUCTION
 - MORGAN COIL ~~WAS~~ USED AS WORKHORSE
- THE ONE DIFFERENCE BETWEEN MTF + RECYCLER TEST STANDS CAUSED PROBLEM
 - WIERD INTERACTION BETWEEN HP1351 MUX + PDI
 - FIXED BY CHANGING PDI INPUT CONFIGURATION
- DETERIORATION IN SIGNAL CABLE CONNECTIONS AS A RESULT OF WASHING MACHINE MOTION
 - HARD TO DIAGNOSE
 - HAPPENED REPEATEDLY
 - SLIP RINGS ~~THAT~~ WOULD HAVE BEEN CUT EFFECTIVE

SGF octupole - shimming



RGF measurement summary (112 magnets)

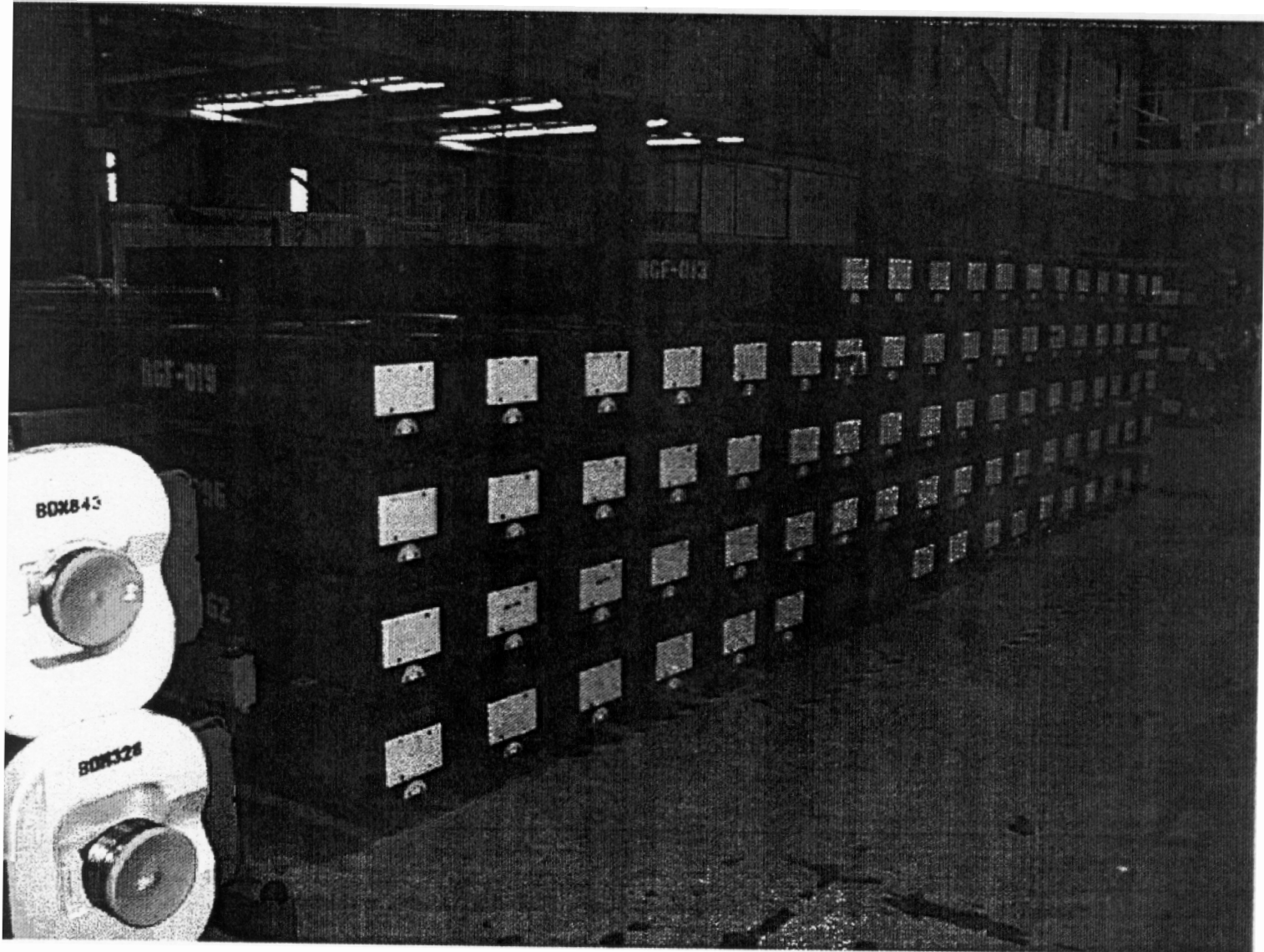
	Ideal	mean	std dev
<i>(dB/B)/dT</i>	0.0	0.09	0.31
DB/B	0.0	-0.04	3.89
<i>b2</i>	619.7	619.74	0.62
<i>a2</i>	0.0	0.31	0.78
<i>b3</i>	8.7	8.61	0.27
<i>a3</i>	0.0	-0.04	0.38
<i>b4</i>	0.0	0.09	0.24
<i>a4</i>	0.0	0.14	0.30
<i>b5</i>	0.0	0.02	0.23
<i>a5</i>	0.0	0.07	0.25
<i>b6</i>	0.0	-0.24	0.28
<i>a6</i>	0.0	-0.11	0.20

Other gradient series also obtained excellent results

COMMENTS

- ~~THROUGH~~ THROUGHPUT HIGH COMPARED TO ELECTROMAGNET MEASUREMENT
- NEEDED SIMPLE, ROBUST, "IDIOT-PROOF" SYSTEMS
(REMOTE LOCATION)
 - FLIP COIL, ZSCAN CERTAINLY MET THAT CRITERIA
 - HARMONICS MEASUREMENT SYSTEM BECAME MORE SO OVER TIME

Finished Recycler Gradient Magnets



Top Ten Things to Learn at IMMW

A Survivor's Tale

Bruce C. Brown
IMMW XI at Brookhaven
23-September-1999

23-Sep-1999 IMMW
IMMW Top Ten
Bruce C. Brown

With the title I offer, you should get a few 'David Letterman' class laughs. You won't. It's mostly a sad tale. You will find it funnier than I do, but please keep that to yourself.

A few points can be just stated. Most will require an illustration.

Keep in mind that I have followed the Main Injector magnets to the accelerator. I am no longer an active data collector. But I am still extracting information and living with its 'features'.

23-Sep-1999 IMMW
IMMW Top Ten
Bruce C. Brown

#10:

Know What Your Customer Needs

Sometimes the obvious can get lost. You probably need to understand some technical features of the application. Then ask, "What are the crucial questions?"

Following the measurement of 600 magnets for the Fermilab Antiproton Source, we were informed that 50-100 magnets from the Main Ring would be available for testing during the construction of the collider overpass. So, we planned to build a new probe and use existing computing and electronic systems. Routine...until we really listened. The crucial information needed concerned injection fields for the Main Ring (400 Gauss). We had experience for Tevatron injection fields (6600 Gauss) and PBar Source fields (1.7 T). Our management was surprised to realize that we would require more than order of magnitude in sensitivity. Yes, we did find new problems which demanded carefully shielded probes.

23-Sep-1999 IMMW
IMMW Top Ten
Bruce C. Brown

#9:

What Your Customer Needs May Not Be Enough

It will not take long to learn more than your typical customer. They probably will not know about the cross checks and redundancy which will provide reliable measurements. They may need help to understand magnet physics issues such as hysteresis or measurement issues such as the benefits of integral over point measurements. You may find that learning more of the accelerator beam dynamics or other requirements-oriented issues is fun.

Typically the customer doesn't care about the next time the magnet will be used. We measured a few magnets for a calorimeter calibration beam line. 4-5 years later they were going into another calibration line. We re-measured them.

23-Sep-1999 IMMW
IMMW Top Ten
Bruce C. Brown

#8:

**Redundancy is so nice.
In fact it is Crucial**

As production began on the Main Injector Dipoles, a minor crisis developed. The field for 120 GeV operation was stronger for new magnets than for the initial production. If the source was a steel difference, we needed to expeditiously understand what needed to be controlled in the steel making process. Because we had redundant strength measurements, including reference magnet differences, we could dismiss potential measurement system problem with a couple of hours or work (really less than that). We confidently moved on to the issues of steel quality and our steel measurements without concern for magnet measurement problems.

23-Sep-1999 IMMW
IMMW Top Ten
Bruce C. Brown

#7:

Humans will Error - 99% Accuracy is Great Work

Watching 18 months of Tevatron magnet measurement convinced me that 99% accuracy was as good as you could achieve. You let people (measurers) make the choices, but the computer must make the measurement, including reading the switches and hardware identification. So we built the PBar Source measurement system and the measurer controlled it but only put in the magnet name. After 600 magnets were measured, we had no errors, *except for measurements on 6 magnets with the wrong label.*

After I quoted this for a decade, a TV show on medical disasters featured a Harvard researcher who reported that human accuracy is 99% at best. Systems which achieve a lower error rate are automated or use answers only after cross checks.

23-Sep-1999 IMMW
IMMW Top Ten
Bruce C. Brown

#6:

We learned at IMMW to Identify Probes Electronically

About 10 years ago at an IMMW, we presented our system for identifying probes using digital input registers which read codes wired into the probe connectors. Another group described having not only probe and instrument coding, but they also included a wire through each connector that could be checked with the computer. Before a measurement began, the computer checked that each connection was complete.

The planning for a probe identification system was included in the Main Injector measurement system. It was mostly implemented but was not included in the initial measurement protocol. At the peak of effort, other projects also required measurements. Data was analyzed with the wrong probe properties. Man months of effort were spent by the data users trying to deal with the resulting confusion. The Main Injector Measurement System now identifies probes.

23-Sep-1999 IMMW
IMMW Top Ten
Bruce C. Brown

#5:

**Remember Hanft's Law:
Unexamined Data is (Probably) Wrong
Data**

The plan for a measurement is only a working plan when you have collected data, demonstrated that the data was collected and monitored the continued data collection. The data quality is likely to be no better than you have demanded of it.

The Main Injector measurements were monitored to demonstrate the magnet quality. Uniformity of better than 0.1% was needed. The measurement system needed strength measurements to 0.03%. Accelerator modeling will find much higher precision to be useful. Repeat measurements at 500 A show RMS strength variations of 0.002% (2×10^{-5} or 0.2 units). This demonstrates that the 10 kA supply provided current control to 20 mA. However, the current readback has variations of 0.02% !!!

23-Sep-1999 IMMW
IMMW Top Ten
Bruce C. Brown

#4:

**Don't Count on Hanft's Law:
OR
Old measurements are nice.
(Keep them On-Line)**

Reported Measurements are Really Nice.

How did we find the probe identification error? We had old measurements. The PBar quadrupole strength was monitored by comparing to a reference magnet with our FLATCOIL measurement program. Rotating coil harmonics were monitored only for field shape. But the data was spinning on-line and was directly comparable to newer measurements. When the data was extracted and analyzed, it demonstrated the design features expected for the various magnet lengths. When compared to new measurements with the 'improved' system, most agreed at the 0.2% level. Disagreements were almost precisely 6% (a probe radius wrong by 3%).

23-Sep-1999 IMMW
IMMW Top Ten
Bruce C. Brown

#3:

Empower Your Measurers: Display Cool Things On-line

- Let them see the harmonic components by displaying raw signals with the dominant contribution suppressed.
- Display time graphs of magnet current changes.
- When possible, compare current measurements against expectations (from previous measurements or design properties)

23-Sep-1999 IMMW
IMMW Top Ten
Bruce C. Brown

#2:

**Congratulate Yourself on Success
When it counts, the project is in trouble**

I was visiting at DESY when the PMES (HERA proton superconducting magnet measurement group) received data back from their newly commissioned measurement system at the magnet factory in France. Room temperature measurements had been made on the first prototype HERA Quadrupole. The 12-pole component was unacceptably large. There were significant effects due to magnetic properties of the stainless steel collars.

The measurement group had saved the day. But management was busy obtaining suitable stainless for the next prototype. I took it upon myself to congratulate the measurement group.

23-Sep-1999 IMMW
IMMW Top Ten
Bruce C. Brown

#1:

Take Time to Enjoy Magnets and Measurements

- We have cool computer tools.
- We buy and build neat electronics.
- We often feature incredible mechanical stuff.
(Cryogenics is really cool. :-))
- Magnets are fascinating. There is still much to learn.
- The people who do magnet measurements are the greatest.

23-Sep-1999 IMMW
IMMW Top Ten
Bruce C. Brown

Session Summary: Session TU3

Tuesday, September 21, 1999, 1:30 –3:00 p.m.

Chair: Malgorzata Tkatchenko

Session TU3 : which we could call “using magnetic measurement in your every day work”

In the first talk [Richard Thomas](#) (BNL) described the smart, automated method used to check the polarity in RHIC magnets. A barcode label is placed on each magnet to indicate the configuration of the magnet. To ensure that the magnet configuration corresponds to the barcode, a Hall probe rotation is performed with subsequent harmonic analysis. This is a very good idea when you have plenty of different magnet configurations, in particular for superconducting magnets.

The second talk by [Dejan Trbojevic](#) (BNL) reported on the complete process, starting from magnetic and mechanical measurement to finish with completing of database for RHIC magnets. This database is used for magnet assembly, their installation, alignment, operation and as a diagnostic tool for accelerator physicist for simulating beam dynamics.

[V. K. Makoveev](#) (JINR) reported on neutron radiation damage on Hall probes used with JINR magnetometer. The conclusion was that the sensitivity is reduced by 3.7 %, but recovers by 1 % after 68 days, starting from exposure to the fast neutron flux of $1.5 \cdot 10^{15} \text{ n/cm}^2$.

[Animesh Jain](#) (BNL) finished this session giving the talk about a new type of measurement. The measurement of helicoidal dipole with the help of the straight coil. Detailed error analysis has shown that the measurement coil has to be made of several segments. The great number of segments will improve the maximum error. The final conclusion was that the experimental results in the helicoidal dipole were consistent with expectations based on numerical simulations.

Session Summary: Session TU4

Tuesday, September 21, 1999, 3:30 –5:00 p.m.

Chair: Gebhard Moritz

It was a mixed session with totally different topics.

[Mike I. Green](#) reported about the ‘Status of Magnetic Measurements at LBNL’. After the completion of the magnets for the ‘Low Energy Ring’ of PEP II at SLAC the group was dissolved. Mike is back at the Lab as a consultant.

[Jacques Billan](#) from CERN talked about ‘Search coils for LHC’. Jacques established a real ‘coil factory’ at CERN – up to 1800 very accurate coils will be made. Out of these individual and identical search coils radial and tangential coils are built. No skew bucking coils are needed because the parallelism of the coils is better than 1 mrad. The coils are made either using single wire or MWS multiwire. They are carefully calibrated at specific test benches. If I can give you an advice: Don’t make your own coils, buy them from Jacques.

Next talk was given by [Doug Evans](#) from TRIUMF about ‘Magnet Measurements for the ISAC Project’. The project includes 132 dipoles, quadrupoles and sextupoles, all resistive and DC. The measuring tools are a 3D-Mapping Table with hall probes and a Rotating Coil System. They developed for this project a new 3m long probe arm, made out of Boron Fiber wrapped with Kevlar.

Next was [Zachary Wolf](#) from SLAC. He presented ‘Measurements for the PEP II Interaction Region Permanent Magnets’. It was a huge effort to measure these 2 dipoles and 2 quadrupoles. It included the measurement of the magnetic moments of the permanent magnet blocks, the field quality of each slice, the field strength and quality of the assembled magnet and the fiducialization. Measurement devices were Helmholtz Coils, Rotating Bucking Coil and Stretched Wire. I like to mention a special coil with well known magnetic moment that was used for test and calibration purpose before each run and the well designed kinematic mount of the rotating coil (ball/cone), in order to avoid any constraints on the coil.

The last speaker of this session was [Laurent Deniau](#) from CERN. The title of his presentation was ‘Effect of the rectangular Coil Windings on Magnetic Field Measurements using Rotating Coils System’. He first calculated the coil flux in a filamentary approximation (zero dimension coil). In this approximation he could determine –with some assumptions- the coil sensitivity factors from the known data of a real coil. Then he handled a rectangular coil with several approximations and got correction factors for the simple filamentary approximation. Graphs showed that the effect can not be neglected if one wants to measure harmonics down to 0.1 unit. Papers are available on the web:

<http://home.cern.ch/m/mtauser/www/html/internalnotes1998.html>

Session Summary: Session WE1

Wednesday, September 22, 1999, 8:30 a.m. –12:00 noon

Chair: D. Evans

[Louis Walckiers, CERN:](#)

Measurements for the Acceptance Tests of the LHC Superconducting Magnets.

The LHC requires more than 7000 total magnets of 60 types. Approximately 1200 dipole cold masses to measure as well as about 400 MQ plus 100 MQM or MQY quads. The magnets will be tested in industry with the assistance of CERN personnel and help from other labs. When the magnets arrive at CERN, more tests will be conducted including alignment tests, stability tests and field quality tests. A one pass mole will be used for the MB centering technique. A 15 meter long rotating coil will be used to check MB field quality. The warm/cold alignment correlation will be established on a reduced no. of magnets using a cold mole system and a stretched wire system.

[Phil Schlabach, FNAL:](#)

Measurements of HGQ Model Magnets.

7 Models have been built and 6 tested. Warm measurements were done during fabrication followed by a full set of cold measurements to verify each magnet. The apparatus used included a FEI mole from SSC for warm measurements and a new 0.82 m. long probe wound on 4.1 cm. O.D. G10 shaft for cold measurements. Measurements included harmonics, transfer functions, field angle & twist, end field meas. and injection field meas. The results showed good agreement between meas. and calculated results. Development is on going to improve results due to Eddy Currents.

[Fabrice Simon, CEA:](#)

Magnetic Measurements on LHC Prototype Quadrupoles at Room Temperature.

The mole used for these measurements was built at CERN and has 5 radial coils, is 750 mm. long and has 400 turns. It was calibrated in a dipole and a quadrupole. Room temperature meas. were carried out in industry so the goal for the meas. system was that it be simple, fast and safe. The system proved to be reproducible to 0.05 units. The mole measured at 5 different positions and the meas. data and calculated data agreed well. More coils were needed however to detect a trend and correct possible imperfections. A complete meas. took less than 3 hours.

[Phil Schlabach, FNAL:](#)

Plans for Measurement of LHC IR Quads During Production.

There will be 2 prototype magnets and 9 FNAL quads. Field meas. to be done with rotating coils and alignment with a stretched wire system. A short (about 1 m. long) rotating coil to be used during fabrication meas. and a long rotating coil (total 16 m. long) to test production magnets. At the moment the hardware is being built for the warm meas. system and the parts are being acquired for the cold meas. system. There are already 3 stretched wire systems operational for alignment. The plan is for the probes to be ready by next summer, the software by next spring and the first full length prototype meas. by next October.